

# Relatório de Conclusão de Curso

Martina Garcia de Cezar

THERMAL EFFECTS OF PLANTS IN CITIES:  
AN ANALYSIS USING DYNAMIC FLOW APPROACH

Florianópolis  
2020



Universidade Federal de Santa Catarina  
Centro Tecnológico  
Curso de Engenharia Sanitária e Ambiental

Thermal effects of plants in cities:  
An analysis using dynamic flow approach

Graduation work submitted to the Sanitary and  
Environmental Engineering Program of the Federal  
University of Santa Catarina for the conclusion of the  
Sanitary and Environmental Engineering course.  
Supervisor: Prof<sup>a</sup>. Dr<sup>a</sup>. Maria Elisa Magri  
Co-Supervisor: Bruno Molle  
Co-Supervisor: Séverine Tomas  
Co-Supervisor: Bruno Cheviron

Florianópolis  
2020

### Identification sheet of the work

Garcia de Cezar, Martina

Thermal effects of plants in cities: An analysis using dynamic flow approach / Martina Garcia de Cezar ; orientadora, Maria Elisa Magri, orientador, Bruno Molle, coorientadora, Séverine Tomas, coorientador, Bruno Cheviron, 2020.

64 p.

Trabalho de Conclusão de Curso (graduação) - Universidade Federal de Santa Catarina, Centro Tecnológico, Graduação em Engenharia Sanitária e Ambiental, Florianópolis, 2020.

Inclui referências.

1. Engenharia Sanitária e Ambiental. 2. Urban microclimate. 3. Numerical simulation. 4. Urban vegetation. 5. Urban canyon. I. Magri, Maria Elisa. II. Molle, Bruno III. Tomas, Séverine. IV. Cheviron, Bruno. V. Universidade Federal de Santa Catarina. Graduação em Engenharia Sanitária e Ambiental. VI. Título.

Martina Garcia de Cezar

Thermal effects of plants in cities:  
An analysis using dynamic flow approach

This graduation work was considered adequate for obtaining the title of Sanitary and Environment Engineer, and approved in its final version by the course of Sanitary and Environmental Engineering.

Florianópolis, Wednesday 9<sup>th</sup> December 2020.

---

Prof.<sup>a</sup> Maria Elisa Magri, Dra.  
Course coordinator  
Federal University of Santa Catarina

---

Prof.<sup>a</sup> Maria Elisa Magri, Dra  
Supervisor  
Federal University of Santa Catarina

---

Bruno Molle  
Co-Supervisor  
Inrae

---

Séverine Tomas  
Co-Supervisor  
Inrae

---

Bruno Cheviron  
Co-Supervisor  
Inrae

**Board of examiners:**

---

Prof. Leonardo Hoinaski, Dr.  
Federal University of Santa Catarina

---

Prof. João Henrique Macedo Sá, Dr  
Federal University of Santa Catarina

This work is dedicated to my parents, my brother, friends and professors who gave me a support during my degree.

## ACKNOWLEDGEMENTS

Going on an academic exchange is a unique and enriching experience, both professionally and personally. I spent my first six months in France attending Supagro's third year Agronomy course. During this time, I developed different skills related to the study of the environment and agriculture; I learned a new way of observing agricultural production as well as the different elements that its optimal development and analysis require. I would like to thank all the team from the course “Water, Soil and Environment” and my classmates, who made learning a fun experience and who provided me with a strong foundation in the subject I love.

I also had the opportunity to do an internship at Inrae G-Eau unit while on exchange. I would like to thank Bruno Molle for this opportunity and for the support he always provided me, as well as my other tutors Séverine Tomas and Bruno Cheviron, who guided me during this period. Together we developed the project and they were very patient with the various questions I had, always allowing for a rich knowledge exchange. I had an amazing time, and learned a lot about an interesting, multi-disciplinary and challenging theme. Thanks also to all of the other interns who were always supportive and helped me during this time.

Thank you to all the EnLarge Project partners, who I had the privilege to work with and learn from during the project development.

Thanks to Emmanuel Bozonnet and the VegDud Project for providing the results of the ClimaBat platform, which were important to test the model proposed by this study.

Thanks to my friends Bruna, for the help with English questions, support, and Deborah for the friendship and knowledge exchange in the conduction of this study.

Thanks to the whole team of Sanitary and Environmental Engineering of the Federal University of Santa Catarina and all the friends I made during these six years of graduation. You have been fundamental to my formation, both personal and professional. I will carry the friendships I have made for the rest of my life, thank you for the support and all the moments we spent.

Finally, a special thanks to my family, who always support me in all the choices I made in my life.

## RESUMO

### **Título: Efeito térmico das plantas nas cidades: Uma análise utilizando a abordagem de dinâmica de fluxo.**

Em um cenário global de crescimento populacional, alta urbanização, esgotamento de recursos e aumento da intensidade das ilhas de calor urbanas, são necessárias iniciativas para construir cidades resilientes e abordar a ligação entre alimentação, água e energia. Assim, este estudo aborda a vegetação urbana como uma alternativa que permite a integração de diversas atividades em sua prática (tratamento de água, agricultura urbana e redução de custos energéticos) e melhorar a qualidade de vida da população com, por exemplo, o aspecto que será tratado principalmente neste trabalho: a capacidade de mitigar as temperaturas externas que as paredes e coberturas verdes podem oferecer, na escala do microclima urbano. Uma primeira versão para uma ferramenta de apoio à decisão foi proposta, para ser integrado a um grande sistema como parte do projeto JPI EnLarge. Esta primeira análise desenvolvida traz duas modelagens trabalhando com os softwares Optirrig, ANSYS / Fluent, Vensim e ENVI-met e é baseada no balanço energético existente entre o edifício, o substrato e a planta, em interação com os fluxos turbulentos presentes em um cânion urbano. Assim, para avaliar a aplicabilidade dos modelos inicialmente propostos simulando um cânion urbano de referência (sem cobertura vegetal), foi realizada uma comparação entre os resultados simulados e os observados com um estudo de caso. Resultados satisfatórios foram obtidos nas primeiras simulações com o modelo 1 e modelo 2 estudados, considerando as simplificações adotadas. Os dois modelos geraram resultados com precisões próximas e os resultados iniciais são um ponto de partida para a continuidade do estudo sobre a unidade elementar de uma cidade, o cânion urbano.

#### Palavras-chave

Telhado verde, cânion urbano, microclima, ilhas de calor, vegetação urbana, simulação numérica

## **ABSTRACT**

### **Title: Thermal effects of plants in cities: An analysis using dynamic flow approach**

In a global scenario of population growth, large urbanization, resource depletion and increased occurrence of urban heat islands, initiatives to build resilient cities and with the Nexus food, water and energy are needed. Therefore, this study approaches urban vegetation as an alternative that makes it possible to integrate various activities with its practice (e.g. water treatment, urban agriculture and reduce energy costs) and improve the quality of life of the population with for example the aspect that will be mainly discussed in the work that is the ability to mitigate the outdoor temperatures that green walls and roofs can generate on the urban microclimate scale. A first analysis of two models to create a tool to help decision-making is proposed and will later be integrated into a large system under the JPI EnLarge Project. This models use the Optirrig, ANSYS Fluent, ENVI-met and Vensim software's and is based on the existing energy balance between the building, substrate and plant system and their interactions with the turbulence that is present in an urban canyon. Thus, to evaluate the applicability of the initially proposed models modeling a reference urban canyon (without green covers), a comparison of the simulated results and those obtained with a case study was performed. Satisfactory results were obtained in the first simulations with model 1 and model 2 studied, considering the simplifications adopted. The two models provided results with close precision and the initial results are a starting point for the continuity of the study on the elementary unit of a city, the urban canyon.

#### Keywords

Green roof, green wall, urban canyon, urban microclimate, urban vegetation, numerical simulation.



## LIST OF FIGURES

Figure 1: Energy balance of the Parisian territory from May to September 2009.....	17
Figure 2 : Variation of energy consumption by Parisian businesses centers between 1990 and 2009.....	18
Figure 3 : Green wall, building of the Institute of Research for Development (IRD), Montpellier, France at 12:48, July 24, 2019.....	19
Figure 4 : Permeable pavements (Montpellier France).....	20
Figure 5: Fountain (Montpellier France) .....	20
Figure 6 : Water misting at Mecca, (Saudi Arabia).....	20
Figure 7 : Creation of a water slide in the soil (Wiegbrug, Amsterdã).....	20
Figure 8: At 55,000 square feet, Higher Ground Farm is the second largest rooftop farm in the US. Topping the Boston Design Center.....	21
Figure 9 : Possible implementation schemes for greywater collection, treatment, and reuse in the same building with green walls: a) floor-by-floor and b) unified.....	21
Figure 10: Basic components of typical Green Roof.....	23
Figure 11 : Diagrammatic representation of varying types of green walls.....	23
Figure 12: Schematic of climatic scales and vertical layers found in urban areas. PBL – planetary boundary layer, UBL – urban boundary layer, UCL – urban canopy layer. ....	28
Figure 13 : Generalized mean (spatial and temporal) wind velocity ( $u(z)$ ) profile in a densely developed urban area including the location of sublayers of the surface layer. The measures on the height scale are the mean height of the roughness elements ( $zH$ ), the roughness sublayer ( $zr$ , i.e. the "blending height" at which the individual influence of each building ceases to be recognizable), the roughness length ( $z0$ ) and zero-plane displacement length ( $zd$ ). Dashed line – profile extrapolated from the inertial sublayer; solid line - actual profile. ....	29
Figure 14 : Effect of packing density ( $H/W$ ) on flow regimes over urban-like ‘building’ arrays in a wind tunnel.....	30
Figure 15 : Typical flow patterns in urban canyon. ....	30
Figure 16 : Mechanisms of mass and heat transfer between building (grey), vegetal canopy (green), substrate (orange) and atmosphere (white). ....	31
Figure 17 : Principles of the Optirrig model. Climatic forcings appear in rose, parameters in green, main state variables in medium blue and auxiliary variables in light blue cells (see text for details). ....	32
Figure 18 Thermodynamic interactions between the built and the natural environment .....	33
Figure 19 : Schematic representation of the coupled model 1.....	36
Figure 20 : Schematic representation of the coupled model 2. ....	36
Figure 21 : Geometry of the shadow on a canyon street. ....	39
Figure 22 : Geometry of the conduction in the system vegetal canopy + substrate + building .....	43
Figure 23 : Theoretical domain of calculation, which includes the input and output characteristics (e.g. speed and temperature profiles) and the heat and mass transfer between the atmosphere and the model walls. Walls, for this spatial scale, refers to a composite interphase, such as building walls, asphalt or systems like building-substrate-vegetation with properties such as density, specific heat, thermal conductivity, roughness, emissivity, moment and thermal conditions.....	45
Figure 24: Illustration of the location of the traced profiles for the analysis of the results obtained in the simulations, ‘v1’, ‘v2’ and ‘v3’ are the vertical profile and the ‘t1’ is the transversal profile in the canyon.....	45
Figure 25 : Example diagram for the analysis of the climatic effects of green walls and roofs in urban canyon. ....	48

Figure 26: Image of the green wall pilot by Ecosec with the column 1 indicated, Montpellier, July 2019.....	49
Figure 27 : Experimental bench ClimaBat.....	50
Figure 28 : Thermal photos green wall pilot at (a) 8h00; (b) 14h30; and (c) 17h30. ....	52
Figure 29: Simulation results for geometry A for the left temperature and right velocity profiles, domain height of 4 metres.....	53
Figure 30: Simulation results for geometry B for the left temperature and right velocity profiles, domain height of 2 metres.....	53
Figure 31 : Results obtained in the refinement of the mesh for the ClimaBat pilot Reference canyon, transverse (t1) velocity profile.. ....	54
Figure 32 : Results obtained in the refinement of the mesh for the ClimaBat pilot Reference canyon, transverse (t1) temperature profile.. ....	54
Figure 33 : Principles of the Optirrig model modified version vegetal walls and roofs.....	57
Figure 34 : 3D Study Area.....	58
Figure 35 : 2D Study Area.....	58
Figure 36 : Results obtained in the ClimaBat pilot reference canyon in ENVI-met Lite.....	58
Figure 37 : Simulation result of the potential air temperature and wind direction profile at 5 p.m. on August 22, 2012.....	59

## LIST OF TABLES

Table 1 : Types of green roofs.....	22
Table 2: A review of the cooling effect of different urban envelopes in an urban canyon (space above the street and between the buildings) .....	25
Table 3: ENVI-met features.....	34
Table 4: List of parameters used for the experimental validation of the day 2012-08-17 at 17:30.....	50
Table 5: Results for the VegDud reference canyon in the Ansys Fluent program with turbulence model "k-e standard", thermal model "radiation" for the surfaces and simple-accuracy. Where TambEXT, U and HR_1 are the inputs data, Tsimulated is the result of the simulation and Tobserved is the temperature measured in the reference canyon.....	56
Table 6: Results for the VegDud reference canyon in the ANSYS Fluent program with turbulence model "Stress Reynolds", thermal model "temperature" for the surfaces and double-accuracy. Where TambEXT, U and HR_1 are the inputs data, Tsimulated is the result of the simulation and Tobserved is the temperature measured in the reference canyon.....	56

## ACRONYMS AND ABBREVIATIONS

CFD	Computational Fluid Dynamics
CPU	Central Processing Unit
EFB	European Federation Green Roofs & Walls
WEF	Water, Energy and Food
H/W	Canyon aspect ratio
IRD	Institute of Research for Development
PET	Physiologically Equivalent Temperature
UBL	Urban boundary layer
UCL	Urban canopy layer

**SYMBOLES**

$\theta_{fc}$	Field capacity of the water	
$\Delta G$	Energy stored or restored	$W m^{-2}$
$\theta_{wp}$	Permanent wilting point of the water	
A	Azimuth of the sun	$^{\circ}$
A	Plane area	$m^2$
a'	Angle of the normal to the street plan with the direction North-South facing South	$^{\circ}$
AET	Actual evapotranspiration	mm
CO <sub>2</sub>	Concentration of carbon dioxide in the ambient	$g m^{-3}$
C <sub>p</sub>	Partition coefficient	-
c <sub>p,a</sub>	Specific heat of the air at constant pressure	$J kg^{-1} K^{-1}$
c <sub>pf</sub>	Specific heat of the vegetal canopy	$J kg^{-1} K^{-1}$
C <sub>s</sub>	Sand-grain roughness constant	-
c <sub>s</sub>	Specific heat of the street	$J kg^{-1} K^{-1}$
D <sub>c</sub>	Distance between the two buildings	m
D <sub>o</sub>	Height of displacement of the plant canopy	m
E	Emissivity	-
ES	Actual evaporation	mm
e <sub>s</sub> - e <sub>a</sub>	Vapour pressure deficit of the air	Pa
ES <sub>0</sub>	Substrate potential evaporation	mm
ET <sub>0</sub>	Potential evapotranspiration	mm
ETM	Maximal evapotranspiration	mm
G <sub>b</sub>	Generation of turbulence kinetic energy due to buoyancy	
G <sub>k</sub>	Generation of turbulence kinetic energy due to the mean velocity gradients	
H	Building height	m
H	Sun height	m
h <sub>f</sub>	Height of the vegetal canopy	m
h <sub>s</sub>	Height of the substrate	m
I	Direct solar radiation perpendicular to the building façade	$W m^{-2}$
I	Electric current flow	A
I <sub>r</sub>	Fraction intercepted by the green wall or roof	-
K	Turbulence kinetic energy	$m^2 s^{-2}$
K <sub>c</sub>	Crop coefficient	-
K <sub>cmax</sub>	Maximal value for the crop coefficient	-
k <sub>ct</sub>	Thermal conductivity of the concrete tanks	$W m^{-1} K$
k <sub>i</sub>	Materials conductivity	$W m^{-1} K^{-1}$
K <sub>s</sub>	Sand-grain roughness height	m
L	Latent heat flow	$W m^{-2}$
L	Plane thickness	m
LAI	Leaf Area Index	$m^2 m^{-2}$
L <sub>o</sub>	Obukhov stability length	-
p <sub>a</sub>	Density of air at constant pressure	Pa
p <sub>f</sub>	Density of the vegetal canopy	$kg m^{-3}$
P <sub>max</sub>	Maximal root depth of the water	mm

$\rho_s$	Density of the street	$\text{kg m}^{-3}$
$p_{v\text{fsat}} - p_{va}$	Deficiency of air vapor pressure compared to leaf cells	Pa
$Q_a$	Anthropogenic flux	$\text{W m}^{-2}$
$Q_{\text{wall}}$	Heat flux through plane	W
$R$	Thermal resistance	$\text{K W}^{-1}$
$R_1$	Water reserves in the subsurface	mm
$R_2$	Variable-depth root-zone	mm
$R_3$	Water reserve in the deep reservoir	mm
$r_a$	Aerodynamic resistance	$\text{s m}^{-1}$
$R_e$	Electric resistance	$\Omega$
$R_{\text{kru}}$	Limit of the easily available water reserve	mm
$R_n$	Net radiation flux	$\text{W m}^{-2}$
$r_s$	Stomatal resistances	$\text{s m}^{-1}$
$r_{s,\text{min}}$	Minimal stomatal resistance	$\text{s m}^{-1}$
$S$	Sensible heat flow	$\text{W m}^{-2}$
$S_n$	Nitrogen stresses	
$S_w$	Water stresses	
$T_a$	Ambient air temperature	K
$T_{\text{DM}}$	Total Dry Matter	mm
$T_f$	Effective surface temperature	K
$TP$	Actual transpiration	mm
$TP_0$	Potential transpiration	mm
$TP_0$	Crop transpiration	mm
$TT$	Sum of temperature	K
$U$	Wind velocity	$\text{m s}^{-1}$
$u^*$	Friction velocity	$\text{m s}^{-1}$
$V$	Electric voltage	V
$V_r$	Maximal root growth rate of the water	mm
$W$	Width of the space between buildings	m
$y_0$	Aerodynamic roughness length	m
$Y_M$	Contribution of the fluctuating dilatation in compressible turbulence to the overall dissipation rate	
$z_d$	Zero-plane displacement height	m
$z_o$	Surface roughness length	m
$Z_u$	Distance of the green wall	m
$\Gamma$	Psychrometric constant	$\text{kPa } ^\circ\text{C}^{-1}$
$\Delta$	Slope of the saturation vapour pressure temperature relationship	$\text{Pa K}^{-1}$
$E$	Turbulence dissipation rate	$\text{m}^2 \text{s}^{-2}$
$K$	Von Karman's constant	-
$\Delta f$	Shear stress profile	Pa
$\sigma_k$	Turbulent Prandtl for k	-
$\sigma_\varepsilon$	Turbulent Prandtl numbers for $\varepsilon$	-
$\Psi_m$	Dimensionless function for the change in curvature of the wind profile	-
$\omega_g$	Water content of the soil	$\frac{\text{kg}_{\text{water}}}{\text{m}^3_{\text{soil}}}$

## TABLE OF CONTENTS

<b>1 INTRODUCTION</b>	<b>15</b>
1.1 OBJECTIVES	16
<b>1.1.1 General Objective</b>	<b>16</b>
<b>1.1.2 Specific Objective</b>	<b>16</b>
<b>2. BIBLIOGRAPHIC REVIEW</b>	<b>16</b>
2.1 URBAN HEAT ISLANDS	17
2.2 ALTERNATIVES TO REDUCING THE IMPACTS OF URBAN HEAT ISLANDS	18
<b>2.2.1 Creating islands of freshness</b>	<b>18</b>
<i>2.2.2.1 Materials with a higher albedo and lower roughness</i>	18
<i>2.2.2.2 Water for cooling purposes</i>	19
<i>2.2.2.3 Implementing urban vegetation</i>	20
<i>2.2.2.3.1 Green roof</i>	22
<i>2.2.2.3.2 Green wall</i>	23
2.3 MODELING THE THERMAL EFFECTS OF PLANTS IN CITIES	24
<b>2.3.2 Plant, substrate and atmosphere</b>	<b>30</b>
2.4 SUMMARY OF TOOLS USED TO CONDUCT THIS STUDY	31
<b>2.4.1 Optirrig</b>	<b>31</b>
<b>2.4.2 ANSYS Fluent</b>	<b>33</b>
<b>2.4.3 ENVI-met</b>	<b>33</b>
<b>2.4.4 Vensim</b>	<b>35</b>
<b>3. METHODOLOGY</b>	<b>35</b>
3.1 OPTIRRIG	37
<b>3.1.1 Energy balance in the vegetal canopy</b>	<b>38</b>
<i>3.1.1.1 Net Solar radiation (<math>R_n</math>)</i>	38
<i>3.1.1.2 Sensible heat flux (<math>S</math>)</i>	39
<i>3.1.1.3 Latent heat flux (<math>L</math>)</i>	41
<i>3.1.1.4 Stored heat flux (<math>\Delta G</math>)</i>	42
<b>3.1.2 System properties</b>	<b>44</b>
3.2 ANSYS	44
<b>3.2.1 Geometry</b>	<b>44</b>
<b>3.2.2 Physical model</b>	<b>46</b>
3.3 ENVI-MET	47
	13

3.4 VENSIM	48
<b>4. RESULTS AND DISCUSSIONS</b>	51
4.1 GREEN WALL PILOT BY ECOSEC	51
4.2 MODEL 1 – CLIMABAT DATA	52
4.3 MODEL 2 – CLIMABAT DATA	58
<b>5 CONCLUSION</b>	59
<b>6 BIBLIOGRAPHIC REFERENCES</b>	61
<b>APPENDIX 1</b>	67
<b>APPENDIX 2</b>	61
<b>APPENDIX 3</b>	62
<b>APPENDIX 4</b>	63

## 1 INTRODUCTION

Urban microclimate is a term in Climatology used to describe a set of climatic conditions of a small area of cities. It refers to areas with climatic characteristics like temperature, humidity, precipitation which are possibly different from the rest of the city (ZAVATTINI, 2013). One type of urban microclimate is known as urban heat islands (UHI), a phenomenon observed in dense cities. Due to low use of high albedo materials, waterproofing of urban public space, eradication of any place of water in the city and human circulation, the temperature of cities is much higher compared to the less urbanized peripheral regions, especially overnight (APUR, 2012). The size and structure of an UHI varies in time and space, according to meteorological conditions and urban characteristics (OKE, 2006).

Human health and the environment are affected because of higher temperatures in large cities. For example, it was estimated that between 1979 and 2003, excessive heat exposure contributed to more than 8,000 premature deaths in the United States, which exceeds the total number of deaths resulting from hurricanes, lightning, tornadoes, floods, and earthquakes for the same period in the United States (Center for Disease Control and Prevention, 2006). High temperatures favor cardiovascular problems and according to the characteristics of the urban agglomeration, a high concentration of pollutants in the air can induce respiratory diseases compromising human health. Furthermore, UHI can negatively impact the environment, since (i) it increases energy consumption for air conditioning of structures in search of greater thermal comfort for the residents (SAILOR, 2002), (ii) it elevates greenhouse gas emissions and air pollution (LI-WEI, 2009), (iii) it poses danger to aquatic systems (JAMES, 2002) and, (iv) it has impacts on animals (KAISER, 2016).

Urban heat islands are attracting more and more attention every day. It happens because their effect is expected to be stronger over the years. By 2050, the world's population is projected to reach 9.31 billion (UN, 2014) and 66% of the world population is expected to live in urban areas, two factors that directly influence the possibility of UHIs. In this context, researches on sustainable urban areas to increase the community resilience against challenges exacerbated by climate change, population growth, and resources depletion are necessary. The present research is part of the JPI EnLarge project, developed in the Institute INRAE, France, in partnership with several countries, which aims to implement a decision support tool to test various solutions for changing the urban metabolism under three aspects: water, energy and food (WEF). Particularly, the present monography aimed to address the question of agricultural and urban vegetation section of the JPI EnLarge project, studying the mitigation of UHIs from the implementation of green walls and roofs. This technique allows for a wider range of different applications for the main objective of the project: the WEF nexus and the formation of more resilient cities. It seeks to link urban agriculture with the processes of agricultural production, waste and water recycling that will result in a reduction of energy consumption and increase the quality of life of the population. The innovative urban agriculture practices promote direct and indirect effects to the urban environment, such as the purification of air, CO<sub>2</sub> and dust capture, noise reduction in urban centers, quality of life improvements of the population, as well as mitigating the effects of high temperatures in cities thanks to evaporation and shadow from vegetation.

The present work presented the extent to which incorporation of vegetation envelopes can influence the reduction of temperature in the UHI, mainly at their close neighborhood, and also alter their microclimate.

## 1.1 OBJECTIVES

The following sections describe the general objective and the specific objectives of this work.

### 1.1.1 General Objective

This work aimed to model temperatures variations caused by the incorporation of green roofs and walls in the city and their effects on urban microclimate, using an urban canyon as a study case.

### 1.1.2 Specific Objective

- Create a simulation architecture to simulate the climatic effect of vegetation in cities;
- Propose a way to integrate the results of the simulation into the Vensim software, which performs dynamic system modeling;
- Follow the implementation of a prototype of green wall with thermal photos to evaluate the direct impact of the wall on the temperature of its surface;
- Test the ability of the proposed simulation architecture to simulate a reference canyon (surfaces without vegetation) with the data from the Climabat pilot.

## 2. BIBLIOGRAPHIC REVIEW

Thirty papers were analyzed and were then organized in a table according to their topic (general overview and sustainability, nutrient recovery and recycling, and modeled effects on temperature). In addition, all articles were organized with an identification, author, year, document type, keywords and main conclusions. Documents of modeled effects on temperature were further organized with the specification of their analysis of scale, model type, fixed parameters, and input/output data of the model.

The methodology used to organize this bibliographic study follows a predetermined pattern to produce a database with all the bibliography easily accessible. Appendix 1 includes tables with the bibliographic research, and Appendix 2 the table with the fixed parameters used in the literature.

The results from the bibliographic study show that urban microclimate is an area of study strongly connected to the particularities of each city, mainly its geometry and the reigning climatic conditions. Urban microclimate is a challenging study area due to the randomness and instability of the natural phenomena. Different ways of reducing UHI impacts were analyzed in the following sections.

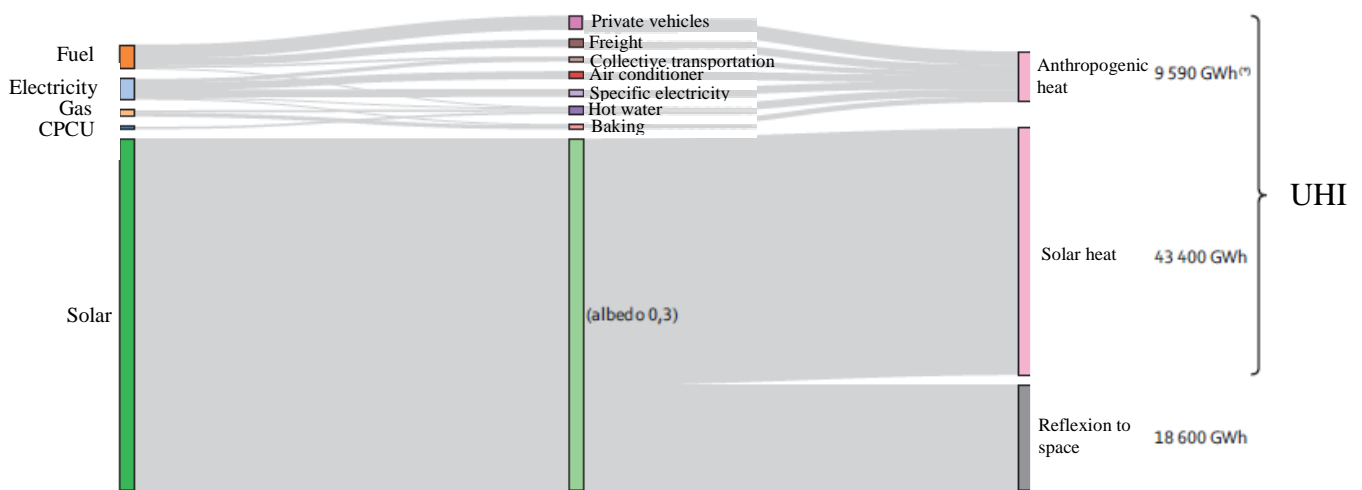


## 2.1 URBAN HEAT ISLANDS

As pointed out by the climatologist specialized in urban climatology Oke (2017), decades of research have shown that cities are almost always warmer than their surroundings. This phenomenon, known as the UHI, is one of the clearest examples of inadvertent climate modification due to humans.

The formation of UHI results from two main heat sources, as shown in the energy balance in Figure 1. One of the heat sources is solar radiation: the characteristics of the city (e.g., surface albedo) are a factor that contributes to the influence of the solar radiation in the formation of UHI. Another source of heat is the anthropogenic related, since every activity that consumes energy is a precursor of heat in urban centers (APUR, 2012).

Figure 1: Energy balance of the Parisian territory from May to September 2009.

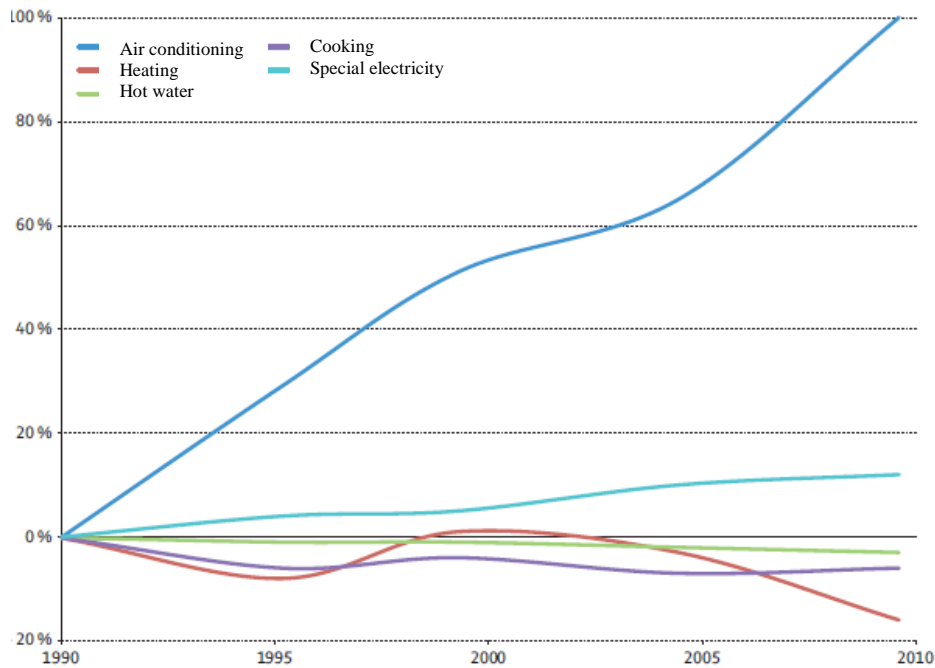


(\*) GWh (for <Giga Watt hour>) is a quantity of energy. A 100 Watts bulb that runs for 10 hours consumes 1 kWh (for <kilo Watt hour>). 1 GWh is 1 million kWh

Source: adapted from CEREN (2011).

One particular anthropic activity is the air conditioning of the buildings. As shown in Figure 2, energy consumption of Parisian businesses areas has significantly increased in the past 20 years. Another activity with great influence is the automobile circulation: in addition to contributing to the formation of UHI, it increases air pollution with gases released in the combustion processes. On the short term, these effects can be minimized with the use of electric vehicles.

Figure 2 : Variation of energy consumption by Parisian businesses centers between 1990 and 2009.



Source: adapted from CEREN (2011)

## 2.2 ALTERNATIVES TO REDUCE IMPACTS OF URBAN HEAT ISLANDS

As UHI have negative impacts on human health and the environment, and their effects are expected to worsen each year, it is necessary to find ways to attenuate temperatures where UHI are formed. Today, various ways of cooling cities are being studied and applied, each with its particular mechanisms and efficiency.

### 2.2.1 Creating islands of freshness

Islands of freshness are known as urban centre areas where the received radiation presents a high percentage of reflection or dissipation (e.g., transpiration). There are several ways to create them, including the use of coating materials with high albedo and low roughness, spaces with water for refreshment purposes or the implementation of vegetation in cities. Those mechanisms minimize the impacts of urbanization by reducing the storage of heat in urban centers.

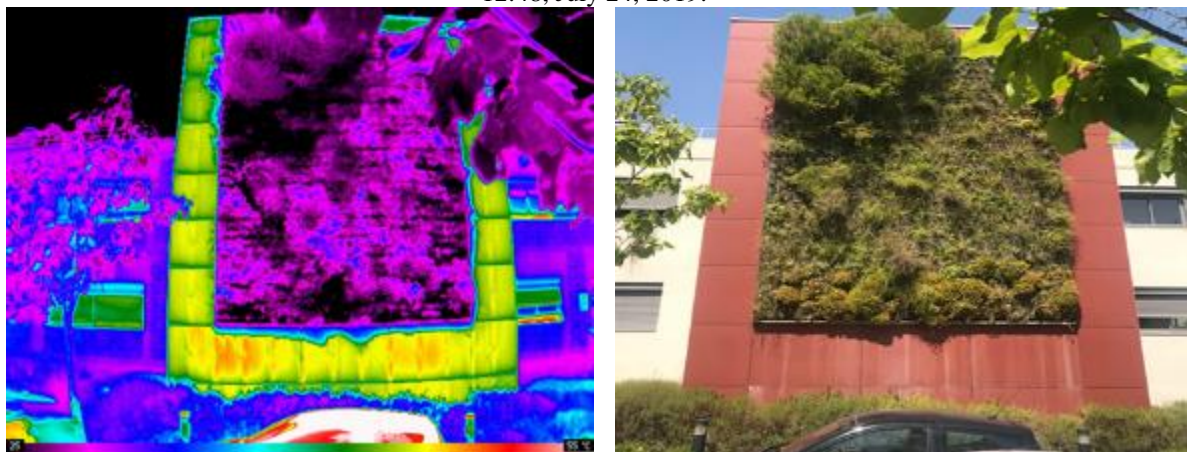
#### 2.2.2.1 Materials with a higher albedo and lower roughness

The cladding materials (external envelope) used in large urban centers are commonly dark and of low albedo. These characteristics favor high heat absorption, since the darker the material is, the smaller is its albedo, and consequently the more radiation is absorbed by the surface. This generates an increase in the temperature of these surfaces and induce the ambient air heating (DJEDJIG, 2013). Other aspects, such as the roughness of the surface coating

material, have a direct impact on surface temperature. Rough surfaces have more room to absorb incident rays, and thus they have a higher heating potential (APUR, 2012).

Figure 3 shows different brightness temperatures in distinct types of building coatings. Under the assumption that the difference between the surface temperature and the brightness temperature is small, we take the values of brightness temperature as the surface temperature of the building walls (GAO et al, 2016). For example, a surface with red paint that has a surface temperature of 47°C, shows an increase of approximately 14°C, compared to a surface with white paint that has 33°C. If we compare the red surface with the vegetal wall that has 30° C, the temperature difference is approximately 17°C. This means that surfaces with vegetation have lower temperatures on their surface compared to the others, and therefore with greater potential to cool the ambient air.

Figure 3 : Green wall, building of the Institute of Research for Development (IRD), Montpellier, France at 12:48, July 24, 2019.



Source: Author, 2020.

High albedo surfaces are called cool surfaces, and they hold greater potential to reflect sunlight, when compared to green surfaces. However, even if the vegetation absorbs the same amount of sunlight as a traditional coating, it can still dissipate much of that energy as latent heat (evapotranspiration). It is more effective than a cool coating, since the reflected radiation by the cool surface will be further intercepted by the street or nearby buildings, which intensifies the lighting of the considered urban scene and prevent radiation dissipation (APUR, 2012; DJEDJIG, 2013).

#### 2.2.2.2 *Water for cooling purposes*

Water can absorb thermal energy from the incoming solar radiation due to its heat capacity. Moreover, water evaporation is a sink for sun radiated energy. Due to this property, it is possible to instrument evaporation, in particular its temporality, in order to answer questions of the climatic discomfort according to the places and their uses in a dynamic way.

Figure 4 : Permeable pavements (Montpellier France)



Figure 5: Fountain (Montpellier France)



As shown in Figures 4, 5, 6 and 7, there are different ways of promoting attenuation of UHI using water. These measures can be taken permanently (e.g., fountain) or temporarily, for example by creating a water slide in the ground or water misting. All these options promote air humidity elevation and the reduction of surface temperature where the water is applied. It results in greater thermal comfort for pedestrians and it can even be energy saving, when the technique is used on the surface of air conditioned buildings. Depending on each technique its effect is more or less significant. The effect depends on the type of technique used and the meteorology of the place. In addition, depending on the place where water will be used, it is possible to use reused water for this purpose (e.g., greywater) in order to reduce the environmental footprint and financial impacts of this technique.

Figure 6 : Water misting at Mecca, (Saudi Arabia).



Figure 7 : Creation of a water slide in the soil (Wiegbrug, Amsterdã).



### 2.2.2.3 Implementing urban vegetation

Vegetation, through evapotranspiration, shading of the soil and thermal insulation of the foliage, allows an energy balance with the predominance of latent flows, which helps to humidify the surrounding air and prevents extreme temperatures (GIVONI, 1991, WILMERS, 1991). In addition, the leaf area index of the vegetation can reach several times the surface area of the soil that it shades, due to the different leaf layers, thus amplifying the benefits.

There are several ways to promote urban vegetation, such as gardens, parks, green lanes on highways, trees in the streets and implementation of green walls and roofs in buildings. Green roofs, as shown in Figure 8, promote the possibility of stimulating innovative forms of urban agriculture by combining food production, design of harmonious urban landscape, reuse of local organic materials (from vegetation maintenance), reuse of greywater (from bathrooms) and yellow water (urine), as sources of water and nutrients for large-scale plants production near consumers, stimulating global food security (BOER, 2018; GRARD, 2015).

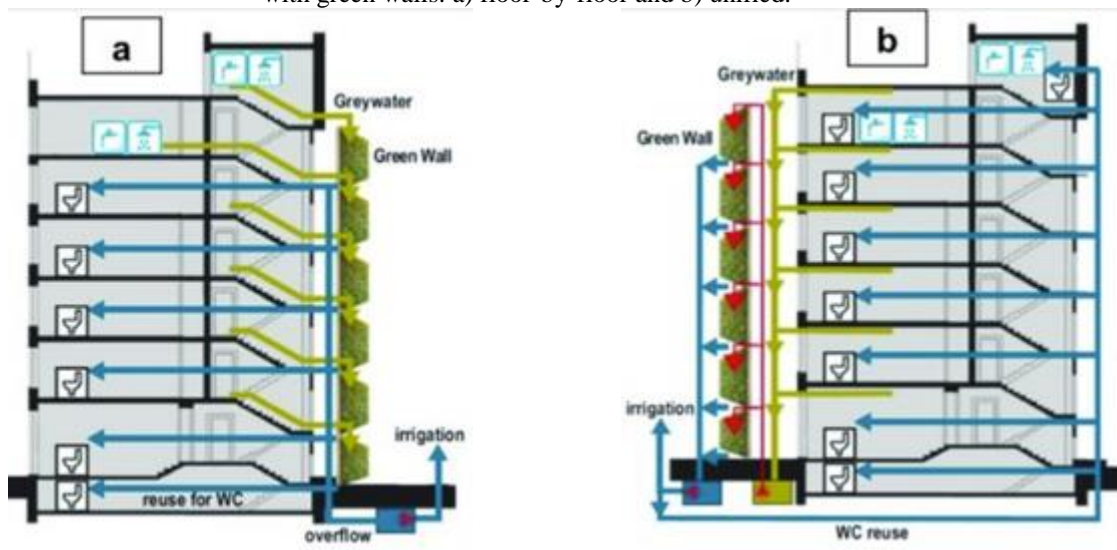
Figure 8: At 55,000 square feet, Higher Ground Farm is the second largest rooftop farm in the US. Topping the Boston Design Center.



Source: <sustainablebusiness.com>.

Moreover, green walls as living ecosystems, in which practically the same processes take place as in a constructed wetland, make it possible to use this system as an efficient form of wastewater treatment, mainly greywater, which represents 70% of the total wastewater produced in a residential building (MASI et al, 2016). Thus, systems such as the one illustrated in Figure 9, can be employed as an innovative way to optimize the benefits of implementing plant walls.

Figure 9 : Possible implementation schemes for greywater collection, treatment, and reuse in the same building with green walls: a) floor-by-floor and b) unified.



Source: MASI et al, 2016.

The process of greening surfaces offers an alternative to introduce vegetation into the cities by using the area of buildings. In many cases, roofs and walls are unutilized spaces, but they have a direct influence on the internal and external environment of the building and the resulting temperature (DJEDJIG, 2013).

Along with the micrometeorological benefits of implementing green walls and roofs in cities, green walls can also promote benefits in hydrology and ecology and to the community. The presence of vegetation can lead to a significant improvement in air quality through fixation of pollutants (particles, aerosols), reducing the occurrence of respiratory diseases (NOWAK, 2006). Green walls are also aesthetically pleasing and can affect our mood and well-being, by

offsetting some of the stress of city living (HERZOG, 2008). Moreover, green walls could help cut the amount of noise that enters buildings. Their influence on urban ecology comes from the fact that the presence of green areas promotes the biodiversity of the region with greater species diversity, genetic diversity and ecosystem diversity (MILLER, 2007). In terms of hydrology, green walls can promote a delay in the beginning of runoffs due to the absorption of water by the substrate and its drainage systems (BENGTSSON, 2005). They also decrease the total runoff in the city, as a part of it is retained and evaporates.

Despite all the benefits and savings of greening cities, public and private sectors give low priority to environmental issues. This scenario becomes even more complex as scientific indications show that vegetation must be well distributed throughout the city for its environmental benefit to be effective, since parks and small areas of vegetation are only effective locally and investments in this practice must be larger (GIVONI, 1991). Another challenge of implementing green walls and roofs is the search for alternatives that reduce installation costs and the need for several artificial components. According to Ottel  et al (2011), the design, transportation, specialized assembly and maintenance of the system, make the ecological footprint of these systems quite high.

#### 2.2.2.3.1 Green roof

Green roofs use plants to improve roof's insulation performance or appearance, or both. They consist of vegetation and growing medium ("substrate"), and could also be referred as a roof garden in some situations. They can be classified into three types: intensive, semi intensive and extensive. The main differences between these three types of green roofs are summarized in the Table 1:

Table 1 : Types of green roofs..

<b>Types</b>	<b>Extensive</b>	<b>Semi-intensive</b>	<b>Intensive</b>
Use	Ecological Landscape	Garden/Ecological Landscape	Garden/Park
Type of vegetation	Moss-Herbs-Grasses	Grass-Herbs-Shrubs	Lawn/Perennials, Shrubs, Trees
Benefit	W,T,B	W,T,B,A	W,T,B,A
Depth of Substrate	60-200mm	120-250mm	150-400mm
Weight	60-150 kg/m <sup>2</sup>	120-200 kg/m <sup>2</sup>	180-500 kg/m <sup>2</sup>
Cost	Low	Periodic	High

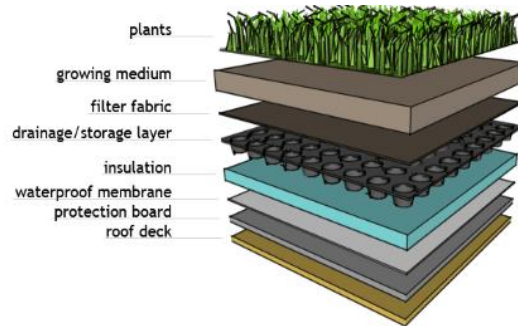
Legend: W= Water, T= Thermal, B= Biodiversity, A= Amenity

Source: European Federation Green Roofs & Walls (EFB)

In general, extensive green roofs have the advantage of lower implementation costs, they do not necessarily require irrigation and maintenance is minimal, as it requires a simple system with low technology employed. However, intensive green roofs have more advantages in terms of greater contribution to urban climate and biodiversity, as well as more social, recreational and agricultural benefits (EFB, 2019).

A green roof is an engineered system that must meet basic roofing requirements. As shown in Figure 10, the system must have layers that protect the building from leaks, to allow excess water drain, retain sufficient water to support vegetation, prevent plant roots from penetrating the roof membrane and in some cases, they also insulate the building (KAMARULZAMAN, 2014).

Figure 10: Basic components of typical Green Roof.

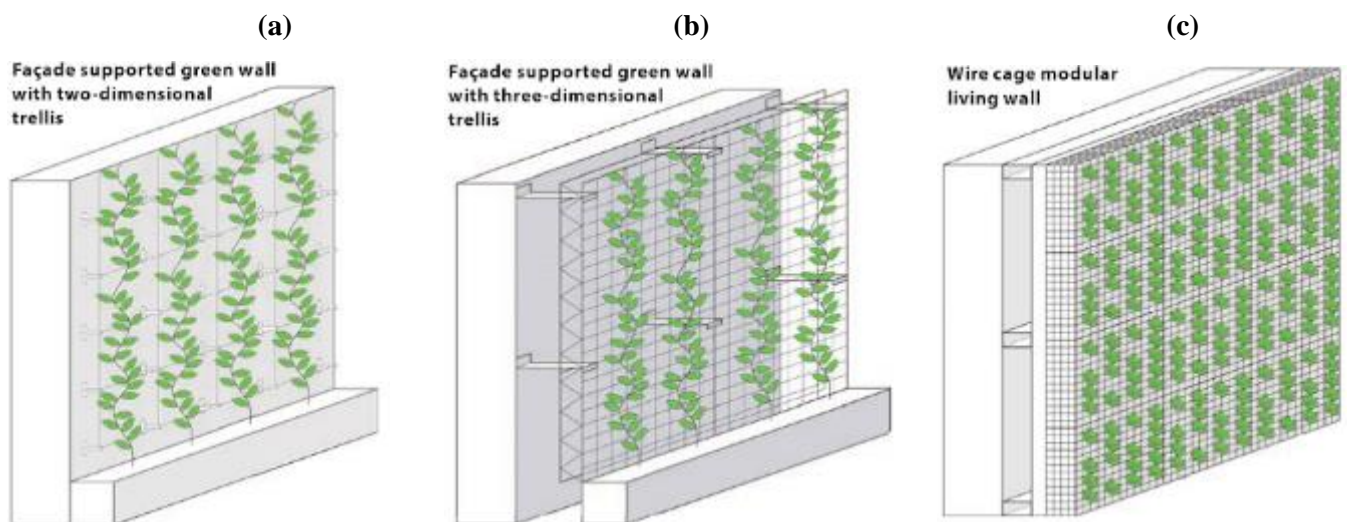


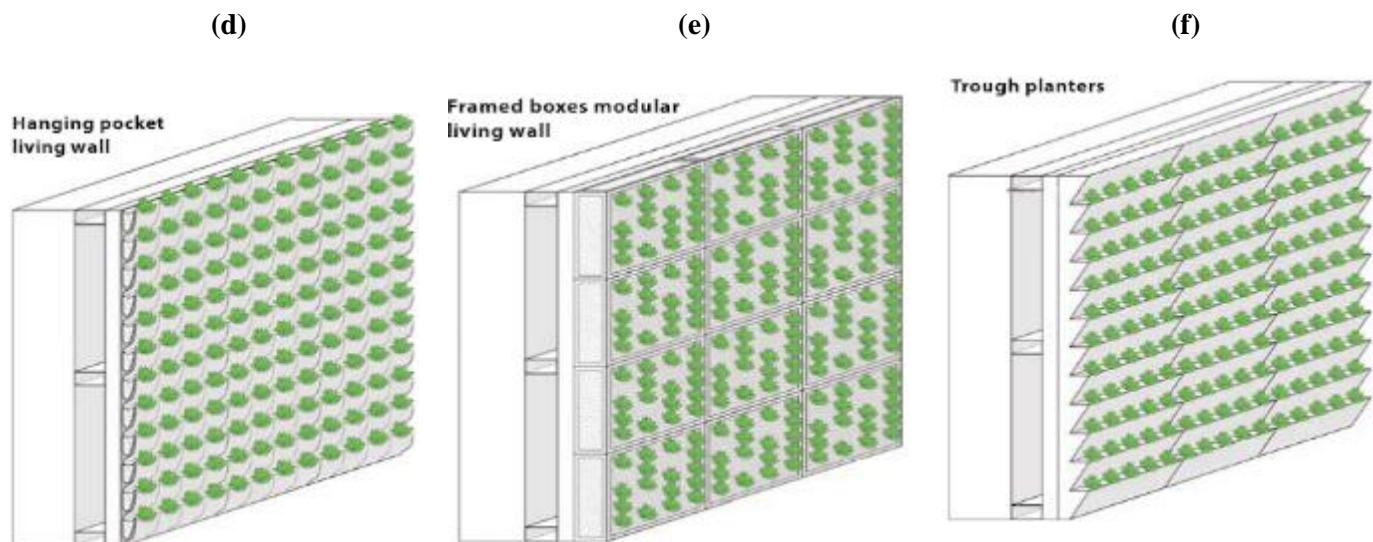
Source: KAMARULZAMAN, 2014.

### 2.2.2.3.2 Green wall

Green wall is a way of describing all types of vertical vegetation. There are different techniques for implementing a green wall, as illustrated in Figure 11. They can mainly be classified into two types: façade greening and living walls.

Figure 11 : Diagrammatic representation of varying types of green walls.





Source: WOOD et al, 2014.

The category of façades greening corresponds to the traditional configuration of this sort of technology, and it is based on the use of creepers with the capacity of autofretage or supported by supports located close to the wall. This technique is economical and easy to apply as plants rooted in the soil or in containers grow freely and derive their support (Figure 11, types “a” and “b”). The limitations of the practice are related to the vertical range of the vines, the very slow growth rate, and possible problems with infiltration and physical damage to the building, in cases where the wall is not adequately protected (WOOD, 2014; CAETANO, 2014; DJEDJIG, 2013).

Living walls are considered the most modern systems, as they use an innovative premise of adding growth media directly to the vertical surface, releasing plants from direct soil dependence. To make this possible, the system incorporates a technical scheme of modular containers with a rooting growth medium or porous surfaces (felts, sponges, plates and fibrous webs), as shown in Figure 11 types “c”, “d”, “e”, “f” and “g”. As this volume of substrate in living walls is generally very limited, it means that its functioning in semi-hydroponic, requires controlled irrigation to supply water and nutrients to plants (DJEDJIG, 2013).

Implementing living walls instead of greening façades has the following advantages: i) they offer a greater thermal insulation due to their different layers; ii) they have virtually no expansion limits, which prevents damage to the building structure due to the independence of the masonry; iii) they also activate an immediate visual effect, allow the use of a wide variety of ornamental plants, facilitate the installation and replacement process with modular functionality, and allow the creation of decorative murals (CAETANO, 2014).

### 2.3 MODELING THE THERMAL EFFECTS OF PLANTS IN CITIES

The UHI is a phenomenon directly linked to the city's morphology and weather conditions. From the energy balance per unit area present in Equation 1 (TAHA, 1997), it is possible to establish that the main causes of UHI are: reduced evapotranspiration (L), increased net



radiation ( $R_n$ ), increased thermal storage ( $\Delta G$ ), low convection ( $S$ ) and the anthropic heat ( $Q_a$ ) (GARTLAND, 2008).

$$R_n + Q_a = S + L + \Delta G \quad (\text{Equation 1})$$

Where:

$R_n$ : The net radiative flux. It corresponds to the radiative flux absorbed, all wavelengths combined;

$Q_a$ : The anthropogenic flux. It corresponds to heat produced by all human activities;

$S$ : The sensible heat flow. It corresponds to convective heat transfer (vertical) or advection (horizontal);

$L$ : The latent heat flow. It corresponds to evaporation produced by surface water, vegetation and permeable surfaces;

$\Delta G$ : The energy stored or restored by building materials.

Therefore, considering the predominance of buildings in the large urban centers, improving their energy performance is essential for sustainable urban development. The use of innovative materials, such as green envelopes in buildings, has been studied as an alternative to reduce both directly and indirectly the effects of high heat and aridity on urban microclimates. Table 2 shows the results of studies on the effect of different envelopes in buildings to attenuate the effect of UHIs. Due to the complexity of the system involved in calculating the climate effect of vegetation in the urban microclimate and the simplifications adopted, most models were validated through experimentation.

Table 2: A review of the cooling effect of different urban envelopes in an urban canyon (space above the street and between the buildings)

Reference	Method	City	Software	Reduction in an urban canyon temperature (K)
Alexandri et al, 2008	Roofs and walls with vegetation	Riyadh	C++, ECOTECH and CFD	9
Saneinejad et al, 2012	The drying process of a wet porous surface	Zurich, Switzerland	ANSYS Fluent, BE-HAM, RAD	4
Sodoudi et al, 2014	Vegetation and green roofs	Tehran, Iran	ENVI-met	1
Djedjig et al, 2015	Green wall	La Rochelle, France	Python, TRNSYS	3
Gagliano et al, 2017	Roofs and walls with high albedo	-	ANSYS Fluent	1
Zhang et al, 2017	Green roof	Jinan, China	PHOENICS	-
Ali et al, 2018	Green roof	Wuhan, China	ENVI-met	1 - 2

An-Shik et al, 2015	Augmented tree/grass coverage ratios of 4.3/21.8%.	Taipei, Taiwan	ANSYS Fluent	2
Pastore et al, 2013	Integration of plants with the built environment	Palermo, Italy	ENVI-met and EnergyPlus	3
Ambrosini et al, 2014	Green roof	Teramo, Italy	ENVI-met	8
Zhang et al, 2019	Independent vegetation spaces	Seoul, South Korea	ANSYS and C	1
Spangenberg et al, 2008	Incorporating street trees	São Paulo, Brazil	ENVI-met	1
De Munck, 2013	Vegetation and green roofs	Paris, France	MESO-NH and TEB	0.5 - 3

Source: Author, 2020

From the studies developed on the interactions between the surface of cities and the urban microclimate, we can infer that:

- The most effective scenario in the process of reducing the temperature inside an urban canyon occurs when the green wall and roof are applied to the building structure together (ALEXANDRI et al, 2008). However, the wall alone has a greater impact both on reducing the temperature inside the canyon and on the structure of the building compared to the green roof (DJEDJIG, 2013). On the other hand, the green roof influences more directly the higher altitudes of the building, but has little influence on the canyon and the building as a whole (ZHANG et al, 2017).
- The warmer and drier the climate, the greater the effect of vegetation is on attenuating urban temperatures (SODOUDI et al, 2014; DJEDJIG, 2013; ALEXANDRI et al, 2008).
- The morphology of the city, which is characterized by high roughness, tends to decrease wind speed in the lower layers of the city. Since convection is directly linked to wind speed, this decline in wind speed decreases convection and accentuates thermal storage in urban centers, resulting in higher surface temperatures (JACOBSON, 2005).
- In addition to measured temperature, there are studies that analyze the thermal comfort indices. The use of thermal comfort indices helps in understanding the thermal perception of users of open spaces. Among them PET (Physiological Equivalent Temperature) is an index based on the thermal balance of the human body, which indicates the effects of the thermal environment in terms of thermal stress for heat/cold and comfort (KRUGER, 2018).

Also, the previous studies presented in Table 2 on the effect of green cover in cities to reduce extreme temperatures, show that depending on the type of vegetation used and the climatic characteristics of the city, the attenuation of the temperature in the urban centre can be from 0°C to 9.1°C. Zhang et al (2017) studied the influence of green roof on exterior surface temperature taking a residential area in Jinan (China) as an example and using the PHOENICS software to establish three-dimensional building model and simulates thermal environment

under the different green conditions. Jinan is a city characterized by a long, hot, humid summer, with precipitation and partially covered skies; the winter is very cold, dry and with almost no clouds. The main conclusions of the Zhang et al (2017) study were that from the height of the pedestrian line at 1.5m, the setting of ground greening lawn is helpful to alleviate outdoor high temperature, and the range of temperature reduction is about 2~4°C. In addition, they pointed that the green roof has little influence on the temperature distribution at outdoor pedestrian height.

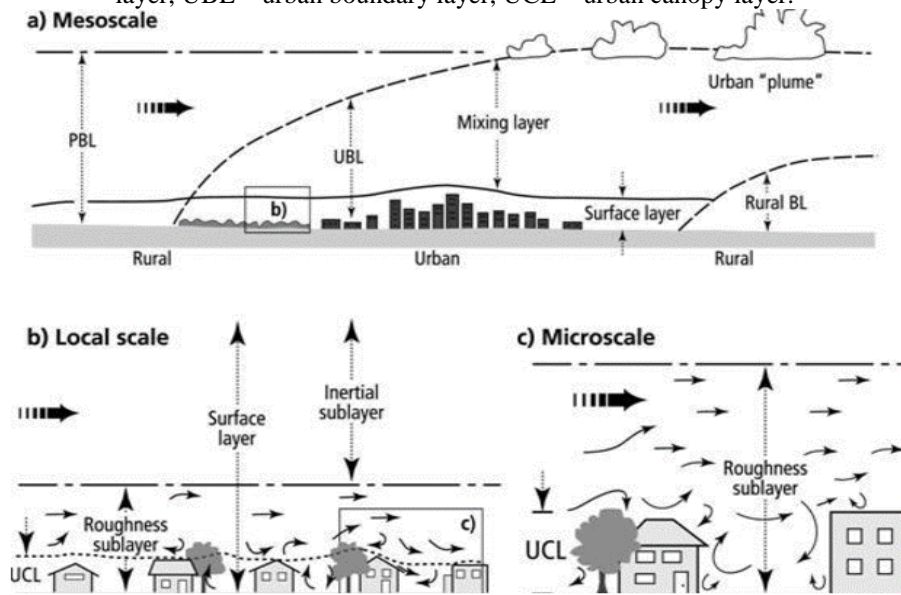
On the other hand, Alexandri et al (2008) used as a methodology a two-dimensional, prognostic (dynamic) micro-scale model developed and programmed in C++, to describe heat and mass transfer in a typical urban canyon, ECOTECH software for radiative calculations and a CFD code (WinAir4) for the simulation of air transport. From this research, it was concluded, when both walls and roof are covered with vegetation, that a city like Riyadh (hot and dry) has a maximum temperature decrease up to 11.3°C and Hong Kong (humid) has maximum temperature decrease up to 8.4°C.

Therefore, seeing all the aspects that can be considered in the practice of urban vegetalization and the variability of efficiency in reducing the temperature in cities displayed in the literature, it is important to develop tools to help decision-making for its implementation. As experimentation is long and expensive, a first approach through simulation is of interest.

### **2.3.1 Scale of study**

In urban areas, there are different microclimatic scales that are defined within the planetary boundary layer (the lowest part of the atmosphere) whose behaviour is directly influenced by friction effects denoting its "contact" with the planetary surface. As shown in Figure 12, there are three scales of interest: the mesoscale, the local scale and the microscale (OKE, 2006). In these different scales, the characteristic (also "effective" or "phenomenological") roughness corresponds to the average height of the obstacles (formed by the buildings and trees, for example) typically associated with maximum flow mixing thus energy dissipation near roughness crests. More generally, turbulence mixes gradients of momentum, energy (including air temperature), moisture, gases and particles vertically and horizontally (JACOBSON, 2005).

Figure 12: Schematic of climatic scales and vertical layers found in urban areas. PBL – planetary boundary layer, UBL – urban boundary layer, UCL – urban canopy layer.



Source: OKE, 2006.

According to Figure 12, we can highlight the presence of the urban boundary layer (UBL), the canopy layer (UCL) and the surface layer. In the surface layer, there are two sublayers: the inertial sublayer, where vertical velocities thus mixing are expected to be negligible, and the roughness sublayer, that is the range at which the specific (thermal and aerodynamic) influence of each obstacle in the city can be felt. The flow characteristics of these sublayers are mainly influenced by wind and the so-called footprint (soil zone most affected for example by amount of heat and concentration carried by turbulent wind, MESTAYER et al, 2011).

Figure 13 shows the average wind profile in an urban canopy without large buildings or obstacles. Wind speeds vary in time and space, constantly interacting with the city's morphology. In the UCL zone, the wind velocity profile will decrease when getting closer to the building surface, and is represented by an exponential form (BRITTER et al, 2003). The representation of the wind velocity, scaled between the (constant) building height is shown in the Equation 2, and becomes from an extension of Cionco (1965) model for the velocity profile within a vegetative canopy and Macdonald (2000) laboratory experiments that insert the parameter required to describe the urban canopy in the equation  $\lambda f$  (shear stress profile).

$$\frac{u}{u_{Hr}} = \exp[-9,6 \lambda f (1 - \frac{z}{hr})] \quad (\text{Equation 2})$$

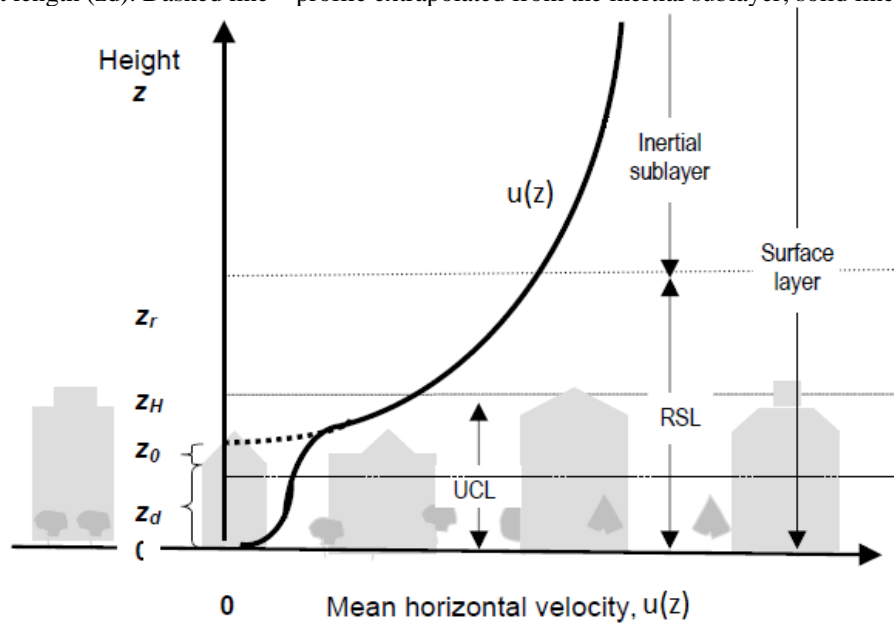
This approach (Equation 2) is simple and describes the laboratory experiments well; however, it does rely on knowledge of the wind speed at the building height (the height at which the velocity profile is changing most rapidly), which may not be easily defined (BRITTER et al, 2003).

On the other hand, in the inertial sublayer it is possible to apply the Monin-Obukhov similarity theory that represents the wind velocity with the Equation 3:

$$u(z) = \frac{(u^*)}{\kappa} \left\{ \ln\left[\frac{z-z_d}{z_0}\right] + \Psi_m\left(\frac{z}{L_o}\right) \right\} \quad (\text{Equation 3})$$

Where  $u^*$  is the friction velocity,  $\kappa$  is von Karman's constant (0.41),  $z_0$  is the surface roughness length,  $z_d$  is the zero-plane displacement height,  $L_o$  is the Obukhov stability length, and  $\Psi_m$  is a dimensionless function that accounts for the change in curvature of the wind profile away from the neutral profile with greater stability or instability (OKE, 2006) .

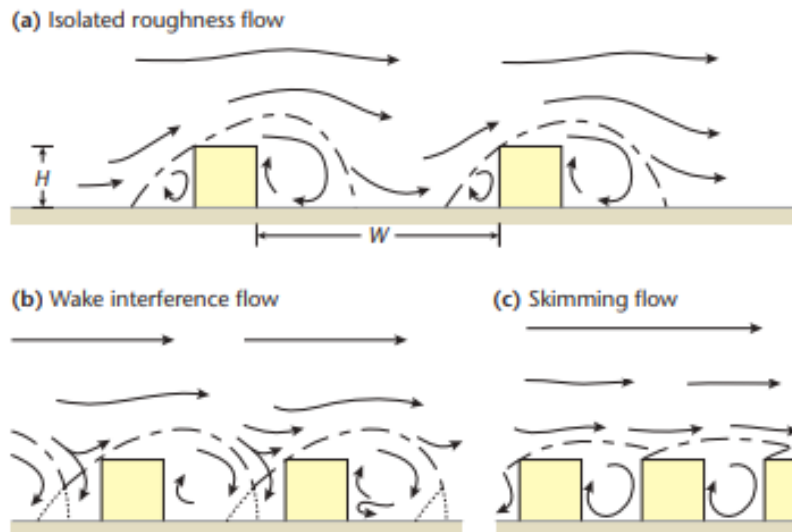
Figure 13 : Generalized mean (spatial and temporal) wind velocity ( $u(z)$ ) profile in a densely developed urban area including the location of sublayers of the surface layer. The measures on the height scale are the mean height of the roughness elements ( $z_H$ ), the roughness sublayer ( $z_r$ , i.e. the "blending height" at which the individual influence of each building ceases to be recognizable), the roughness length ( $z_0$ ) and zero-plane displacement length ( $z_d$ ). Dashed line – profile extrapolated from the inertial sublayer; solid line - actual profile.



Source: OKE, 2006.

Among all the scales analyzed, the smallest one is that of the street and the street canyon mentioned in Table 2, the elementary unit of the system. The understanding of this lower scale is necessary to understand the phenomena that occur on larger scales. Units of street delimited by two continuous rows of buildings are known as street canyons. This geometry is often described by the canyon aspect ratio ( $H/W$ ), which is defined as the ratio of the building height ( $H$ ) to the width of the space between buildings ( $W$ ). This morphological parameter is directly governing its ability of capturing solar radiation and promoting/combating aerodynamic confinement within the canyon. In a canyon street, taking into account the period of the day without shadow in the canyon, the absorption of solar energy becomes more important as the  $H/W$  ratio increases (AIDA, 1982). Depending on the wind direction, its intensity, and the  $H/W$  aspect ratio, the nature of the air flux may vary. According to Oke et al (2017), as shown in Figure 14, there are three types of flow, which depend on the aspect ratio, in areas of reasonably uniform building height and when the airflow in the urban boundary layer is approximately normal to street axis: (a) isolated roughness flow (wide streets,  $H/W < 0,35$ ); (b) wake interference flow ( $0,35 < H/W < 0,65$ ) ; (c) skimming flow (generation of a vortex inside the canyon,  $H/W > 0,65$ ).

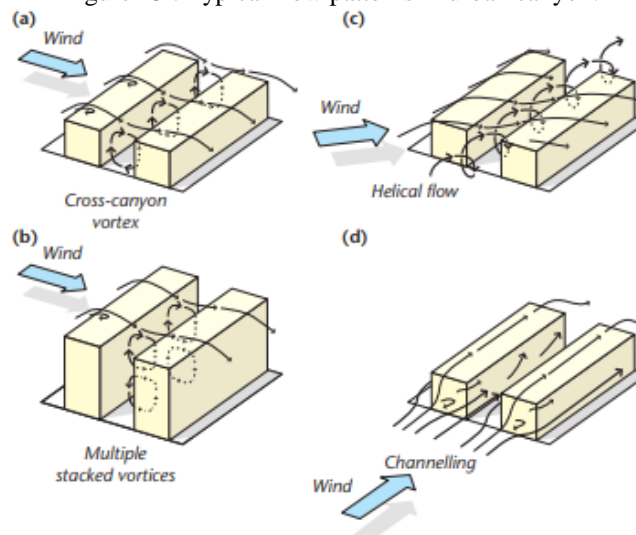
Figure 14 : Effect of packing density ( $H/W$ ) on flow regimes over urban-like ‘building’ arrays in a wind tunnel.



Source: OKE et al, 2017 (Modified after: Oke, 1988 constructed using data of Hussain and Lee, 1980)

Taking into account the streets and interceptions, it is possible to classify the typical flow patterns in urban canyons. Figure 15 shows the four types of flow patterns that is driven by the above-roof wind, especially its horizontal direction relative to the axis of the canyon (angle-of-attack,  $\phi_c$ ): (a) cross-canyons vortex ( $\phi_c = 90^\circ$ ), (b) multiple stacked vortices in a deep canyon ( $\phi_c = 90^\circ$ ), (c) helical flow along a canyon ( $\phi_c \sim 45^\circ$ ), (d) along channeling and jetting along a canyon ( $\phi_c < 30^\circ$ ).

Figure 15 : Typical flow patterns in urban canyon.

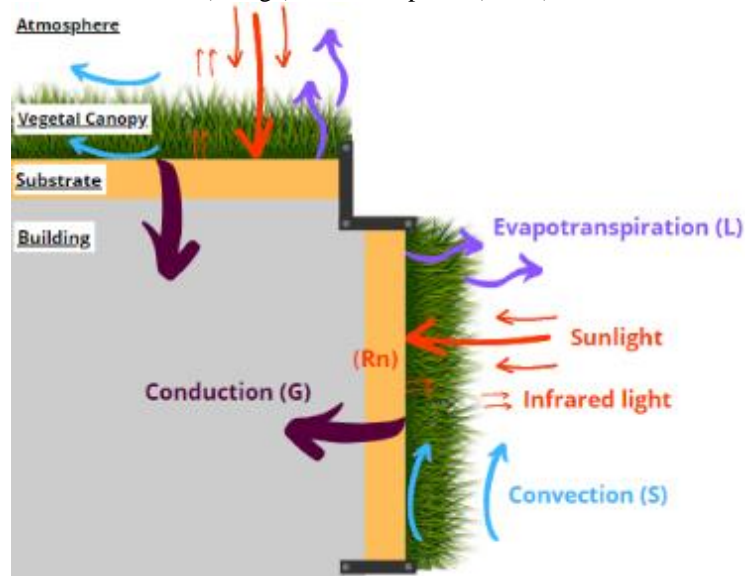


Source: OKE et al, 2017 (Modified after: Oke, 1997; Belcher, 2005).

### 2.3.2 Plant, substrate and atmosphere

The study of the impact of green walls and roofs on the temperature of an urban microclimate demands to analyze the thermal and hydraulic exchanges between building, vegetal canopy and atmosphere approached by Djedjig (2013). For this, the dominant thermal and water transfer phenomena must be considered. Figure 16 shows in a simplified way the order-1 mechanisms of mass and heat transfer between the layers of the system.

Figure 16 : Mechanisms of mass and heat transfer between building (grey), vegetal canopy (green), substrate (orange) and atmosphere (white).



Source: Author, 2020.

The mechanisms involved are convection (sensible heat exchange by water or air displacement), phase change through evapotranspiration (latent heat exchange), conduction (heat exchange by contact and without particle displacement, from/to the building), radiative exchange (related to sun exposure) and liquid water transfers within the substrate and plants. We can infer that beside drip irrigation within the substrate, all "natural" mass and heat transfer mechanisms are directly linked to the weather conditions (e.g., wind and solar radiation intensity and direction), the physical properties of the materials involved (e.g., thermal conductivity, specific heat, albedo, emissivity, water content) and the biological properties (e.g., water stress and plant growth which dissipate energy intercepted by solar rays through evapotranspiration).

Taking into account the complexity of the processes involved in this system, different models are proposed in the literature to calculate the heat transfer between vegetation, buildings and the atmosphere. They use different simplifications that facilitate the approach, depending on the type of model that is intended to be used and parameters focussed. There are two main types of approaches with dedicated targets: one is the study of green envelopes effects on the attenuation of temperatures inside buildings, and the other one is the study of green envelopes effects to mitigate the temperature inside urban canyons. In Section 3 of this work, we present the methodology of the monography, focusing on this second type of approach and its mechanisms in detail, as well as on the relevant spatial scales, simplifications and assumptions done to build a first candidate model.

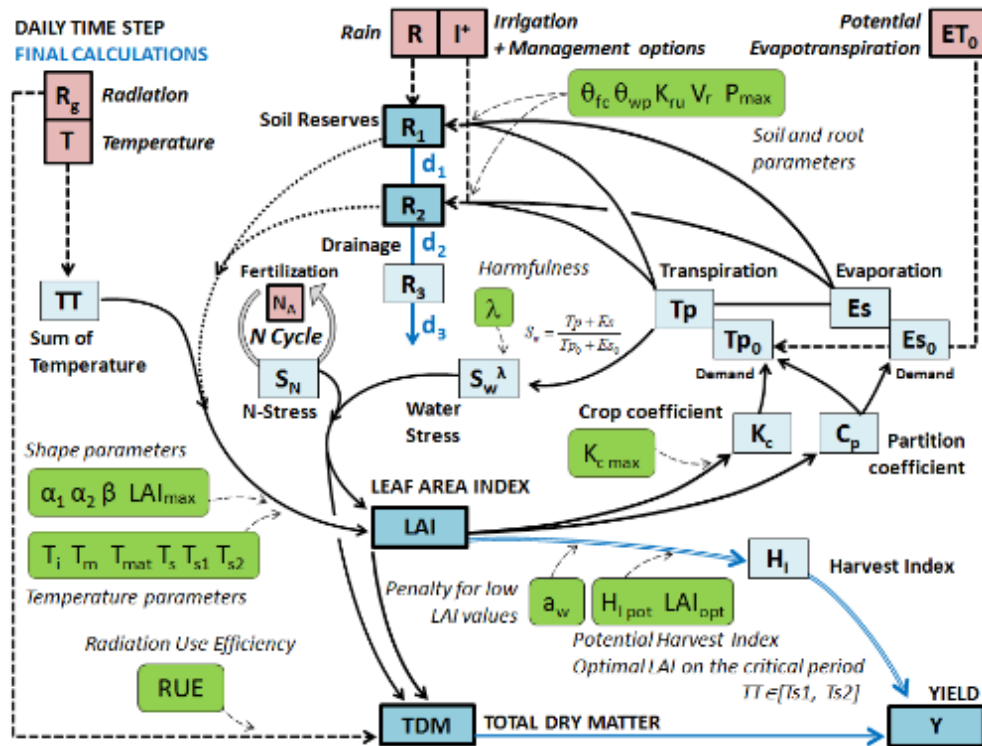
## 2.4 SUMMARY OF TOOLS USED TO CONDUCT THIS STUDY

### 2.4.1 Optirrig

Optirrig aims at the generation, analysis and optimization of irrigation scenarios for various crops cultivated in classical field conditions. It relies on "as simple as possible"

agronomic calculations whose principles appear in Figure 17 and puts the effort on deciphering relevant irrigation strategies within constrained optimization limits (e.g. limited water availability vs. objectives of minimal crop yield and profitability). Mailhol et al. (1997, 2011) describe this model in details.

Figure 17 : Principles of the Optirrig model. Climatic forcings appear in rose, parameters in green, main state variables in medium blue and auxiliary variables in light blue cells (see text for details).



Source : Cheviron et al, 2016.

Model forcing's are radiation, air temperature, rain and potential evapotranspiration, plus the irrigation strategy and additional site management parameters, as for example the sowing date.

Model key variables are water reserves in the subsurface (R1) and the variable-depth root-zone (R2), Leaf Area Index (LAI) development and Total Dry Matter (TDM) accumulation.

Model auxiliary variables are the sum of temperatures over zero vegetation value (TT), the crop (Kc) and partition (Cp) coefficients, the potential (ES0, TP0) and actual (ES, TP) evaporation and transpiration, water (Sw) and nitrogen (Sn) stresses, and eventually water reserve in the deep reservoir (R3).

The most crucial role is played by LAI which is the main proxy of crop growth and status, being a function of both water availability and thermal time, then in turn controlling the production of biomass as well as the values of the crop and partition coefficients, taken as functions of LAI.

Model parameters fall in several groups with distinct roles: shape and temperature parameters dictate the form of the LAI curve with increasing thermal time; radiation use efficiency controls biomass production which also depends on radiation interception as a



function of LAI (see arrow between LAI and TDM), there is a maximal value for the crop coefficient ( $K_{cmax}$ ) and there are characteristic values for the parameters of the water budget: field capacity ( $\theta_{fc}$ ), permanent wilting point ( $\theta_{wp}$ ), limit of the easily available water reserve ( $r_{kru}$ ), maximal root growth rate ( $V_r$ ) and maximal root depth ( $P_{max}$ ).

### 2.4.2 ANSYS Fluent

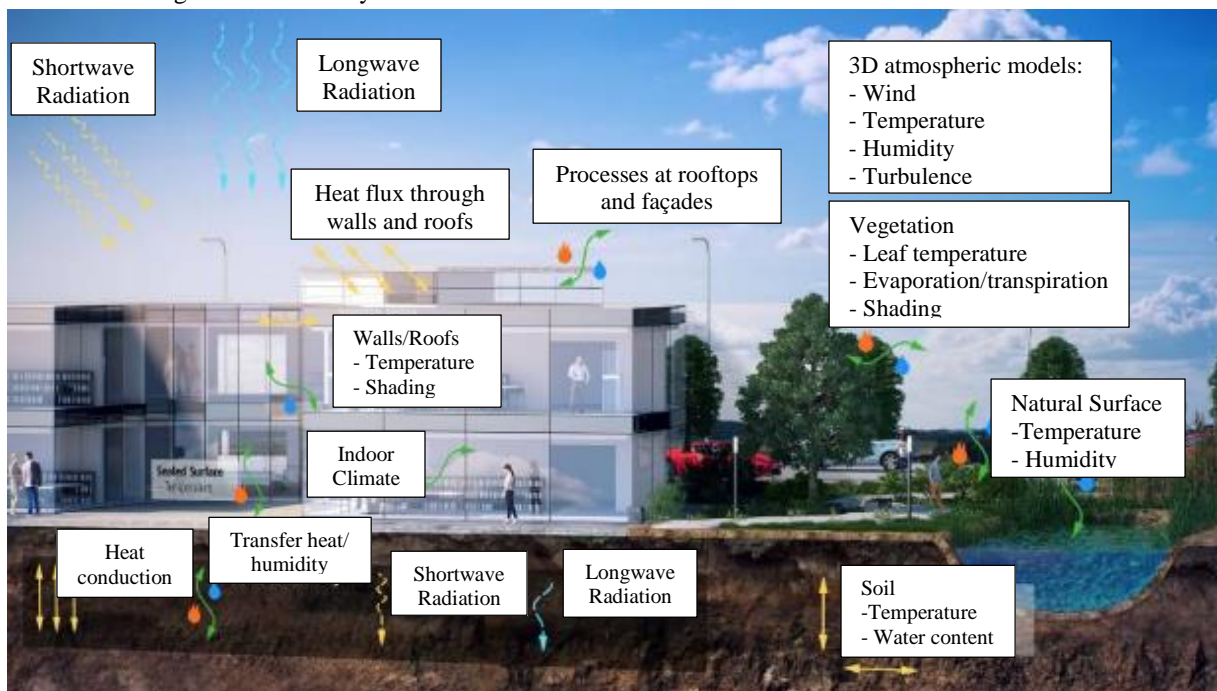
ANSYS is an engineering simulation software that allows calculations in several areas among them: structures mechanics, fluid flow, thermal transfers, electromagnetics, topology optimization, fluid-structure interaction, fluid-solid heat transfer, polymer extrusion, geometry modeling.

In this project, ANSYS Fluent was used, which is a Computational Fluid Dynamics (CFD) simulation tool that adopted the finite volume method and a high-precision algorithm, which is more selective for the turbulence models and whose mesh can be freely adjusted to meet all kinds of simulation including at small scales. The software was selected to start the analysis of green walls and roofs climatic effects in an urban environment, to evaluate the attenuation of an UHI thanks to vegetation.

### 2.4.3 ENVI-met

“ENVI-met V4 is a holistic three-dimensional non-hydrostatic model for the simulation of surface-plant-air interactions not only limited to, but very often used to simulate urban environments and to asses the effects of green architecture visions” (ENVI-met, 2020). With a typical horizontal resolution from 0.5 to 10 m and a typical time frame of 24 to 48 hours with a time step of 1 to 5 seconds, the model is designed for microscale analyses (Figure 18).

Figure 18 Thermodynamic interactions between the built and the natural environment



Source: Adapted from ENVI-met, 2020

As presented in the Figure 18, the model calculation includes:

- Shortwave and longwave radiation fluxes with respect to shading, reflection and re-radiation from building systems and the vegetation;
- Transpiration, evaporation and sensible heat flux from the vegetation into the air including full simulation of all plant physical parameters (e.g. photosynthesis rate);
- Dynamic surface temperature and wall temperature calculation for each facade and roof element supporting up to 3 layers of materials and 7 calculation points in the wall/ roof;
- Water and heat exchange inside the soil system including plant water uptake;
- 3D representation of vegetation including dynamic water balance modelling of the individual species;
- Dispersion of gases and particles;
- Calculation of biometeorological (Mean Radiant Temperature, PMV/PPD, PET or UTCI);
- Atmospheric model: Wind field ENVI-met includes a full 3D CFD model. It solves the Reynolds-averaged non-hydrostatic Navier-Stokes equations for each grid in space and for each time step. The effects of vegetation are included as drag forces in the wind field. For detailed building physics simulation, the wind flow close to each facade and roof segment is calculated;
- Turbulence: E-epsilon 1.5 order closure (“E-epsilon” or “k-epsilon” model). Two prognostic equations for turbulent energy production and its dissipation (epsilon) are used to simulate the distribution of turbulent energy. Exchange coefficients in the air are calculated using the Prandtl-Kolmogorov relation. For low wind situations, the 1st order mixing length model can be used instead of the E-epsilon model (which often fails in this situations).

Several studies use ENVI-met to investigate the influence of site parameters for thermal comfort study and urban design (SODOUDI et al, 2014; ALI et al, 2018; PASTORE et al, 2013; AMBROSINI et al, 2014 ; SPANGENBERG et al, 2008). Overview articles of microclimate tools for predicting the thermal comfort and design strategies in outdoors spaces indicate ENVI-met as one of the most suitable tools for this kind of analyses (ALBDOUR et al, 2019; SUNARYA, 2020). However, this program has some limitations, such as only generate validated results of microclimate data for 24 to 48 h in each simulation and it takes a long time when running the simulation depending of the study zone extension, grid resolution and computational resource which limits the possibility of testing different analysis configurations and periods (RAMESH, 2017).

There are four version of ENVI-met, with different features, as show the Table 3.

Table 3 ENVI-met features.

All Features	LITE (Beginners, Testing)	STUDENT (Students, PhD)	SCIENCE (Universities)	BUSINESS (Architects, Urban Planners and other professional Users)
License Type	No number of seats	Up to 2 seats	Volume license	Up to 5 seats
Commercial Use	×	×	×	✓

Model Size	50x50x40	unlimited	unlimited	unlimited
Full 3-D Microclimate Model	✓	✓	✓	✓
Complete Software Environment	✓	✓	✓	✓
Parallel Simulation on Multiple CPU Cores	✗	✗	✓	✓
Detailed Analysis of Building Energy Parameters	✗	✓	✓	✓
Detailed Building Physics (Facade Temperatures and Energy Fluxes, Microclimate at Facade)	✗	✓	✓	✓
Roof and Facade Greening	✗	✓	✓	✓
Simulation of Blue Technologies (Water Spray, Wet Surfaces)	✗	✓	✓	✓
Full Forcing	✗	✓	✓	✓
Multi-Pollutant Dispersion with Chemistry	✗	✓	✓	✓
High-Resolution Radiation Modelling with IVS	✗	✓	✓	✓
NetCDF Outputs	✓	✓	✓	✓
BIO-met	✗	✓	✗	✓
Personal Support via e-mail	✗	✗	✗	✓

Source: ENVI-met, 2020.

#### 2.4.4 Vensim

Vensim is industrial-strength simulation software for improving the performance of real systems. It emphasizes model quality, connections to data, flexible distribution, and advanced algorithms. Its development is based on the fact that each variable is defined by data and parameters, a parameter could come from the definition of another variable. Simulations take place at different temporal scales to highlight complex interactions between simple variables. Such tool is interesting to analyze the sensitivity of circular economy loops and point their weakness and strength.

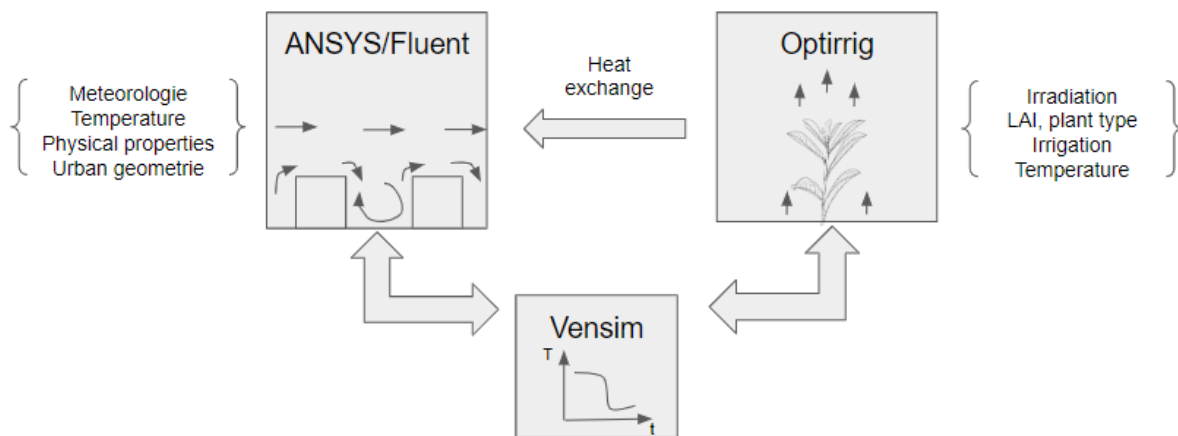
### 3. METHODOLOGY

The bibliographical review allowed us to compare numerous simulation tools to select the most appropriate for this study. The project aimed at using the Vensim software, like the Enlarge group that this project belongs, to integrate this analysis in a decision-support tool to test different solutions to modify urban metabolism in three aspects: food, water and energy. But after running the first test using Vensim, we noticed that the necessary micro-meteorological description coupling irrigation, plant and building was too complex to be modeled in Vensim. The complexity of the equations that had to be undertaken is not supported by such tool. Therefore, different possibilities were examined to simplify this problematic in

the Vensim program. Thus, came the initial idea Model 1 to couple the ANSYS Fluent software for the mechanical and thermal transfer part with the Optirrig software for the irrigation and plant part. The final step was to build a simulation architecture to perform a temperature sensitivity analysis in the building-plant-canyon system, to evaluate the most significant parameters to be used as an input in the Vensim simulations.

The use of existing programs to model the atmospheric flow (ANSYS Fluent) and the hydraulic and thermal functioning of the crop (Optirrig) allows such an approach to obtain consistent results with fewer simplifications. This approach relies on the use of a modified version of Optirrig that undertakes heat exchange due to the interaction between the plant, substrate and the atmosphere. Then, the data provided by Optirrig are inserted in ANSYS Fluent to evaluate the impact of green walls and roofs on the attenuation of the temperature in a street canyon. ANSYS Fluent will provide the urban aspects more relevant in the system and the outdoors temperatures in the urban canyon and Optirrig the heat exchanges produced by the system building, substrate and plant to be introduced in ANSYS Fluent and as an input parameter in Vensim, as shown in Figure 19.

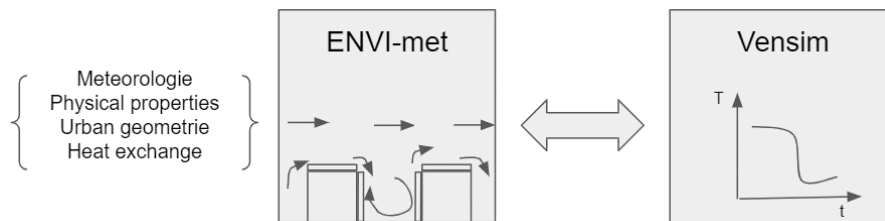
Figure 19 : Schematic representation of the coupled model 1.



Source : Author, 2020.

After this first attempt of modelling (Figure 19) another possibility to simplify the system was evaluated. Model 2 was studied with the support of ENVI-met software, a microclimate model designed to simulate the surface-plant-air interactions in the urban environment. The principle of Model 2 is the same as Model 1, however ENVI-met provided the aspects more relevant in the system and the outdoors temperatures in the urban canyon as an input parameter in Vensim.

Figure 20 : Schematic representation of the coupled model 2.



Source: Author, 2020.

### 3.1 OPTIRRIG

#### Ad hoc adaptations and/or parameterization

- Surface drip irrigation was modeled, to ensure low variations in soil water content and deliver enough irrigation to prevent any water stress, keeping water content slightly beyond field capacity. This was modeled with daily irrigation amounts, either fixed or weekly variable, decided from plant needs as estimated from the  $ET_0$  term (maximal evapotranspiration being estimated from plant characteristics as  $ETM = K_c ET_0$ ). The presence of sensors to monitor soil water status was simulated by using the "adaptive" mode of Optirrig in which irrigations are decided on the basis of a threshold level of soil water reserve (and not from an irrigation calendar). This ended in the form of an approximate apparent permanent regime in terms of soil water status, with no spatial discretization of soil water content.

- "Soil" means here a substrate of a few centimeters of depth and no significant root growth needs to be modeled, which suggests using only the R1 and R2 reservoirs.

- A fixed LAI value of about 2-3 was assumed at first, for systems not aiming at biomass production. Then, this LAI value was used to estimate radiation interception on the one hand, and the potential evaporation and transpiration on the other hand, hypothesizing enough water is present for the plant to satisfy the  $ET_0$  demand (that is, the actual evapotranspiration AET equals the maximal evapotranspiration ETM and potential evapotranspiration  $ET_0$ ).

Hence, an adapted version of Optirrig should be able to provide (i) the AET term that intervenes in the latent heat exchange and (ii) the radiation interception term that is part of the  $R_n$  term through the LAI.

- Still for the sake of simplicity the substrate used for vegetal roofs and walls were represented as rectangular boxes with heat exchanges only in directions perpendicular to the buildings (i.e., vertically for the vegetated roofs and horizontally for the vegetated walls). This reduces the problem to one dimension and assumes that LAI values mentioned above show no spatial patterns or significant heterogeneities.

- Another hypothesis is that the canopy is thin enough for heat storage to be negligible in the vegetal parts of the system (CONVERTINO, 2019).

- Also from literature, the energetic processes of chemical origin associated to photosynthesis are deemed negligible in front of the other energetic processes at play, as is the thermal conduction term in plant stems and structure, in comparison with heat exchange through evapotranspiration (latent heat) and convection (sensible heat), or conduction through the almost saturated substrate and the buildings (SAUDREAU, 2007; DJEDJIG, 2013).

### 3.1.1 Energy balance in the vegetal canopy

The energy balance on the surface of the green wall and roof is represented on Equation 4, Bowen (1926):

$$Rn = S + L + \Delta G \quad (\text{Equation 4})$$

Where:

- Rn : Net Solar radiation ( $\text{W m}^{-2}$ );
- S : Sensible heat flux ( $\text{W m}^{-2}$ );
- L: Latent heat flux ( $\text{W m}^{-2}$ );
- $\Delta G$  : Stored heat flux ( $\text{W m}^{-2}$ ).

Each variable of the energy balance equation will be described in the next sub-sections. This expression indicates that all solar energy absorbed by the green wall and roof system will be divided into three other forms of energy: latent heat, sensible heat and a part will be stored and propagated through the system by conduction.

With the calculation of the energy balance, it is intended to obtain the system's potential of dissipating the energy absorbed by the sun, as well as the physical properties of the layers (e.g., density, specific heat and thermal conductivity), for a given hypothetical situation. These system proprieties are fundamental as input results for the next simulation step in the ANSYS Fluent software.

#### 3.1.1.1 Net Solar radiation ( $Rn$ )

To calculate Net Solar radiation, Optirrig (CHEVIRON et al, 2016) calculates the fraction intercepted by the green wall or roof ( $ir$ ) as a function of LAI that can be approximated in most cases as:

$$ir = \frac{LAI}{(0.5+LAI)} \quad (\text{Equation 5})$$

From Equation 5, it is possible to know what portion of all the radiation received by the plant may actually be absorbed. The fraction that is not intercepted by the foliage is partly reflected, another part goes through the foliage to be absorbed or reflected by the substrate and can once again be intercepted by the lower part of the foliage of the plant or transmitted back to the atmosphere. In this study, the fraction that goes through the foliage is rather weak (~15%) and its effects was not directly accounted for as we focus on first order terms. However, as the "canopy term"  $C_p$  in Optirrig governs the partition between crop transpiration ( $Tp_0$ ) and substrate evaporation (ES0) demands, the effects of radiation interception and transmission affect water budget modelling thus evapotranspiration and the latent heat term.

Thus, if we consider the time of day when the building's façade is not shaded by the nearby building and have a perpendicular radiation in its surface, the net solar radiation in  $\text{W m}^{-2}$  can be established from Equation 6. In this equation, the variable  $I$  ( $\text{W m}^{-2}$ ) is the direct solar radiation perpendicular to the building façade/roof.

$$Rn = I . ir \quad (\text{Equation } 6)$$

In this first simulation of this model, the Equation 6 was used. However, with the interest of inserting in the equation the periods of the day where the wall is exposed to shadow, and the different angles of irradiation, it is necessary to take into account the daily shadow variation on the vegetation to calculate this variable in the energy balance study.

Therefore, for the periods of day when the wall is exposed to interference from shadow of nearby buildings, the net radiation is derived from the incidence of the sun over the day, the distance and height of the neighboring buildings. The Equation 7 can calculate the net solar radiation, in all the surface of the wall. For this, it is necessary to find the value of “Hx”, that is the surface that receives the radiation according to Equation 8 (RIAU et al, 1989).

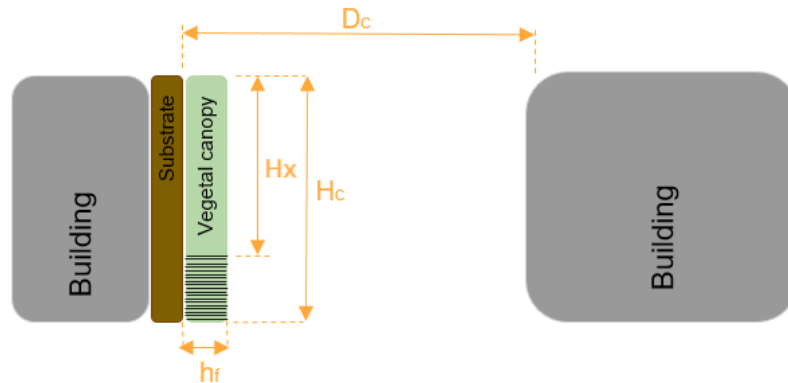
$$Rn = I . ir . Hx \quad (\text{Equation } 7)$$

$$X = \frac{(Dc - Lc)tg(h)}{\cos(a-a')} \quad (\text{Equation } 8)$$

Where:

- a : Azimuth of the sun;
- a' : Angle of the normal to the street plan with the direction North-South facing South;
- h : Sun height (m);
- D<sub>c</sub> : Distance between the two buildings (m), according to Figure 21;
- h<sub>f</sub> : Height of the plant canopy (m), according to Figure 21.

Figure 21 : Geometry of the shadow on a canyon street.



Source: adaptation of RIAU et al (1989)

### 3.1.1.2 Sensible heat flux (S)

Sensible heat flux is a consequence of the heat exchange between materials, which generates temperature variation of the same by convection. One of the possible equation to calculate sensible heat flux is given by Verma (1989) and its "compatibility" with Optirrig is discussed in the following:

$$S = p_a \cdot c_{p,a} \cdot \frac{(T_f - T_a)}{r_a} \quad (\text{Equation 9})$$

Where:

- $p_a$  : Density of air at constant pressure ( $\text{kg m}^{-3}$ );
- $c_{p,a}$  : Specific heat of the air at constant pressure ( $\text{J kg}^{-1}\text{K}^{-1}$ );
- $T_f$  : Effective surface temperature (K);
- $T_a$  : Ambient air temperature (K);
- $r_a$  : Aerodynamic resistance (Monin Obukhov model) ( $\text{s m}^{-1}$ ).

The Equation 9 tells us that the sensible heat depends on the volumetric mass and the thermal capacity of the air, the variation of the material temperature and the aerodynamic resistance provided by the environment in which the system is located.

To calculate  $r_a$ :

$$r_a = \frac{\text{Ln} \left[ \frac{z_u - d_o}{z_{om}} \right] \text{Ln} \left[ \frac{z_u - d_o}{z_{oH}} \right]}{\kappa^2 u} \quad (\text{Equation 10})$$

Where :

- $\kappa$  : constant of Von Karman's (0,41) (SANEINEJAD et al, 2012)
- $u$  : wind speed measured at the distance ( $z_u$ ) of the green wall ( $\text{m s}^{-1}$ )

The lengths of roughness ( $z_{om}$ ,  $z_{oH}$ ) and the height of displacement ( $d_o$ ) are calculated according to the height of the plant canopy ( $h_f$ ) (BALICK et al., 1981).

$$d_o = 0,701 h_f^{0,975} \quad (\text{Equation 11})$$

$$z_{om} = 0,131 h_f^{0,997} \quad (\text{Equation 12})$$

$$z_{oH} = 0,1 z_{om} \quad (\text{Equation 13})$$

In the above terms, only  $T_a$  directly appears as input data or state variables of Optirrig but still there are indirect connections between some of these terms and Optirrig:

- The first possible connection is through wind velocity in the  $r_a$  term, which also appears in the definition of the ET0 climatic demand – but the latter is usually calculated at a daily time step in the Penman-Monteith equation. Therefore, this a loose connection that does not seem to necessitate coherence checks between  $u$  in  $r_a$  and the wind velocity term in ET0, unless hourly ET0 is used.
- The second possible connection is between the value of LAI and that of crop height. This connection exists in classical uses of Optirrig (e.g. maize, wheat, sorghum) but in the present



case the characteristic roughness lengths can probably be freely chosen, in association with fixed values of LAI.

Finally, the unknown left in Equation 9 is  $T_f$  and "effective surface temperature" is understood as "the temperature of the vegetal canopy layer" as represented in Figure 17.

### 3.1.1.3 Latent heat flux ( $L$ )

Latent heat flux is a form of heat transfer between materials, related to changes in phase between liquids, gases, and solids. In this energy balance,  $L$  was represented by the evapotranspiration of the system, resulting from the sum between the loss of plant water by transpiration and the loss of soil water by evaporation. The AET is calculated as such by Optirrig thus available from the simulation of this model.

However, in order to obtain a more accurate result that leads to more determinate parameters it is necessary to consider a more complete equation such as the Penman-Monteith (1948) in the Equation 14, that is the version extended with introducing resistance factors (FAO-56). This equation combined the energy balance with the mass transfer method and derived an equation to compute the latent heat flux (evapotranspiration) from uniform expanses of vegetation. This equation take into account an open water surface from standard climatological records of sunshine, temperature, humidity and wind speed.

$$L = \frac{\Delta(R_n - G) + \frac{p_a c_{p,a}(e_s - e_a)}{r_a}}{\Delta + \gamma \left(1 + \left(\frac{r_s}{r_a}\right)\right)} \quad (\text{Equation 14})$$

Where  $R_n$  is the net radiation,  $G$  is the soil heat flux,  $(e_s - e_a)$  represents the vapour pressure deficit of the air,  $p_a$  is the mean air density at constant pressure,  $c_{p,a}$  is the specific heat of the air at constant pressure,  $\Delta$  represents the slope of the saturation vapour pressure temperature relationship,  $\gamma$  is the psychrometric constant, and  $r_s$  and  $r_a$  are the stomatal and aerodynamic resistances.

Stomatal resistance, which is a factor that evaluates the opening and closing of plant stomata, is a fundamental value to classify the effects of osmotic and water conditions on photosynthetic efficiency in plants (MELO et al., 2010). This factor considers the type of plant used in the system ( $r_{s,min}$ ) and the percentage of influence that solar radiation, leaf surface temperature and soil water content have on the stomatal resistance, as shown in the Equations 15, 16, 17, 18 and 19 (AVISSAR and PIELKE, 1991; SAILOR, 2008; STANGHELLINI and DE JONG, 1995).

To calculate  $r_s$ :

$$r_s = r_{s,min} f_1(I) f_2(T_f) f_3(\omega_g) f_4(p_{v,f,sat} - p_{va}) f_5(CO_2) \quad (\text{Equation 15})$$

$$f_1(I_s) = 1 + e^{-0,034(I_s - 3,5)} \quad (\text{Equation 16})$$

$$f_2(T_f) = \frac{e^{0,3(T_f - 273,15)} + 258}{e^{0,3(T_f - 273,15)} + 27} \quad (\text{Equation 17})$$

$$f_3(\omega_g) = \begin{cases} 0 & \text{if } \omega_g^{\min} > \omega_g \\ \frac{\omega_{g\max} - \omega_{g\min}}{\omega_g - \omega_{g\min}} & \text{if } \omega_g^{\min} > \omega_g > \omega_g^{\max} \end{cases} \quad (\text{Equation 18})$$

$$f_4(p_{v,f,sat} - p_{va}) = 4 \times 10^{-3} + e^{-0,73 \left[ \frac{0,622 \times 10^3}{p_{atm}} \right] (p_{v,f,sat} - p_{va})} \quad (\text{Equation 19})$$

Where:

$\omega_g$ : The water status given by the water content of the soil ( $\text{kg}_{\text{eau}} \text{m}^{-3}_{\text{substrat}}$ );

$(p_{v,f,sat} - p_{va})$ : Deficiency of air vapor pressure compared to leaf cells;

$\text{CO}_2$ : The concentration of carbon dioxide in the ambient;

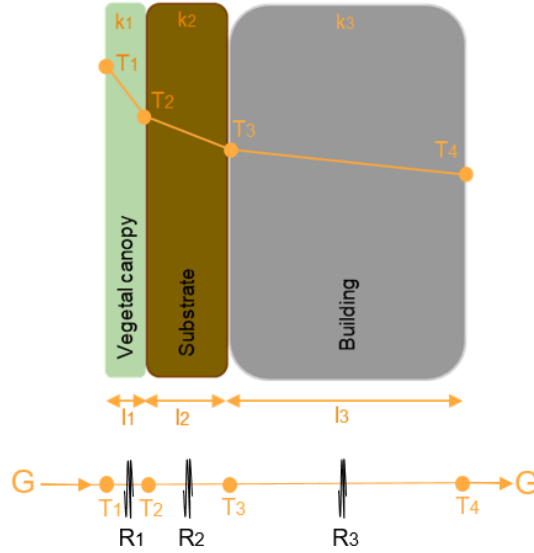
$r_{s,\min}$  : Minimal stomatal resistance ( $\text{s m}^{-1}$ ).

In this analysis, the influence of  $\text{CO}_2$  concentration was ignored, since it was not taken into account in the energy balance of the vegetal canopy the metabolic activities of the plant and it can be considered constant. The multiplicative factor  $f_5(\text{CO}_2)$  in the equation was equal to 1. We can emphasize too that the plants under hydric stress reduce their metabolic activities, transpiration rate and do not contribute to the energy dissipation of the system through evaporation (NOGUEIRA et al., 1998). Therefore, maintaining the green wall and roof with an adequate hydrological state is fundamental to assure the benefits related to the decrease of surface temperature, humidification of the air and softening of the indoor and outdoor temperatures of the building.

#### 3.1.1.4 Stored heat flux ( $\Delta G$ )

One part of the energy that is intercepted by the system is propagated through conduction mechanisms. Conduction is the propagation of thermal energy between nearby molecules resulting from a temperature difference. In this system, the conduction that occurs in the vegetal canopy can be ignored, since the heat capacity of the canopy layer is small compared to the other existing fluxes from/to substrates and building (CONVERTINO, 2019). Therefore, even if the energy balance considered in this work is on the surface of the canopy, to obtain the value of the stored heat flux, the conduction has to be considered in these other two layers.

Figure 22 : Geometry of the conduction in the system vegetal canopy + substrate + building



Source : Author, 2020.

As shown in Figure 22, there is an analogy between the diffusion of heat and the electrical charge. For one-dimensional steady heat conduction through the wall, the Fourier's law of heat conduction for the wall can be expressed as for the vegetal canopy like the equations below (BERGMAN, 2011):

$$Q_{wall} = -\frac{k_i A (T_2 - T_1)}{l_1} = -\frac{T_2 - T_1}{R_1} \quad (\text{Equation 20})$$

$$R_t = \frac{l}{kA} \quad (\text{Equation 21})$$

Where  $Q_{wall}$  is the heat flux through plane (W),  $k_i$  is the materials conductivity ( $W\ m^{-1}K^{-1}$ ),  $l$  is the plane thickness (m),  $A$  is the plane area ( $m^2$ ) and  $R_t$  is the thermal resistance ( $K\ W^{-1}$ ). The Equation 20, for heat flow, is analogous to the relation for electric current flow  $i$ , expressed as:

$$i = -\frac{V_2 - V_1}{R_e} \quad (\text{Equation 22})$$

$$R_e = \frac{l}{\sigma_e A} \quad (\text{Equation 23})$$

Where  $R_e$  is the electric resistance ( $\Omega$ ),  $V_1 - V_2$  is the voltage difference (V) across the resistance and  $\sigma_e$  is the electrical conductivity (S/m). The analogy between both equations is evident, with an analogies between the  $Q_{wall}$  and the  $I$ , the  $R_e$  and  $R_t$  and the difference  $T$  and  $V$ . Thus it make possible to represent the heat transfer through the composite wall ( $\Delta G$ ) from these resistances like shows the Equation 25.

$$T_1 - T_4 = Q \left( \frac{l_1}{k_1 A} + \frac{l_2}{k_2 A} + \frac{l_3}{k_3 A} \right) \quad (\text{Equation 24})$$

$$\Delta G = \frac{T_1 - T_4}{R_1 + R_2 + R_3} \quad (\text{Equation 25})$$

### 3.1.2 System properties

The study of the energy balance in the vegetal canopy allows obtaining of output data such as heat generation of the system (or dissipation). This variable is an input for the next step of the model in ANSYS Fluent program, to represent the green cover.

The first idea of the energy balance analyses was to obtain a specific set of characteristics for the entire system (plant canopy, substrate and building) such as albedo, emissivity, density ( $\text{Kg m}^{-3}$ ), specific heat ( $\text{J Kg}^{-1}\text{K}^{-1}$ ) and thermal conductivity ( $\text{W m}^{-1}\text{K}^{-1}$ ). However, these characteristics require a greater complexity than expected and a very specific information that, for an initial study, has become difficult to perform.

## 3.2 ANSYS

For the simulation in ANSYS Fluent, the required steps are: determination of the geometry of the fluid zone, discretization or mesh of the domain, add the data of the chosen physical models and hypotheses, and the numerical resolution where the equations will be solved from algorithmic interactions until the required convergence.

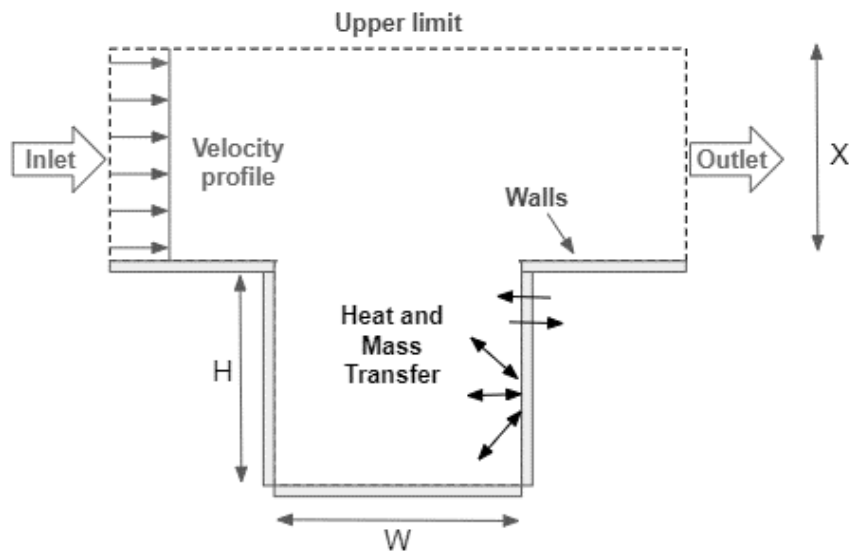
Also, in order to assess model 1's ability to solve the problem in question, the strategy used was first to carry out simulations with ANSYS Fluent and a reference canyon, the canyon that has no green cover (tested in this monography). Based on these results, the next step was to study the green canopy representation in the ANSYS Fluent with the data provided by Optirrig.

### 3.2.1 Geometry

The geometry used in the simulation was a two-dimensional (2-D) urban canyon. It is considered the elementary unit of the urban atmosphere scale, which allows for a finer analysis, with fewer accumulated errors. Thus, the system consists of a building height (H) and a street width (W) to the limit condition of the simulation (X), as shown in Figure 23.

The boundary layer of the analysis corresponds to a height from the ground to study turbulent phenomena and their interactions with different characteristics of the urban environment. For the study of fluid dynamics in an urban microclimate, it is recommended to use a boundary layer that includes an area where turbulence caused by the obstacle (e.g., provided by the building) is dissipated, as studied by Saneinejad et al (2012), Bottillo et al (2013), Gagliano et al (2017), Alexandri et al (2008). For this work, the boundary layer (X) initial consider was 4H and it was considered a longitudinal and constant wind flow to the direction of the urban canyon for the first step of this analyses.

Figure 23 : Theoretical domain of calculation, which includes the input and output characteristics (e.g. speed and temperature profiles) and the heat and mass transfer between the atmosphere and the model walls. Walls, for this spatial scale, refers to a composite interphase, such as building walls, asphalt or systems like building-substrate-vegetation with properties such as density, specific heat, thermal conductivity, roughness, emissivity, moment and thermal conditions

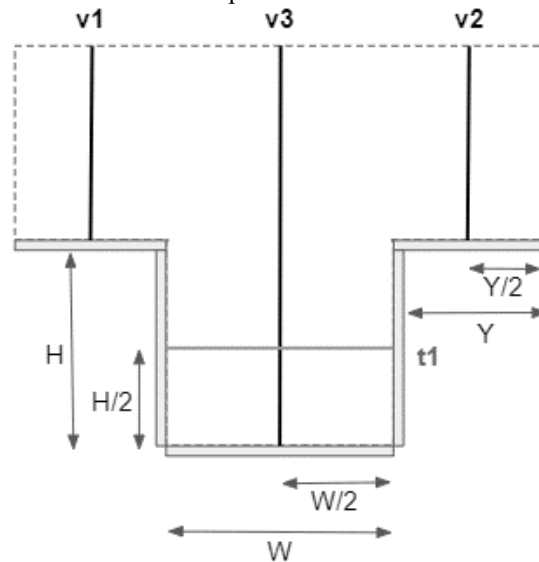


Source: Author, 2020.

Creating the most appropriate mesh is the first challenge: to optimize the CPU (central processing unit) and to ensure that results are independent from mesh. As the objective of the project is to analyze the climatic effect on vegetation in urban environments, mesh has to be thinner as possible in the urban canyon and close to the vegetal canopy, and larger away from it.

Also, in order to obtain a more representative comparison of the results obtained for the different simulated domains, tree vertical profiles and one horizontal profile were drawn to compare the results of the graphics for the different simulations and overlaps to better analyze the results (Figure 24)

Figure 24: Illustration of the location of the traced profiles for the analysis of the results obtained in the simulations, 'v1', 'v2' and 'v3' are the vertical profile and the 't1' is the transversal profile in the canyon.



Source: Author.

### 3.2.2 Physical model

Fluent code offers several turbulence schemes including multiple variations of the k- $\epsilon$  models, as well as k- $\omega$  models, and Reynolds Stress turbulence models. In street canyon flow and thermal stratification studies, the standard k- $\epsilon$  turbulence model is commonly used (GAGLIANO et al., 2017 and BOTTILLO et al., 2013) and was adopted in this project as first step of modeling. However, some studies claim that the standard k- $\epsilon$  turbulence model is not the most appropriate for this type of analysis. As it can derive errors of over 40% and the most appropriate would be Low-Reynolds Number Modeling (LRNM) (SANEINEJAD et al., 2012, BLOCKEN et al, 2009 and DEFRAEYE et al., 2010). In a second phase, this turbulence model was used to check possible errors in the result with the standard k- $\epsilon$  turbulence model. Also, more complex models such as Reynolds Stress Model that do not suppose an isotropic turbulence was used.

In the derivation of the k- $\epsilon$  model, the assumption is that the flow is fully turbulent, and the effects of molecular viscosity are negligible. The standard k- $\epsilon$  model (LAUNDER et al, 1972) is a model based on model transport equations for the turbulence kinetic energy (k) and its dissipation rate ( $\epsilon$ ):

$$\frac{\partial}{\partial t}(\rho k) + \frac{\partial}{\partial x_i}(\rho k u_i) = \frac{\partial}{\partial x_j} \left[ \left( \mu + \frac{\mu_t}{\sigma_k} \right) \left( \frac{\partial k}{\partial x_j} \right) \right] + G_k + G_b - \rho \epsilon - Y_M + S_k \quad (\text{Equation 26})$$

$$\frac{\partial}{\partial t}(\rho \epsilon) + \frac{\partial}{\partial x_i}(\rho \epsilon u_i) = \frac{\partial}{\partial x_j} \left[ \left( \mu + \frac{\mu_t}{\sigma_\epsilon} \right) \left( \frac{\partial \epsilon}{\partial x_j} \right) \right] + C_{1\epsilon} \left( \frac{\epsilon}{k} \right) (G_k + C_{3\epsilon} G_b) - C_{2\epsilon} \rho \left( \frac{\epsilon^2}{k} \right) + S_\epsilon \quad (\text{Equation 27})$$

Where:

$G_k$ : represents the generation of turbulence kinetic energy due to the mean velocity gradients;

$G_b$ : is the generation of turbulence kinetic energy due to buoyancy;

$Y_M$ : represents the contribution of the fluctuating dilatation in compressible turbulence to the overall dissipation rate;

$C_{1\epsilon}$ ,  $C_{2\epsilon}$  and  $C_{3\epsilon}$ : are constants and the default values are 1.44, 1.92 and 1.3 respectively;

$\sigma_k$  and  $\sigma_\epsilon$ : are the turbulent Prandtl numbers for k and  $\epsilon$ , respectively and the default values are 1.0 and 1.3;

$S_k$  and  $S_\epsilon$  : are user-defined source terms.

This model is a finite-difference numerical solution technique based on integration over the control volume to solve the model equations with appropriate boundary conditions. The final converged steady-solutions are obtained by solving iteratively the steady transport equations. The results can be considered as converged when the residuals have a value smaller than  $10^{-3}$ .

### 3.2.3 Boundary conditions

The characteristics of the system requested by ANSYS Fluent depend on the models that are enabled for the simulation.

In addition to the characteristics of the materials present in the domain density ( $\text{kg m}^{-3}$ ), specific heat ( $\text{J kg}^{-1}\text{K}^{-1}$ ) and thermal conductivity ( $\text{W m}^{-1}\text{K}^{-1}$ ), it is necessary to define the boundary conditions related to momentum and thermal.

One of the requested parameters of momentum is the sand-grain roughness height ( $k_s$ ) in meters and the sand-grain roughness constant ( $C_s$ ). According to the ANSYS Manuel is recommended to use the value 0,5 for the  $C_s$  and it is possible to obtain  $k_s$  value through the Equation 28 and Equation 29, that relates the aerodynamic roughness length  $y_0$  with its equivalent  $k_s$  for the atmospheric boundary layer proposed by Blocken et al (2007). The Equation 28, represents the aerodynamic roughness length  $y_0$  (m) over a vegetation canopy (JACOBSON, 2005; SELLERS et al 1996).

$$y_0 = hc(1 - 0.91e^{-0.0075LAI}) \quad (\text{Equation 28})$$

$$k_s = \frac{9.793 \cdot y_0}{C_s} \quad (\text{Equation 29})$$

Where:

$hc$ : is the canopy height above the ground of the top of the vegetation canopy (m);  
 $LAI$ : is the one-sided leaf area index ( $\text{m}^2 \text{m}^{-2}$ ).

Radiation was the chosen thermal boundary conditions because it allows the interaction between Optirrig and ANSYS Fluent. The parameter heat generation rate ( $\text{W m}^{-3}$ ) in this option corresponds to a volumetric energy produced or dissipated by the selected element. Thus, in the selected element that corresponds to the properties of the green wall or roof, this parameter corresponds to the sum of the energy dissipated by the sensitive and latent heat flow and is the data that we intend to use from Optirrig to represent the plants in ANSYS Fluent.

### 3.3 ENVI-MET

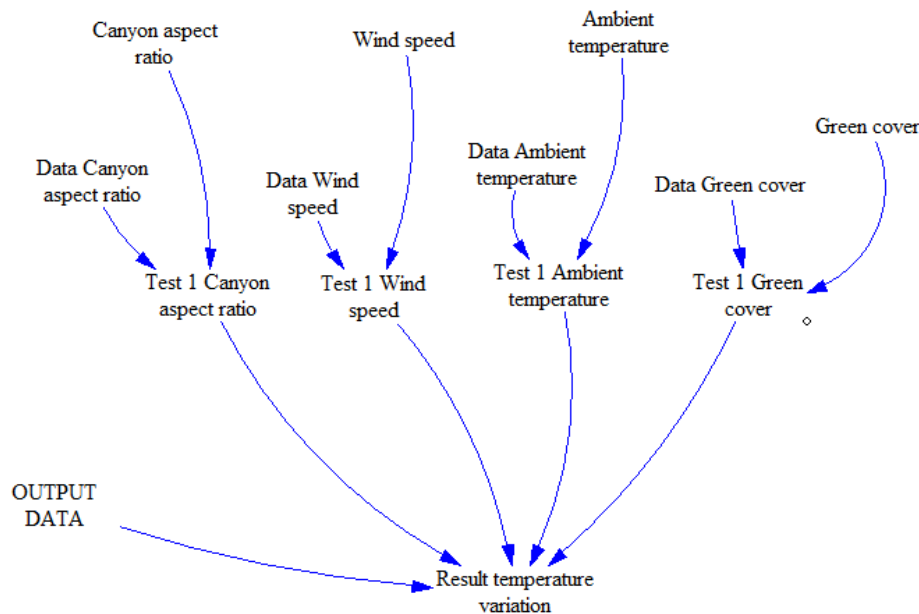
For the analyses with model 2, the Lite (free) version of ENVI-met, available through the ENVI-met website, was used. This version is limited in the domain area, parallel-computing and features presenting or visualizing detail output analysis. Despite the limitations, the free version can be used to produce output data of hourly air temperature and relative humidity and thus, the development of modelling site parameters using ENVI-met might produce the useful workflow that can be used globally for Urban Planners or designers, for a first analyses of the system. For this reason, simulations with this software in a reference canyon (without green covers) was performed in this study.

For the choice of the simulation geometry and mesh, the criterion for choosing the ideal formulation was the combination of mesh and geometry that generated the most accurate simulation results when compared to the real results obtained in the pilot.

### 3.4 VENSIM

The idea of the simulations architectures proposed, as previously mentioned, is to do a sensitivity study with the aid of Model 1 and/or Model 2 to obtain the most determinant variables of the system in relation to the temperature change within the urban canyon provided by green wall and/or green roof. With the most determinant variables of the system and the data related to the sensitivity study it is possible to know the relation that each variable has in the system as a whole and derive from it a scheme as proposed in the following Figure 25.

Figure 25 : Example diagram for the analysis of the climatic effects of green walls and roofs in urban canyon.



Source: Author, 2020.

The proposed diagram suggests that the most relevant parameters for the study in question are the urban aspects such as the geometry of the urban canyon (with the canyon aspect ratio  $H / W$ ) and the meteorological data of the study case (e.g.; wind speed, relative humidity and ambient temperature). With this input data, the program would provide the temperature variation within the urban canyon found from the comparison between the proposed scenario and the previously simulated scenario data, to find the result that is most similar to the desired one.

### 3.5 STUDY CASE

To illustrate the study of the urban microclimate conducted in section 1, the green wall pilot by Ecosec was accompanied. For the evaluation of the applicability of the model 1 and 2 proposed, with the support of the VegDUD Project<sup>1</sup> (MUSY et al, 2012) and his ClimaBat experiment<sup>2</sup>, it was possible to perform the first model simulations for an urban canyon case.

<sup>1</sup> ANR-Villes Durables VegDUD project: The role of plants in sustainable urban development; an approach based on issues related to climatology, hydrology, energy management and atmospheres (2010-2013).

<sup>2</sup> Directed by Rabah Djedjig, Emmanuel Bozonnet and Rafik Belarbi and presented in the thesis of Djedjig, 2013.



### 3.5.1 Green wall pilot – Montpellier, France

During the month of July, 2019, in Montpellier (France), the company Ecosec, French company specialized in dry toilets, installed a green wall pilot to carry out the first analyzes of this type of structure. The green wall pilot, as shown in Figure 26, was made with 18 blocks, containing soil inside, along with a fabric and wire mesh to support it. Different types of plants were used, and the type of irrigation was drip irrigation. Column 1, which has no plants, was used to enable the evaluation of the difference in surface temperature that a dry, a moist and a block with plants can have. For this, the topmost block of the column 1 was not irrigated and the other two were irrigated.

Figure 26: Image of the green wall pilot by Ecosec with the column 1 indicated, Montpellier, July 2019.



Source: Author, 2020.

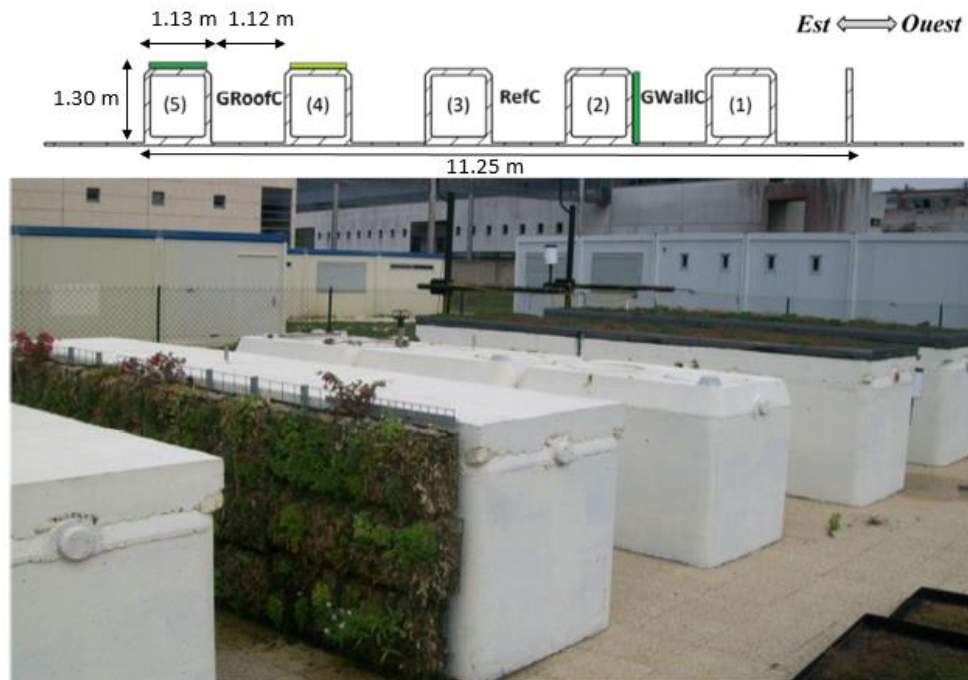
### 3.5.2 VegDUD Project – La Rochelle, France

To evaluate the relevance of the models developed in this study, with the support of the VegDUD project and the data from the developed ClimaBat pilot, it was possible to compare the results of numerical and experimental simulations. The pilot has been developed at La Rochelle University and performed in August 2012. The platform deployment region is characterized by moderate summer temperatures and is a zone classified by the Köppen-Geiger system as cfb (wet maritime temperate climate).

The ClimaBat pilot is made up of 5 rows of small-scale (1:10) buildings, with form a block 5 m long, 1.3 m high and 1.12 m wide and has an aspect ratio (H/W) equal to 1.2. The experiment provides features data from a meteorological station on the university campus and measurements on the surface and inside the urban canyon, as shown in Appendix 3 and Figure 27. The data refer to the canyon with a green wall system on the west façade of the building 2 and the reference canyon which has no vegetation in its façades. The green wall system used in this simulation is the type framed boxes modular living wall, like shows Figure 11 “e”, is made of six types of plants (sedum, mint, thyme, vinca, campanula and delosperma), a substrate

made of chile sphagnum and the system is watered twice a day by an automatic drip watering system.

Figure 27 : Experimental bench ClimaBat



Source: Djedjig (2013)

With the analysis of the available data, five instants of five different days were simulated, on days without rain and at times with higher air temperatures inside the canyon, to represent the reference urban canyon (RefC). The day that marked the highest temperatures on the pilot's surface and inside de canyon (2012-08-17 at 17:30) was selected in order to conduct the firsts analyzes with the model 1 (area and grid calibrations). The simulations in ANSYS Fluent (model 1) and ENVI-met (model 2) were performed with the parameters presented in Table 4, provided by the VegDud project. Thus, to analyse the accuracy of the models simulating the reference canyon (canyon without green cover), it was evaluated if the temperature measured inside the urban canyon was close to the simulated temperature.

Table 4: List of parameters used for the experimental validation of the day 2012-08-17 at 17:30.

Parametre	Description	Value
E	Emissivity of the leaf	0,95
$h_f$	Height of the vegetal canopy (m)	0,07
LAI	Leaf Area Index	3
$c_{pf}$	Specific heat of the vegetal canopy ( $J\ kg^{-1}\ K^{-1}$ )	4180
$\rho_f$	Density of the vegetal canopy ( $kg\ m^{-3}$ )	900
$r_{s,min}$	Minimal stomatal resistance ( $s\ m^{-1}$ )	200
$\omega_g^{max}$	Maximum water content of the soil ( $kg_{water}\ m^{-3}_{soil}$ )	260
$\omega_g^{min}$	Minimum water content of the soil ( $kg_{water}\ m^{-3}_{soil}$ )	5
$\omega_g$	Initial water content of the soil ( $kg_{water}\ m^{-3}_{soil}$ )	75
$h_s$	Height of the substrate (m)	0,12

$k(\omega_g^{\max})$	Maximum thermal conductivity of the substrate ( $\text{W m}^{-1} \text{K}^{-1}$ )	0,5
$k(\omega_g^{\min})$	Minimum thermal conductivity of the substrate ( $\text{W m}^{-1} \text{K}^{-1}$ )	0,1
$\rho_{ct}$	Density of the concrete tanks ( $\text{kg m}^{-3}$ )	2150
$c_{ct}$	Specific heat of the concrete tanks ( $\text{J kg}^{-1} \text{K}^{-1}$ )	914
$k_{ct}$	Thermal conductivity of the concrete tanks ( $\text{W m}^{-1} \text{K}$ )	2,365
$e_{ct}$	Emissivity of the concrete tanks	0,94
$\rho_s$	Density of the street ( $\text{kg m}^{-3}$ )	2290
$c_s$	Specific heat of the street ( $\text{J kg}^{-1} \text{K}^{-1}$ )	926
$k_s$	Thermal conductivity of the street ( $\text{W m}^{-1} \text{K}$ )	3,58
$e_s$	Emissivity of the street	0,81
$R_n$	Net Solar radiation ( $\text{N m}^{-2}$ )	393,84
$U$	Wind speed measured at the distance 1,58 m from the pilot ( $\text{m s}^{-1}$ )	2,05
$WS_{ms}$	Wind direction ( $^\circ$ )	192,2
$p_{atm}$	Atmospheric pressure (Pa)	1017
$TempEXT$	Ambient temperature (K)	298
$RH_1$	Relative Humidity of the air in the reference canyon (%)	29,14
$RH_2$	Relative Humidity of the air in the canyon with green wall (%)	28,99
$TS_{10}, TS_{11}, TS_{13}$	Average of the surface temperatures measured on the façade without greening (oust) of the canyon with green wall (K)	305,5
$TS_{18}, TS_{19}, TS_{21}$	Average of the surface temperatures measured on the façade with greening (oust) of the canyon with green wall (K)	300,2
$TS_8$	Surface temperatures measured on the roof oust of the canyon with green wall (K)	311,7
$TS_{24}$	Surface temperatures measured on the roof west of the canyon with green wall and oust of the reference canyon (K)	313,1
$TS_{40}$	Surface temperatures measured on the roof west of the reference canyon (K)	316,6
$TS_{26}, TS_{27}, TS_{29}$	Average of the surface temperatures measured on the façade oust of the reference canyon (K)	307,5
$TS_{34}, TS_{35}, TS_{37}$	Average of the surface temperatures measured on the façade west of the reference canyon (K)	313,6
$TS_{30}, TS_{32}$	Average of the surface temperatures measured on the street of the canyon (K)	311,1

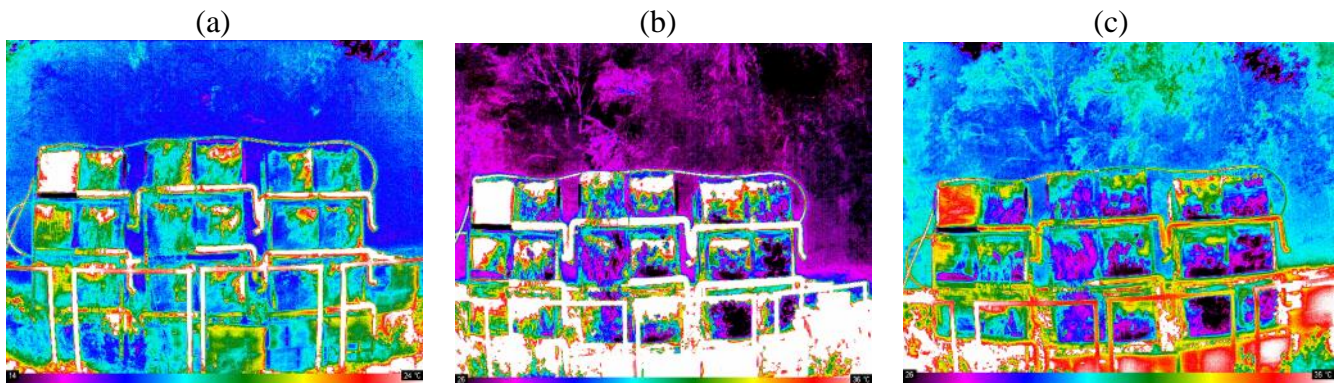
Source: Adapted from ClimaBat pilot of VegDud project and Jacobson (2004).

## 4. RESULTS AND DISCUSSIONS

### 4.1 GREEN WALL PILOT BY ECOSEC

Although the plants did not have abundant green cover, it was possible to obtain positive results of the attenuation of the surface temperature from the vegetal canopy.

Figure 28 : Thermal photos green wall pilot at (a) 8h00; (b) 14h30; and (c) 17h30.



Source: Author, 2020.

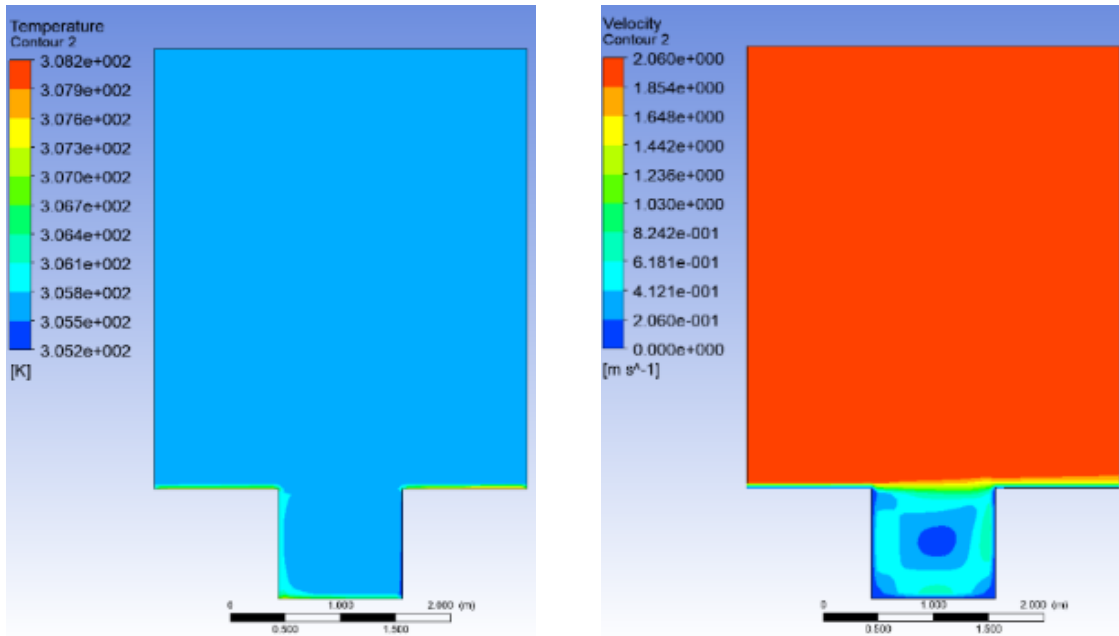
Figure 28 are thermal photos of the pilot at different times of the day. They show a wide variation in the surface brightness of the different materials in the photo and during various times of the day. In all the photos, the non-irrigated block showed a higher temperature and the other two moist blocks showed a variation of their surface temperature according to the moisture accumulation in the block (i.e., the lower part with more water has lower surface temperatures). The blocks with a more abundant green coverage showed lower surface temperatures than the previous two cases. The difference in surface temperature between the three cases was the most significant at 14h30, with more than  $36^{\circ}\text{C}$  in the surface of the dry block, between  $27.5$  and  $36^{\circ}\text{C}$  in the moist block and less than  $26^{\circ}\text{C}$  in the surface with greener coerture. This is since it is the time of the day with the highest solar radiation and thus the low albedo materials absorb more radiation and their surface get more heated. The difference between the dry surface and the moist surface show the impact of the evaporation in the surface temperature. The difference between the moist surface and the vegetal surface shows that the vegetal canopy is more efficient to mitigate the surface temperature with the mechanisms of shadow and evapotranspiration.

#### 4.2 MODEL 1 – CLIMABAT DATA

To start the simulations in ANSYS Fluent the first step is find the best way to represent the system. For this, we try different geometries and types of mesh to have less residual in less time until the system arrives in his convergence.

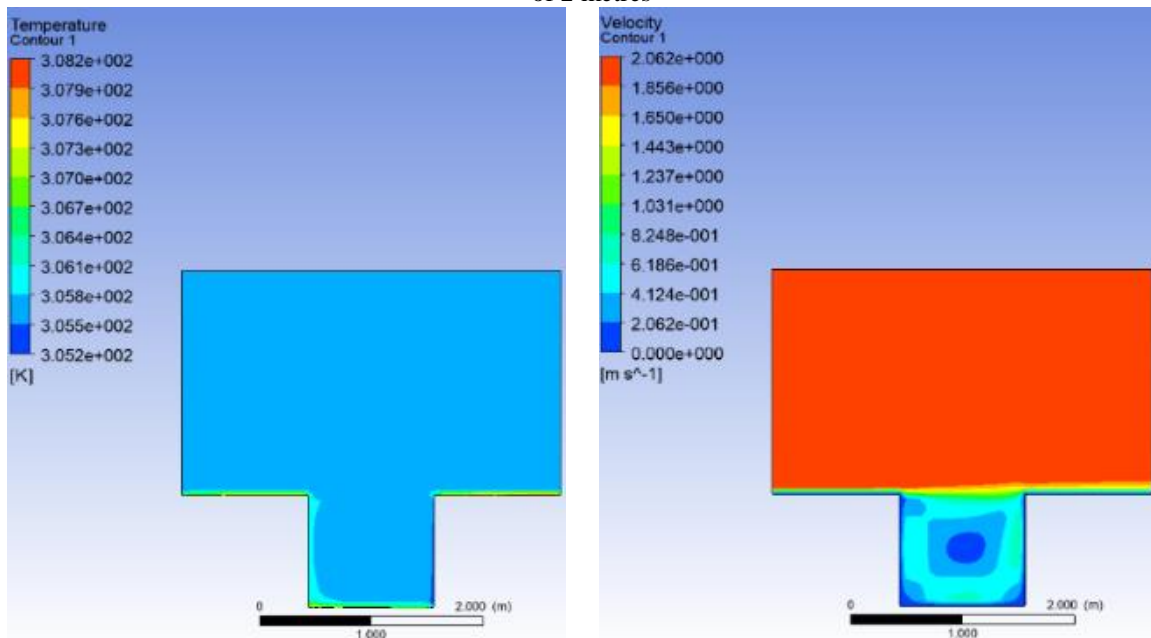
After simulations with different geometries, the first observation was that as we are considering the profile of the wind velocity constant in this first approach, it is possible to use a smaller boundary layer ( $X = 2H$ ) since this will not perturb the conditions inside the urban canyon and will optimize the time of simulation. The following Figures 29 and 30 shows the results of different simulations for the velocity and temperature profiles in the urban canyon with different geometries (A and B) and the same results found. In the Appendix 4 the graphics of the transverse ( $t1$ ) profiles for the velocity and temperature within the canyon are presented for the two studied geometries, as well the three vertical ( $v1$ ,  $v2$  and  $v3$ ) temperature profiles.

Figure 29: Simulation results for geometry A for the left temperature and right velocity profiles, domain height of 4 metres



Source: Author, 2020.

Figure 30: Simulation results for geometry B for the left temperature and right velocity profiles, domain height of 2 metres

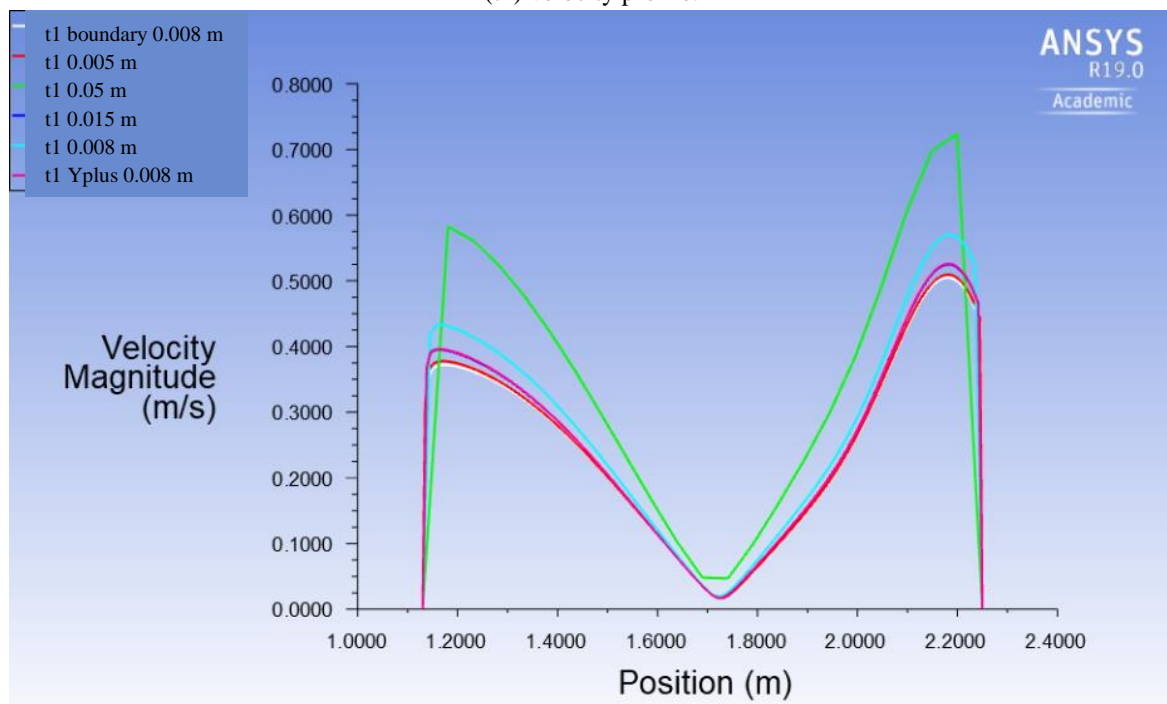


Source: Author, 2020.

After the definition of the study domain, the construction of the ideal mesh begins. The process of choosing the mesh starts from the principle of testing different grid shapes and sizes, for example a thinner grid near the walls and thicker away from them. However, taking into account that the area of study is reduced and our area of interest is the evolution of temperature within the urban canyon, we opted for a homogenous grid and square throughout the area. With

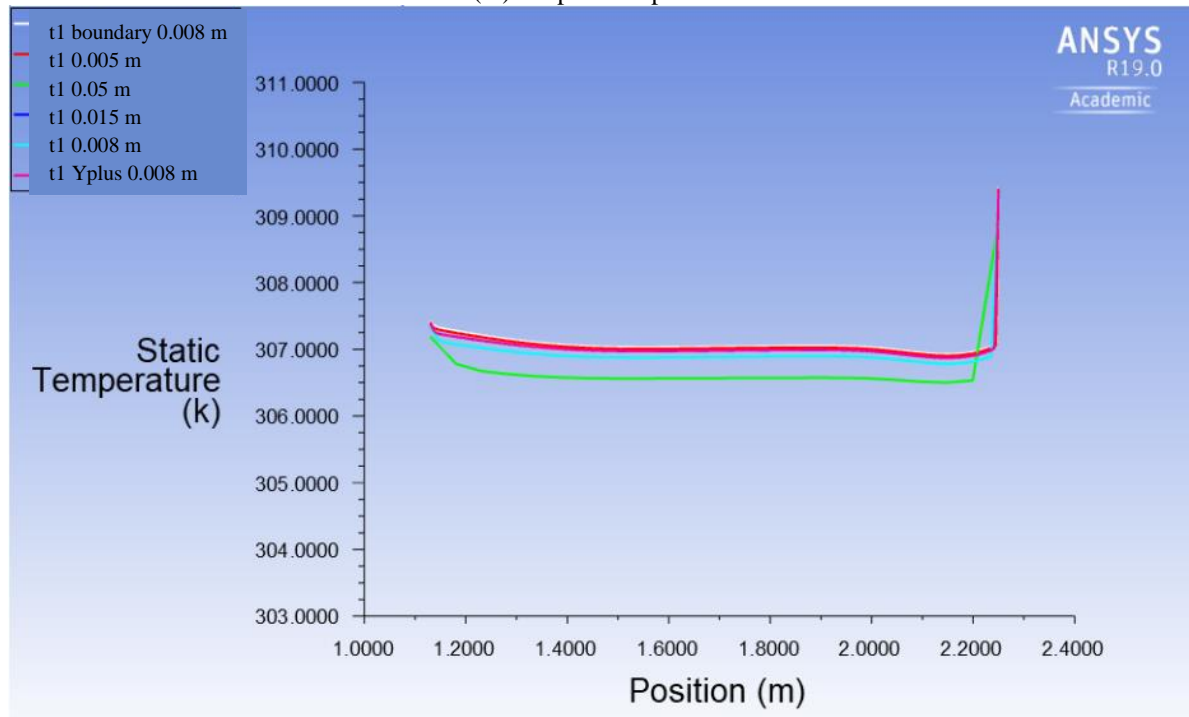
the homogenous and square grid it was possible to get statistic values of the quality of the mesh (e.g.: standard deviation and average) satisfactory. A series of simulation of a grid of 0.05 m to 0.005 m was carried out. The profiles of the results obtained can be observed below and show that as the grid decreases the results converges to the same asymptotic value. Other techniques have been tested to improve mesh quality with the mesh adapt option “boundary” and “Yplus” modes. These adaptations tend to refine the mesh close to the wall. The results can be seen in Figures 31 and 32. The optimal would be to continue testing different mesh, but with limited time for the finalization of the study, the mesh chosen to work with this system was the grid of 0.008 m with a finer mesh close 0,2 m to the walls, represented by ‘boundary 0.008m’ in the graphics.

Figure 31 : Results obtained in the refinement of the mesh for the ClimaBat pilot Reference canyon, transverse (t1) velocity profile.



Source : Author, 2020.

Figure 32 : Results obtained in the refinement of the mesh for the ClimaBat pilot Reference canyon, transverse (t1) temperature profile.



Source : Author, 2020.

The results of these simulations (Figure 31 and 32) refer to the values obtained for the reference canyon (17/08/2012 at 17:30). The temperature obtained inside the canyon was approximately 34.2 °C while the experimental value was 35.26 °C. Thus, there was a difference of 1°C between the two results. At this stage, it is difficult to raise hypothesis about this difference, it is necessary to perform more tests for different periods of the day and different days in order to check if the results obtained experimentally and numerically are compatible. In this way it will be possible to better verify if the generated error was for example by experimental error or numerical error (through the choice of the wrong method of simulation, models for thermal transfers, study zone or mesh) or still if this difference is found for all the situations, showing that the numerical method underestimates the temperatures found.

Table 5 shows the results for the simulation in the reference canyon for five different days at different times, on days without rain and at times with higher air temperatures inside the canyon. The method of simulation used was turbulence model "k-e standard", thermal model "radiation" for the surfaces, simple-accuracy of the solver and the average result of the simulated flow (stationary time).

**Table 5** Results for the VegDud reference canyon in the ANSYS Fluent program with turbulence model "k-e standard", thermal model "radiation" for the surfaces and simple-accuracy. Where TambEXT, U and HR\_1 are the inputs data, Tsimulated is the result of the simulation and Tobserved is the temperature measured in the reference canyon.

Day and Time	TambEXT (°C)	U (m/s)	HR_1 (%)	Tsimulated (°C)	Tobserved (°C)
02/08/2012, 17:00	21,21	3,943	53,71	23,0	25,71
04/08/2012, 17:00	22,29	2,257	56,38	24,2	25,13
12/08/2012, 12:00	21,99	4,111	61,15	23,0	26,13
17/08/2012, 17:30	32,52	2,05	28,99	34,2	35,26
22/08/2012, 12:00	22,73	2,438	44,37	23,5	26,19
25/08/2012, 12:00	20,50	5,736	57,21	21,0	24,81

Source: Author, 2020.

The difference between the simulated and observed results varied between 0.9 and 3.8 °C, for these five cases studied. In order to develop a more efficient simulation method, different combinations of turbulence models, thermal models for surfaces and precision version of the solver were tested. Finally, the combination found that resulted in the most accurate results was with "Stress Reynolds" turbulence model, "temperature" thermal model for surfaces, double-precision version of the solver and stationary time. Table 6 shows the results of the simulations found for this new configuration, where the difference between observed and simulated temperatures varies between 0.4 and 3.1 °C.

**Table 6** Results for the VegDud reference canyon in the ANSYS Fluent program with turbulence model "Stress Reynolds", thermal model "temperature" for the surfaces and double-accuracy. Where TambEXT, U and HR\_1 are the inputs data, Tsimulated is the result of the simulation and Tobserved is the temperature measured in the reference canyon.

Day and Time	TambEXT (°C)	U (m/s)	HR_1 (%)	Tsimulated (°C)	Tobserved (°C)
02/08/2012, 17:00	21,21	3,943	53,71	25,0	25,71
04/08/2012, 17:00	22,29	2,257	56,38	25,5	25,13
12/08/2012, 12:00	21,99	4,111	61,15	24,0	26,13
17/08/2012, 17:30	32,52	2,05	28,99	34,8	35,26
22/08/2012, 12:00	22,73	2,438	44,37	24,0	26,19
25/08/2012, 12:00	20,5	5,736	57,21	21,8	24,81

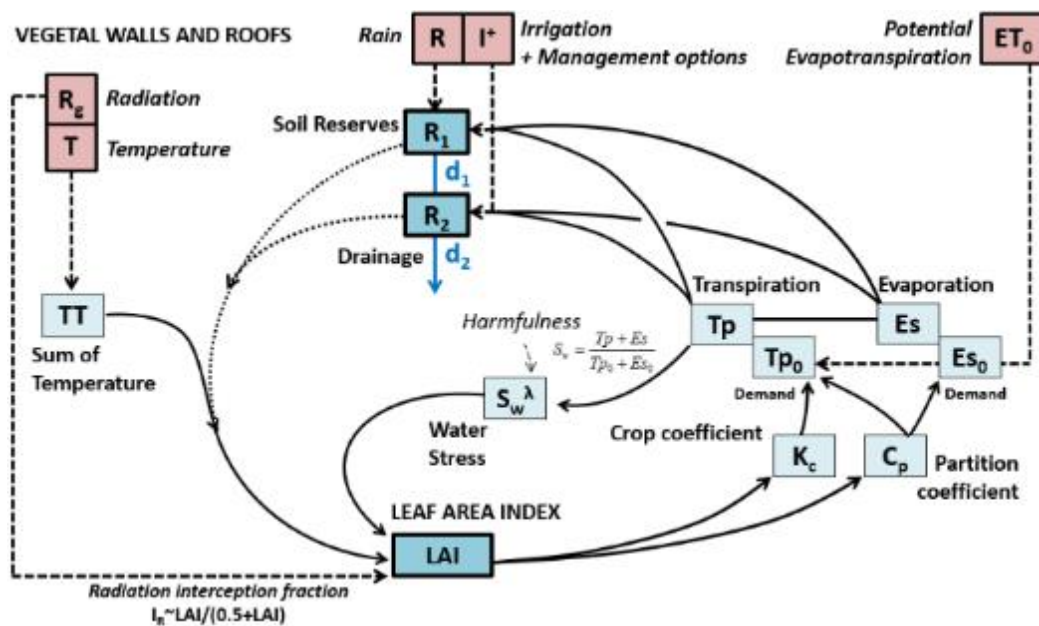
Source: Author, 2020.



In addition, with these tabular results and the temperature and wind speed profiles of the different days, it was possible to verify that the temperature presents a constant characteristic inside the canyon and higher temperatures very close to the walls, this means that the temperature of the canyon's surface has a greater local influence and that the wind speed profile does not directly influence the temperature profile, for the analysis of this study. On the other hand, the wind speed profile shows more variation inside the canyon, the formation of a vortex in the middle of the canyon and higher wind speed outside of the urban canyon, typical characteristics of the smallest microclimate scales, with maximum mixing of flows associated with increased roughness and obstacles. Taking into account that the analysis was carried out with many simplifications, with for example study area in two dimensions, constant velocity profile, stationary time, without introduction of solar radiation and relative air humidity, we can evaluate the accuracy of the model as satisfactory.

Simultaneously with the simulations in ANSYS Fluent, adaptations on the Optirrig program were developed. Among them, the key adaptations were: limited root zone, a constant LAI value, adapted irrigation such as drip irrigation of 5 mm that is triggered when  $R1+R2 < 80\%$  max and no biomass production. These first adaptations begin to assimilate the Optirrig model, which was initially developed to work on classical field conditions, to systems such as green walls and roofs. The model has a smaller water reserve and extension, as well as plants develop, in this first moment, without the objective of producing biomass, but to assure an ideal condition where the plants can evapotranspire, have a good surface cover and humidify the environment. Those characteristics help to guarantee a better thermal comfort on the environments they are inserted in. Figure 33 shows a scheme with the changes made on model.

Figure 33 : Principles of the Optirrig model modified version vegetal walls and roofs.



Source: Author, 2020.

### 4.3 MODEL 2 – CLIMABAT DATA

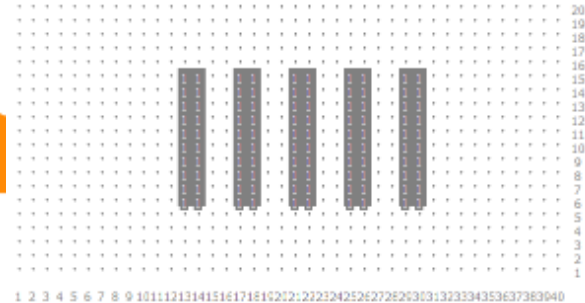
Model 2 is a simulation of the ClimaBat pilot with the ENVI-met software Lite version, presented in the Section 2.4.3. For the simulation, the study area and the database that characterise the study domain were configured in the program. Figures 34 and 35 show the study area in 3D and 2D perspective.

Figure 34 : 3D Study Area



Source: Author, 2020.

Figure 35 : 2D Study Area

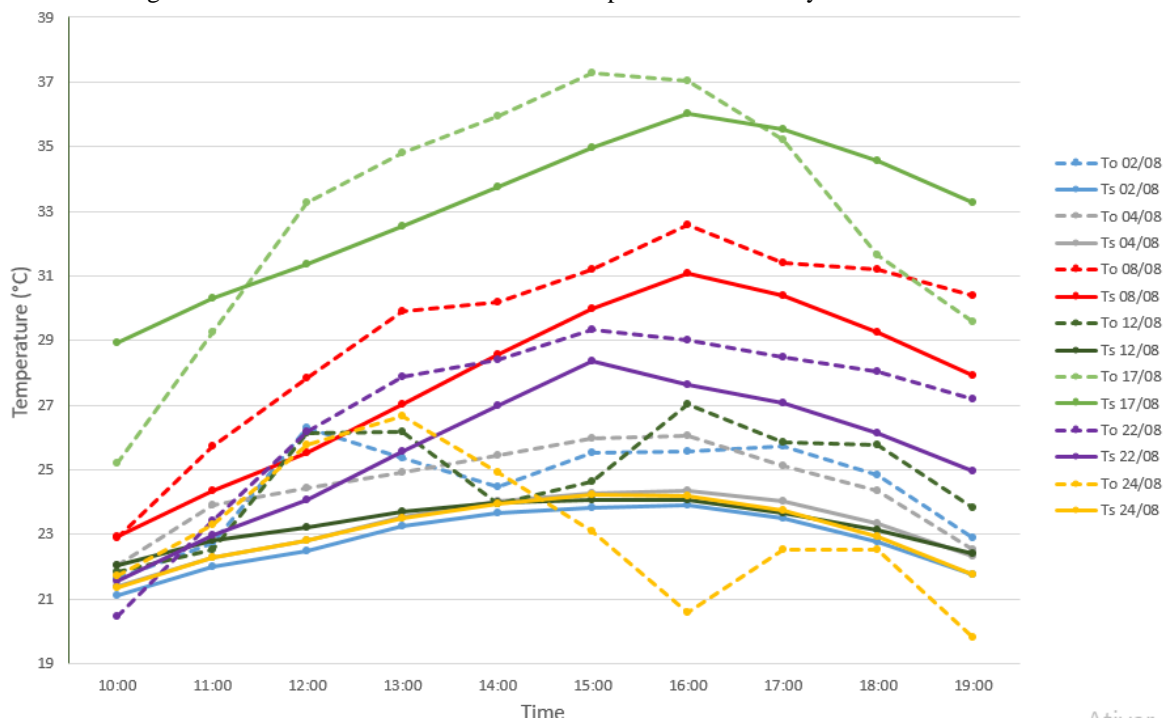


Source: Author, 2020.

For the study area, it was selected, after different tests, an area with 20 x 10 x 10 m, a grid of 0.5 x 0.5 m in the horizontal and 1.0 m cell base in the vertical with 5 sub-cells of 0.20 m, as these configurations show results that are more accurate. For each simulated day, minimum and maximum temperature, average wind speed, wind direction and minimum and maximum relative humidity were set for the 10-hour simulation time, starting at 9 a.m. until 7 p.m.

Thus, seven different days were simulated for the same analysis period. In the Figure 36, there is the temperature profile observed in the pilot ( $T_o$ ) and the simulated temperature in ENVI-met ( $T_s$ ) for each day evaluated at a point in the center of the reference canyon at 0.5 m height from the ground.

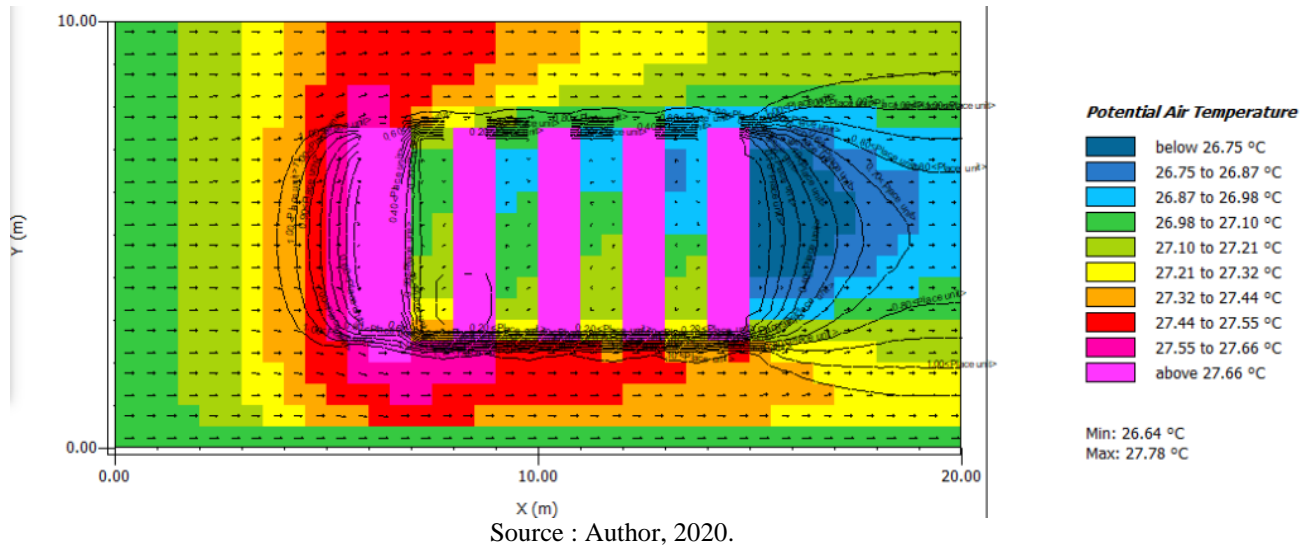
Figure 36 : Results obtained in the ClimaBat pilot reference canyon in ENVI-met Lite.



Source : Author, 2020.

The difference between the simulated and observed results varied between 0.049 and 3.812°C. The accuracy of the results of Model 2 was close to that obtained with Model 1. Taking into account the use of the ENVI-met Lite version, which has several limitations, it can be said that the results were satisfactory. Besides tabular results for the simulation, ENVI-met also generates transversal profiles of the modelling, at the time and height the choice, as shown in Figure 37, which is a cut at 5 p.m. on August 22, 2012 at a height of 0.5 m from the ground.

Figure 37 : Simulation result of the potential air temperature and wind direction profile at 5 p.m. on August 22, 2012.



These profiles, as well as the tabular results, have shown that the wind direction tends to channel inside the canyon, most days from north to south. In addition, depending on the wind direction and the size of the obstacle that the wind flow must pass through, the wind speed measured inside the canyon is lower. However, given that the version used in the simulations does not consider the physical properties of the pilot walls and therefore, the impacts of green envelopes and different surfaces cannot be evaluated. On the other hand, the wind speed and direction showed a small impact on the potential temperature measured inside the canyons, since the simulations of August 12th and 24th resulted in almost identical simulations profiles, although the input data of the wind speeds and relative humidity of each day were quite different.

## 5 CONCLUSION

Urban vegetation has the potential of reducing UHIs, allowing cities to become more resilient and sustainable. It seeks to reconnect large urban centres with nature, biodiversity, containing water runoff and making the city a more pleasant environment to live in, as it has great flexibility in terms of employment and direct benefits for the well-being of the population. Moreover, it is a way to take advantage of underused spaces in cities, which is why policymakers ought to invest in urban vegetation projects, making them more accessible.

The analysis of the thermal impact of green walls and roofs in cities requires understanding the wide range of mechanisms which are part of the system. It also depends on the goal of the study, which can be interpreted in different ways. In this project, we opted for the analysis of

the impact of vegetation on the decrease of outdoor temperatures and a first study of the energy balance between building, plant and atmospheric flows was carried out.

The model 1 simulation architecture to evaluate the thermal impact of plants in cities uses software already used by the INRAE team (Optirrig and ANSYS Fluent). Satisfactory results were obtained in the first simulations, considering the simplifications adopted. The results are starting points for the continuous development of this study of the elementary unity of the city, the urban canyon.

Comparing the two models developed, it can be observed that model 1 allows a greater flexibility in the choice of turbulent models, smaller grids and better characterization of the green envelope (with Optirrig), which allows greater detail in the study area, but a better characterized study area and computational power. On the other hand, despite the less detailed grid and study surface, model 2 also proved to be adequate for this study. Model 2 provided results close to those found in Model 1, in addition to enabling a three-dimensional study and detailed results for different hours of the day. At this stage of the study, it is not possible to identify one model as better than the other, it is necessary to evaluate the results for these study areas with the green walls and roofs. Therefore, it will be possible to determine which of the two models are the most suitable for this type of study.

## 6 BIBLIOGRAPHIC REFERENCES

AIDA, M. **Urban albedo as a function of the urban structure - A model experiment.** *Boundary- Layer Meteorol* 23, 405–413. 1982.

ALBDOUR, S. Mohammad; BARANYAI, Balint. **An overview of microclimate tools for predicting the thermal comfort, meteorological parameters and design strategies in outdoor spaces.** *International Journal for Engineering and Information Sciences* DOI: 10.1556/606.2019.14.2.10 Vol. 14, No. 2, pp. 109–118 (2019)

ALEXANDRIA, Eleftheria; JONES, Phil. **Temperature decreases in an urban canyon due to green walls and green roofs in diverse climates.** *Building and Environment* 43 (2008) 480–493.

ALI, Salman; LI, Baofeng. **Evaluating the Impact of the Morphological Transformation of Urban Sites on the Urban Thermal Microenvironment.** *Buildings MDPI* (2018).

ALLEN, Richard G. **FAO Irrigation and Drainage Paper No. 56.**

AMBROSINI, Dario; GALLI, Giorgio; MANCINI, Biagio; NARDI, Iole; SFARRA, Stefano. **Evaluating Mitigation Effects of Urban Heat Islands in a Historical Small Center with the ENVI-Met Climate Model.** *Sustainability* (2014).

AN-SHIK, Yang; CHIH-YUNG, Wen; CHIANG-HO, Cheng; YU-HSUAN, Juan. **CFD Simulations to Study the Cooling Effects of Different Greening Modifications.** *World Academy of Science, Engineering and Technology International Journal of Environmental and Ecological Engineering* Vol:9, No:7, 2015.

**ANSYS Fluent Theory, Guide** Site: <<https://uiuc-cse.github.io/me498cmfa15/lessons/fluent/refs/ANSYS%20Fluent%20Theory%20Guide.pdf>>.

APUR. **Les îlots de chaleur urbains à Paris, cahier #1.** 2012.

APUR. **Les îlots de chaleur urbains à Paris, cahier #2.** 2014.

AVISSAR, R.; PIELKE, R.A. **The impact of plant stomatal control on mesoscale atmospheric circulations.** *Agricultural and Forest Meteorology* 54, 353–372. 1991.

BALICK, L.K.; SCOGGINS, R.K.; LINK, L.E. **Inclusion of a Simple Vegetation Layer in Terrain Temperature Models for Thermal IR Signature Prediction.** *IEEE Transactions on Geoscience and Remote Sensing* GE-19, 143–152. 1981.

BENGTSSON L., GRAHN L., OLSSON J. **Hydrological function of a thin extensive green roof in southern Sweden.** *Nordic Hydrology*. No 36(3) p. 259–268. 2005.

BERGMAN, T. L.; LAVINE, A. S.; INCROPERA, F. P.; DEWITT, D. P. **Introduction to Heat Transfer**, 6th ed., Hoboken: John Wiley and Sons, 2011.

BLOCKEN, B.; STATHOPOULOS, T.; CARMELIET, J. **CFD simulation of the atmospheric boundary layer: wall function problems**. *Atmospheric Environment* 41 (2), 238–252. 2007.

BOWEN, I.S. **The Ratio of Heat Losses by Conduction and by Evaporation from Any Water Surface**. *Physical Review*, 27, 779. 1926.

BRITTER, R.E.; HANNA, S.R. **Flow and dispersion in urban areas**, *Annual Reviews of Fluid Mechanics*, 35, pp. 469-496. 2003.

CAETANO, Fernando Durso Neves. **Influência de muros vivos sobre o desempenho térmico de edifícios**. Campinas, SP, 2014.

Center for Disease Control and Prevention. **Extreme Heat: A Prevention Guide to Promote Your Personal Health and Safety** (2006).

CEREN (2011). **Bilan énergétique de Paris** Ed. 2009.

CHEVIRON, B. ; R.W. Vervoort, Rami Albasha, Romain Dairon, Camille Le Priol, et al.. **A framework to use crop models for multi-objective constrained optimization of irrigation strategies**. *Environmental Modelling and Software*, Elsevier, 2016, 86, pp.145-157. [ff10.1016/j.envsoft.2016.09.001](https://doi.org/10.1016/j.envsoft.2016.09.001)ff. [ffhal-02604719](https://doi.org/10.1016/j.envsoft.2016.09.001)f.

CIONCO, RM. **Mathematical model for airflow in a vegetative canopy**. *J. Appl. Meteorol.* 4: 517–22. 1965.

CONVERTINO, F.; VOX, G.; SCHETTINI, E. **Heat transfer mechanisms in vertical green systems and energy balance equations**. *Int. J. of Design & Nature and Ecodynamics*. Vol. 14, No. 1 (2019) 7-18.

DE MUNCK, C. **Modélisation de la végétation urbaine et des stratégies d'adaptation au changement climatique pour l'amélioration du confort climatique et de la demande énergétique en ville**. PhD Thesis. Paul Sabatier University, Toulouse, France in French. 2013.

DJEDJIG, Rabah. **Impacts des enveloppes végétales à l'interface bâtiment microclimat urbain**. Génie civil. Université de La Rochelle, 2013. Français. NNT : 2013LAROS421. tel-01141046.

BOER, Marissa A. de; et al. **Uptake of pharmaceuticals by sorbent-amended struvite**

**fertilisers recovered from human urine and their bioaccumulation in tomato fruit.** Water Research. 2018.

DJEDJIG, Rabah; BOZONNET, Emmanuel; BELARBI, Rafik. **Modeling green wall interactions with street canyons for building simulation in urban context.** Urban Climate. 2015.

ENVI-met, 2020. *ENVI-met 4. A holistic Microclimate Modelling System.* [Online] Available at: <http://www.envi-met.info/doku.php?id=intro:modelconcept>. [Accessed 7 2020]

European Federation Green Roofs & Walls (EFB), 6 august 2019: <<https://efb-greenroof.eu>>

FRANKE, J.; HELLSTEN, A.; SCHLUNZEN, H.; CARISSIMO, B. **Best practice guideline for the CFD simulation of flows in the urban environment,** Brussels: COST Office; 2007.

GABLIANO, Antonio; NOCERA, Francesco; ANELI, Stefano. **Computational fluid dynamics for evaluating the urban heat island effects.** ScienceDirect, Energy Procedia 134 (2017) 508-517.

GAO, Z.; BRESSON, R.; QU, Y.; MILLIEZ, M.; MUNK, C. CARISSIMO, B. **High resolution unsteady RANS simulation of wind, thermal effects and pollution dispersion for studying urban renewal scenarios in a neighborhood of Toulouse.** ScienceDirect, Urban Climate 23 (2018) 114-130.

GARTLAND, L. **Heat islands: understanding and mitigating heat in urban areas.** Earthscan. 2008.

GRARD, B.J.-P et al. **Recycling urban waste as possible use for rooftop vegetable garden.** Future of Food: Journal on Food, Agriculture and Society. 2015.

HERZOG, T. R.; STREVEY, S. J. **Contact With Nature, Sense of Humor, and Psychological Well-Being.** Environment and Behavior, v. 40, n. 6, p. 747-776, 20 mar. 2008.

JACOBSON, Mark Z. **Fundamentals of Atmospheric Modeling.** Second Edition. 2005.

JAMES, W. **Green roads: research into permeable pavers.** *Stormwater* 3(2):48-40. 2002.

KAISER, A.; MERCKX, T. ; DYCK, H. V. **The Urban Heat Island and its spatial scale dependent impact on survival and development in butterflies of different thermal sensitivity.** Ecology and Evolution. 2016.

KAMARULZAMAN, Noorazlina; HASHIM, Siti Zubaidah; HASHIM, Hasnan; SALEH, Alia Abdullah. **Green Roof Concepts as a Passive Cooling Approach in Tropical Climate- An Overview.** 2014.

KRUGER, Eduardo Leite; ROSSI, Francine Aídie; CRISTELI, Pablyne Sant'Ana, SOUZA, Henor Artur de. **Calibração do índice de conforto para espaços externos Physiological Equivalent Temperature (PET) para Curitiba.** *Ambient. constr.* [online]. 2018, vol.18, n.3, pp.135-148. ISSN 1678-8621. <https://doi.org/10.1590/s1678-86212018000300272>.

LAUNDER, B. E.; SPALDING, D. B. **Lectures in Mathematical Models of Turbulence.** Academic Press, London, England. 1972.

LHOMME, J.-P.; VACHER, J.-J. **Modelling nocturnal heat dynamics and frost mitigation in Andean raised field systems.** *Agricultural and Forest Meteorology* 112. 2002. 179–193.

LI-WEI, Lai ; WAN-LI, Cheng. **Air quality influenced by urban heat island coupled with synoptic weather patterns.** *Science of The Total Environment* Volume 407, Issue 8, 1 April 2009, Pages 2724-2733

MACDONALD RW. **Modelling the mean velocity profile in the urban canopy layer.** *Bound.-Layer Meteorol.* 97: 25–45. 2000.

MAILHOL, J.C.; OLUFAYO, O.; RUELLE, P. AET and yields assessments based on the LAI simulation. Application to sorghum and sunflower crops, *Agricultural Water Management*, 35, pp.167-182. 1997.

MAILHOL, J.C.; RUELLE, P.; WALSER, S.; SCHÜTZE, N.; DEJEAN, C. Analysis of AET and yield prediction under surface and buried drip irrigation systems using the crop model PILOTE and Hydrus-2D, *Agricultural Water Management*, 98, pp.1033-1044. 2011.

MASI, F.; RIZZO, A.; BRESCIANI, R.; EDATHOOT, A.; PATWARDHAN, N.; PANSE, D. **Greywater Treatment and Reuse in a Municipal Office in Pune by Vertical Gardens.** *Sustainable Sanitation Practice.* 2016.

MESTAYER, P. G. ; ROSANT, J.-M.; RODRIGUEZ, F.; ROUAUD, J.-M. **La Campagne Expérimentale FluxSAP 2010: Mesures de climatologie en zone urbaine hétérogène.** *La Météorologie* - n° 73 - mai 2011.

MILLER, G.T., 2007. **Living in the environment: principles, connections, and solutions.** Thomson Brooks/Cole, Belmont, CA.

MUSY, M.; GUTLEBEN, C.; INARD, C.; et al. **VegDUD project: Role of vegetation in sustainable urban development.** In: 8th International Conference on Urban Climate (ICUC8). Dublin, Ireland 2012.

NOGUEIRA, R.; J. M. C. et al. **Comportamento fisiológico de duas cultivares de amendoim submetidas a diferentes regimes hídricos.** *Pesquisa Agropecuária Brasileira*, v. 33, n. 12, p. 1963-1969, 1998.



NOWAK, D. J. **Institutionalizing urban forestry as a biotechnology to improve environmental quality.** *Urban Forestry & Urban Greening*, v. 5, p. 93-100, 2006.

OKE, T. R.; MILLS, G.; CHRISTEN, A.; VOOGT, J. A. **Urban climates.** Cambridge: Cambridge University Press, 2017.

PASTORE, Luisa; CORRAO, Rossella; HEISELBERG, Per. **The use of Vegetation for Social Housing Renovations: a cases study in the city of Palermo.** CESBP. 2013.

RAMESH, Shalini – **Urban Energy Information Modeling – A Framework for Coupling Macro-micro Factors Affecting Building Energy Consumption.** 2017

RIAU, Valancogne C. ; PIERI, P. **Un modèle simple d’interception du rayonnement solaire par la vigne – vérification expérimentale.** *Agronomie* (1989) 9, 441 - 450.

RUEFENACHT, Lea A.; ACERO, Juan A. **Strategies for cooling Singapore.** 2017.

GIVONI, B. **Impact of planted areas on urban environmental quality: a review. Atmospheric Environment. Part B.** *Urban Atmosphere*, v. 25, n. 3, p. 289–299, 1991.

SAILOR, D. J. **Urban Heat Islands, Opportunities and Challenges for Mitigation and Adaptation.** Sample Electric Load Data for New Orleans, LA. North American Urban Heat Island Summit. Toronto, Canada. 1–4 May 2002. Data courtesy Entergy Corporation.

SAILOR, D.J. **A green roof model for building energy simulation programs.** *Energy and Buildings* 40, 1466–1478. 2008.

SANEINEJAD, Saba; MOONEN, Peter; DEFRAEYE, Thijs; DEROME, Dominique; CARMELIET, Jan. **Coupled CFD, radiation and porous media transport model for evaluating evaporative cooling in an urban environment.** *Journal of wind engineering and industrial aerodynamics.* 2012.

SAUDREAU, Marc et al. **A 3D model for simulating the spatial and temporal distribution of temperature within ellipsoidal fruit.** *Agricultural and Forest Meteorology* 147 (2007) 1–15.

SELLERS, P. J.; LOS, S. O.; TUCKER, C. J. **A revised land surface parameterization (SiB2) for atmospheric GCMs. Part II: The generation of global fields of terrestrial biophysical parameters from satellite data.** *J. Clim.* 9, 706–37. 1996.

SHUTTLEWORTH, W.J., WALLACE, J.S. **Evaporation from sparse crops—an energy combination theory.** *Quart. J. R. Meteorol. Soc.* 111, 839–855. 1985.

SODOUDI, Sahar; SHAHMOHAMODI, Parisa; VOLLACK, Ken; CUBASCH, Ulrich; CHENI, A. I. **Mitigating the Urban Heat Island Effect in Megacity Tehran**. *Advances in Meteorology*. 2014.

SPANGENBERG, Jörg; SHINZATO, Paula; JOHANSSON, Erik; DUARTE, Denise. **Simulation Influence of Vegetation on Microclimate and Thermal Comfort in the City of São Paulo**. *Rev. SBAU, Piracicaba*, v.3, n.2, jun. 2008, p. 1-19

STANGHELLINI, C., JONG, T. de. **A model of humidity and its applications in a greenhouse**. *Agricultural and Forest Meteorology* 76, 129–148. 1995.

SUNARYA, Wendy. **The importance of site on house heating energy modelling in wellington - Integrating EnergyPlus with ENVI-met for site modelling**. *Building Science*. Victoria University of Wellington. 2020.

TAHA, H. **Urban climates and heat islands: albedo, evapotranspiration, and anthropogenic heat**. *Energy and Buildings* 25, 99–103. 1997.

VERMA, S. B. **Aerodynamic resistances to transfers of heat, mass and momentum**. *Estimation of areal evapotranspiration*, no. 177, 1989.

WILMERS, F. **Effects of vegetation on urban climate and buildings**. *Energy and Buildings*, v. 15, n. 3, p. 507–514, 1991.

WOOD, Antony; BAHRAMI, Payam; SAFARIK, Daniel. **Green Walls in High-Rise Buildings: An output of the CTBUH Sustainability Working Group**. p. 16, 2014.

OTTELÉ, M. et al. **Comparative life cycle analysis for green façades and living wall systems**. *Energy and Buildings*, v. 43, n. 12, p. 3419-3429, dez. 2011.

ZAVATTINI, João Afonso. **Climatologia Geográfica - teoria e prática de pesquisa**, Editora: Alinea, (2013).

ZHANG, Linfang; MING, Jin; JIYING, Liu; LINHUA, Zhang. **Simulated study on the potential of building energy saving using the green roof**. *Procedia Engineering* Volume 205, 2017, Pages 1469-1476.

ZHANG, M.; BAE, W.; KIM, J. **The Effects of the Layouts of Vegetation and Wind Flow in an Apartment Housing Complex to Mitigate Outdoor Microclimate Air Temperature**. *Sustainability* 2019, 11, 3081 ; doi : 10.3390/su11113081

## APPENDIX 1

Legend:	General overview and Sustainability	Nutrient recovery and recycling	Model effect on temperature
---------	--	------------------------------------	--------------------------------

ID	Author	Paper	Year	Main Conclusions
1	Paper: APPA Nord-Pas de Calais - 2014	Urban Vegetation - Environmental and Health Issues	2014	It is necessary to take into account any damage caused by particles on trees: abrasion, occlusion of leaf stomata, formation of a crust of particles on the leaf surface that can disturb physiological mechanisms such as bud break, pollination or light absorption. In some cases, depending on their planting density and morphology, trees can alter airflow, which slows down the dispersion of pollutants and would even lead to an increase in pollutants, which are concentrated in certain areas.
2	Julien Bigorgne and Adrien Mangold	Climatic simulations of three Parisian urban forms and lessons in section 2	2014	Heat islands are a problem of night cooling (the city cannot cool down at night unlike the surrounding areas). Therefore, to avoid this, it is necessary to look for diurnal strategies preventing the city from warming up as shadows carried by urban canopies and the runoff of non-potable water on highly exposed floor coverings and also nocturnal strategies to accelerate night cooling with the multiplication of permeable soils sufficiently soaked with water for evaporation purposes.
3	Julien Bigorgne	Urban Heat Islands in Paris section1	2012	Each city has its own heat island depending on its global urban configuration, each city also has its own adaptation solutions. Look at it on a very small scale.
4	M. Musy	The role of plants in sustainable urban development; an approach based on issues related to climatology, hydrology, energy management and environments	2009	The climatic impact of the plant depends in part on the water that the plants can use. However, it is difficult to represent this subsystem in all models that would become very complex. The functioning of plants also depends on their positioning in the urban form. Management (human interventions) and plant growth conditions (climate, access to light, water, soil type, exposure to pollution, human or animal degradation, etc.) are very influential parameters that have not been taken into account, or in a very partial way. It is important to take into account realistic urban conditions. The articulation of physical and quantitative approaches and approaches to the humanities and society remains a difficulty in addressing topics such as the role of the plant.
5	Sebastian Huttner geb. in Scherzingen	Further development and application of the 3D microclimate simulation ENVI-met	2012	ENVI-met is a software for urban microclimate simulations. The large number of users and the diversity of ENVI-met projects are used to support this statement.
6	Marissa A. de Boer et al	Uptake of pharmaceuticals by sorbent-amended struvite fertilisers recovered from human urine and their bioaccumulation in tomato fruit	2018	This study showed that the health risk posed by pharmaceutical micro pollutants, transferred from human urine to struvite- and sorbent-based fertilizers in tomato fruits, is negligible.

7	Grard B.J.-P. et al	Recycling urban waste as possible use for rooftop vegetable garden	2015	Types of urban organic waste composing the growing substrate: Compost of green waste from urban public parks and green spaces, Crushed wood, as well as public spaces, Ground coffee with <i>Pleurotus Ostreatus</i> mycelium. Mixed in four different compositions and a control. The available results show: high levels of agricultural production with limited inputs compared to professional terrestrial gardening, low levels of heavy metal pollutants in the edible parts of crops, especially for Cd and Pb compared to EU standards for vegetables and a positive influence on yields organizing the substrate into layers and improving biological activity by inoculating the earthworm.
8	Esther Sanyé-Mengual et al	Techniques and crops for efficient rooftop gardens in Bologna, Italy	2015	Further research on local food and urban agriculture systems is needed to assess the potential contribution of such systems to urban sustainability, to identify the role of rooftop agriculture and to assess the potential of different forms of urban production. The design of rooftop agriculture can focus on potential local resources that can be used at the construction stage (such as the reuse of elements). The design may include different types of cropping systems, as fruiting vegetables and leafy vegetables have different requirements. Soil techniques for fruiting vegetables and winter cycles of leafy vegetables, while floating production would be attractive for summer leafy vegetable crops, the nutrient film technique would be the least recommended option, unless energy-efficient solutions are applied.
9	Mert Eksia et al	Effect of substrate compost percentage on green roof vegetable production	2015	Adding an appropriate amount of compost to shallow green roof substrates can increase plant growth yields compared to cucumbers and peppers under regular irrigation. In general, adding 60 or 80% compost has given the best results in terms of plant growth and fruit yield, although the differences are not as pronounced as for cucumbers. These amounts are much higher than recommended for roofs of large conventional ornamental greens planted with succulents or other perennials and grasses due to the negative consequences of substrate retention and nutrient runoff. The fact that the roof plots all worked better than the ground garden plot highlights the fact that growing vegetables on a roof can be an advantage because the substrates can be designed to optimize plant health, although the same can be done with raised flower beds in a garden.
10	Veljko Prodanovic et al	Green walls for greywater reuse: Understanding the role of media on pollutant removal	2017	To reduce the impacts caused by the application of green walls and roofs in the city due to its high water consumption and better application results in arid regions, one solution is to use grey water as a source of water and nutrients. To assess the impact of grey water use on walls and their potential to remove pollutants to enable water reuse, this project was put into practice. The results show that coconut and perlite substrates have the greatest potential for pollutant removal and that the combination of the two would produce an even better result. In addition to different types of substrates, the influence of different detention times on process optimization was tested

ID	Author/Year	Paper/Scale	Main conclusion	Type of model	Input
11	Fernando Durso Neves Caetano 2014	The influence of living walls on the thermal performance of buildings <b>Local - building</b>	The living wall pilot system provided an average thermal damping of up to 19°C at the outer surface temperature of the envelope and an average thermal delay of up to 4 hours; inside, the presence of a living wall allowed an average damping of up to 2.73°C at the operating temperature at the hottest time of the day	Comparative experimental analysis	Internal and external surface temperature of the building and operating temperature inside the building
12	Helge Simon et al 2018	Modeling transpiration and leaf temperature of urban trees – A case study evaluating the microclimate model ENVI-met against measurement data <b>Neighbourhood - climatology</b>	The study showed that the ENVI-met microclimate model, operating in full-forcing mode, was able to accurately simulate the transpiration rate and leaf temperature changes of both trees in a complex urban environment. He confirmed that ENVI-met is a viable tool for assessing tree effects on urban microclimate (transpiring cooling effects) as well as for simulating tree vitality parameters under specific microclimate conditions.	ENVI-met: three-dimensional prognostic microclimate model. The principle of this model is that plants use stomatal conductance to maximize CO2 gain while minimizing associated water losses (Jacobs, 1994)	Using meteorological measurements and the ENVI-met full forcing option, half-hourly forcings of wind speed, solar radiation, air temperature and humidity were created as boundary conditions for the model. Input a most accurate representation of the tree's geometry and leaf area density (important for estimating the tree's actual transpiration flow).
13	Ferdinando Salata et al 2016	Urban microclimate and outdoor thermal comfort. A proper procedure to fit ENVI-met simulation outputs to experimental data <b>Neighbourhood - climatology</b>	In this study, great attention was paid to the evaluation of the model's input parameters while describing the procedure performed for the simulations. A general procedure for performing simulations in ENVI-met is suggested	ENVI-met	Three input categories: The "zone input file" is created via a graphical interface and mainly contains the geometric data of the simulated model, the "configuration file" presents the initial calculation parameters and boundary conditions characterizing the simulation and the for the "databases" were used: vegetation, soil stratigraphy and data from each layer. Each file contains parameters used for the equations of the physico-mathematical models implemented by the software. These are all data related to the typology of plants or soil: water content, thermal conductivity, physiological characteristics of leaves and roots
14	Sahar Sodoudi et al 2014	Mitigating the Urban Heat Island Effect in Megacity Tehran <b>Neighbourhood - climatology</b>	The results of the field study clearly show higher temperatures in the central part compared to the green areas of Tehran's 6th urban district, with high-density residential, commercial and industrial areas showing a higher temperature of about 6 -7K. Three different UHI mitigation strategies (high albedo materials, green roofs and vegetation, and hybrid) were simulated from the ENVI-met simulations. The scenarios (HYBRID) show the most important cooling. The average cooling of this scenario is about 1.67 K at 15:00 and 1.10 K at 03:00, although the maximum cooling is about 4.2 K in the green zone between buildings.	ENVI-met: This numerical model simulates aerodynamics, thermodynamics and radiation balance in complex urban structures. It is designed for micro scales with a horizontal resolution of 0.5 to 10 m and a typical time span of 24 to 48 hours with a time step of 1 to 10 seconds. This resolution makes it possible to analyze small-scale interactions between buildings, surfaces and plants. Typical scales of analysis range from a single street to a canyon that can reach a few hundred metres.	Local input data on soil, meteorology and buildings for model initialization in the study area. These include temperature and relative humidity at 2 m, wind direction and speed at 10 m, specific humidity at 2 500 m, soil temperature and relative humidity, indoor building temperature, thermal conductivity divided by the average width of the wall or roof, heat transfer and average albedo of walls and roofs.

ID	Author/Year	Paper/Scale	Main conclusion	Type of model	Input
15	Rabah Djedjig 2013	Impacts of plant envelopes at the urban microclimate building interface <b>Neighbourhood - climatology</b>	This thesis deals with the modelling and experimentation of roofs and green facades in order to evaluate their hygrothermal impacts on buildings and urban microclimates. For this reason he carried out a bibliographic study where he concluded that the models best describe the phenomena of thermal transfer in the foliage and in the substrate neglect the coupling between thermal and water transfers within the plant wall. The implementation under TRNSYS of an aeraulic model describing the intensity of flows as a function of wind speed made it possible to simulate the interaction of green buildings with the microclimate at the scale of a canyon street.	Aeraulic model describing the intensity of flows as a function of wind speed. He considers the vegetation cover as a layer semi-transparent to solar radiation. The thermal inertia of the entire vegetated wall is taken into account and mass and heat transfers are strongly coupled	The ambient air temperature, relative humidity, wind speed at certain altitudes, global solar irradiance on the vegetation module, sky temperature and precipitation. In addition to the external meteorological conditions, the temperature of the lower surface of the substrate layer or the heat flux at this location must also be provided. For each time step, the (n+3) variables are initialized to their values at the previous time step
16	P. G. Mestayer et al 2010	The FluxSAP 2010 experimental campaign, Climatology measurements in heterogeneous urban areas <b>Neighbourhood - climatology</b>	At night, the gaps are reduced, within the limits of the accuracy of the measurements, except for a site with a very vegetal environment, which can give a colder temperature of 2°C at sunrise. During the day, the dispersion is more important, the extreme differences between sites can reach 5°C for the sunniest days, the phase shift between the surface and the depth of 5 cm is about 1 hour for both sites. Surface temperature is directly dependent on local sunlight conditions; thus the storage flow, associated with the gradient at the surface, is negative at night and can also remain so for most of the day on a hidden site, while it is strongly positive all day on a sunny open site. In addition, temperature variations at 1 m in the ground are small at the day and week scales, which validate the choice of this maximum depth for future studies.	Implement five methods for evaluating surface-atmosphere fluxes over a highly variable domain and compare the results obtained.	Measurements of piezometry, water content and temperature in the ground make it possible to monitor water and heat transfers in the ground. Temperature and humidity measurements at the surface and at a height z of a few meters above the surface are analyzed using the average gradient method. Measurements of turbulent flows of sensitive heat. Measurements of scintillometers placed at a height above the canopy allow the evaluation of the integrated sensitive heat flows. Measurements of temperature, humidity and wind speed at several levels on the permanent instrumented mast of the central site make it possible to evaluate flows using the methods of vertical profiles of average quantities or vertical gradients.
17	Eleftheria Alexandri, Phil Jones 2008	Temperature decreases in an urban canyon due to green walls and green roofs in diverse climates <b>Neighbourhood - climatology</b>	In general, the more solar radiation a surface receives, the lower its temperature when it is covered with vegetation. For low air velocities within the canyon, wind direction does not have a significant effect on temperature decreases due to vegetation. In terms of urban geometry, the wider a canyon is, the smaller the effect of green roofs and green walls on temperature reduction. In all climates examined, green walls have a stronger effect than green roofs inside the canyon. Nevertheless, green roofs have a greater effect at the roof level and, consequently, at the urban scale.	A two-dimensional, prognostic, microscale model was used programmed in C++. The differential equations described as heat and mass transfer in air, building materials (considered capillaries - porous bodies), earth and vegetation have been solved with approximations of finite differences, where surface elements are replaced by nodes	Maximum, minimum and average diurnal values of climatic characteristics (total horizontal solar radiation, air temperature, relative humidity, wind speed) for the 24-hour profile of the typical day of the hottest month in each city (METEONORM)
18	Jörg Spangenberg et al 2008	Simulation of the influence of vegetation on microclimate and thermal confort in the city of Sao Paulo <b>Neighbourhood - climatology</b>	The leaf area index (LAI) and leaf area density (LAD) of the canopy are important parameters that have a significant influence on the microclimate. Isolated trees and even rows of trees have a relatively small impact on the decrease in air temperature and, therefore, a limited potential for mitigating urban heat island air temperatures	ENVI-met	Start of simulation (h), Wind speed at 10 m above ground level (m/s), Wind direction, Initial atmospheric temperature (K), Specific humidity at 2500 m (g Water / kg air), Solar adjustment factor, Relative humidity at 2m (%), Relative humidity in all layers (%), Wall albedo and roof albedo. Also add the study area where the simulation took place

ID	Author/Year	Paper/Scale	Main conclusion	Type of model	Input
19	Eleftheria Alexandri, Phil Jones 2004	The Thermal Effects of Green Roofs and Green Façades on an Urban Canyon  <b>Neighbourhood - climatology</b>	This analysis is applied to various geometries and climates and the calculation is performed using a two-dimensional dynamic microscale mass and heat transfer model describing the temperature and humidity distributions in an urban canyon. The algorithm for building materials, soil, vegetation and air has been programmed in C ++. In general, the wider a street is, the more intense the effect, especially with green walls, due to the shading in building materials from plants and the extreme wind speeds prevailing in the canyon. Dry climates tend to increase the benefit of vegetation; due to lower humidity in the climate, plant evapotranspiration, which alters humidity concentrations, has a greater effect on temperatures.	The impact of mass transfer on heat transfer was considered crucial for the rational estimation of the impact of vegetation on temperatures for various moisture concentrations.	Air temperature and humidity inside buildings. Temperature and humidity are also considered constant at a depth of 8.0m in the soil. Meteorological data from Meteonorm.
20	Rabah Djedjig et al 2015	Modeling green wall interactions with street canyons for building energy simulation in urban context  <b>Neighbourhood – climatology and local-building</b>	The green envelope model has been specially developed to overcome some of the limitations and assumptions of previous modelling approaches that assume near-permanent heat transfer and neglect the effect of water transfer on heat transfer. Interactions between buildings, green walls and the street canyon were studied with the addition of a component of the urban canyon. This work made it possible to establish a reference case study that could be used for future digital calibrations and validations of new models for buildings and interactions between the street and the walls of green buildings	Green wall model: the model equations establish the heat balance on the leaf canopy and on the substrate surface. Fluxes are evaluated on the foliage using a resistance scheme that opposes heat and vapor transfer and that incorporates the aerodynamic resistance, the stomatal resistance and the resistance to the diffusion of heat and vapor from the soil surface throughout the leaf canopy	Ambient air temperature, relative humidity, global incoming solar radiation on the wall, sky temperature, wind speed et altitude zu, rainfall, drainage, irrigation and inner boundary condition (conducted flux)
21	Rabah Djedjig et al 2013	Experimental study of the urban microclimate mitigation potential of green roofs and green walls in street canyons  <b>Neighbourhood - climatology</b>	An analysis of experimental data was carried out on three street canyons: a reference street, a street between two buildings with green roofs and one with a green wall to the west. This article presents the results and highlights the radiative, thermal and hygrometric effects of the use of green roofs and facades on the urban microclimate. In terms of thermal comfort in the street canyon, the long wave heat flux from the canyon surfaces can be modelled by a theoretical average radiant temperature, assuming that the body surfaces are black. To assess the mitigation potential of vegetation, we quantify the overheating reduction potential (ORP) by decreasing the temperature in the canyons covered with vegetation compared to the overheating in the reference canyon. The green wall can reduce the overheating of the street canyons by one-third by maintaining moderate temperatures on the green façade by evapotranspiration. The use of green facades can reduce the average radiation temperature by 4°C, which directly affects the thermal comfort in the street canyon	Experimental analysis	Relative humidity, air temperature, wind speed, wind direction, solar radiation and long wave emittance of the street

ID	Author/Year	Paper/Scale	Main conclusion	Type of model	Input
22	Pierre Philippe Kastendeuch et al 2016	Thermo-radiative simulation of an urban district with LASER/F  <b>Neighbourhood - climatology</b>	Modelling from the LASER / F program of the climatic impact of the installation of trees in the city in order to mitigate the thermal discomfort caused by urban heat islands. To this end, the programme was first evaluated and, as a means of evaluating the results demonstrated by the programme, experimental measurements were carried out in the region. It was verified that the program provides good values of net radiation and that the ground heat flux is the two best reproduced variables (determination coefficient of 0.62). However, the result of the latent heat flux calculated by the program and the actual measured at a determination coefficient of only 0.37	LASER/F	
23	Linfang Zhang et al 2017	Simulated study on the potential of building energy saving using the green roof  <b>Neighbourhood – climatology and local-building</b>	Work carried out with the help of the PHOENICS program and the simulation of four different situations of ground cover and roof structures in a neighbourhood. Use of simple equations of the changes between the roof and the environment. It was concluded that the green roof can reduce the building's exterior surface temperature and improve the thermal environment of the roof and its environment. This provides optimization strategies for building energy conservation.	PHOENICS software to establish 3D building model and simulates thermal environment under the different green conditions	Environment temperature (°C), Dominant wind direction, Dominant speed (m/s), Ground floor material , Computational domain , Near-Wall Treatment, Computational grid, Boundary condition , Discrete algorithm
24	L. Guilioni a, J.P. Lhomme 2006	Modelling the daily course of capitulum temperature in a sunflower canopy  <b>Neighbourhood – climatology</b>	A model is proposed to estimate the daily course of capitulum temperature in a sunflower canopy from the beginning of flowering. The model is based on the equations describing the energy exchanges between the soil–plant system and the atmosphere. The local microclimate surrounding the capitulum is explicitly calculated. The model allows the estimation of the temperature really experienced by the capitulum, which significantly differs from air temperature at screen level. To be used in an operational manner the model inputs should be only standard meteorological data and easily recorded parameters. Limitations concerning the estimation of some weather data still remain, such as the atmospheric long wave radiation and the diffuse solar radiation. The calculation of soil heat flux as a fraction of net radiation does not work well at night. More efficient parameterisations should be found. But the comparison between the model and the measured show a good relation in general	The plant canopy is assumed to be horizontally homogeneous and conceived as an electrical circuit transferring sensible and latent heat between the soil–plant system and the air. Horizontal flux divergence is assumed to be negligible. The whole canopy is divided into two main layers: the first layer represents the capitulum above the canopy of leaves and the second layer represents the rest of the canopy: leaves and soil surface. Model development: Basic transfer equation, energy balance equation, capitulum radiation balance, incident radiations received by the capitulum, parameterizing air conductances, parameterizing stomatal conductance	Number of plants per unit area, whole canopy height, height of the leafy part of the canopy, leaf area index, leaf width, canopy albedo, diameter, thickness, albedo (each side), azimuth and inclination angle of the capitulum, fraction of transpirable soil water. OUTPUT: capitulum and leaf temperatures



ID	Author/Year	Paper/Scale	Main conclusion	Type of model	Input
25	T. Winkel et al 2009	Assessing the protective effect of vertically heterogeneous canopies against radiative frost: The case of quinoa on the Andean Altiplano  <b>Neighbourhood – climatology</b>	Night radiative frost is a highly limiting factor for agriculture in Andean highlands. A sensitivity analysis of the model reveals that canopy height, leaf area index, and sky cloudiness have the most important influences on the development of the sheltering effect, while air temperature and air humidity play a minor role under typical radiative frost conditions. As for wind speed, its actual influence remains unclear due to experimental and modelling limitations at low wind speeds. The significance of these results is discussed in terms of the trade-off between stress adaptation and biomass productivity. Continuous data collection throughout an entire quinoa crop cycle showed that, under field conditions prone to nocturnal cooling, leaf temperature gradients up to 2.6 8Cm-1 appeared within the canopy of a traditional quinoa landrace (in most cases, would be sufficient to allow the the crop canopy to escape from lethal freezing)	To the energy balance the heat storage term as well as the transpiration flux can be neglected, the first one because of the small biomass of the leaf blades, the second one because leaf stomata are closed at night. Three hypothetical conditions of vertical heterogeneity in the crop row were considered, according to the difference in the height of the smallest plant relative to that of the tallest plant, for an heterogeneous, an intermediate, and an homogeneous canopy respectively.	In the model, canopy structure is essentially represented by canopy height and leaf area index LAI, and atmospheric conditions by wind speed, sky cloudiness, relative air humidity and air temperature. The model was run successively varying the value of one parameter, all other parameters being kept equal. The output of the model was the difference in leaf temperature between two levels within the canopy, specifically the upper leaf of the smallest plant and that of the tallest plant within a crop row.
26	J. P. Lhomme, J. J. Vacher 2002	Modelling nocturnal heat dynamics and frost mitigation in Andean raised field systems  <b>Neighbourhood – climatology</b>	Model based in a two-layer scheme of the surface–atmosphere interaction, to evaluate the nocturnal heat dynamics in a raised field system. It consists of a substrate layer representing the water within the canals and a vegetation layer representing the crop grown on the platforms. Wider canals or narrower platforms have a positive impact on the minimum crop temperature reached during the night. Increasing water depth also improves frost mitigation. The main crop characteristics, LAI and crop height, both have a positive impact, facilitating the heat transfer from the canals and the air to the crop: the greater they are, the higher the minimum crop temperature with, however, a decreasing marginal benefit. Higher wind velocity or air relative humidity also enhances the frost mitigation effect in accordance with the common knowledge derived from radiation frost models.	Can be run in two different ways according to the data available: (i) if the time series of water temperature is known and used as input, together with the air characteristics at screen height, the model returns the nocturnal variation of crop temperature; (ii) if only the initial temperature of the water is known, the model returns simultaneously the nocturnal variation of crop and water temperatures from the air characteristics measured at screen height. The outputs obtained in running both ways the model have been successfully compared to experimental data collected on a system of raised fields in the vicinity of Lake Titicaca in Bolivia.	
27	Marc Saudreau et al 2007	A 3D model for simulating the spatial and temporal distribution of temperature within ellipsoidal fruit  <b>Neighbourhood – climatology</b>	Model based in a three-dimensional (3D) unsteady heat conduction equation with unsteady and non-homogeneous heat fluxes as boundary conditions. The model quality has been assessed by comparing model outputs to temperature measured with thermocouples at several locations in isolated peach and apple fruits. Results suggested that the model could be used in order to study the microclimatic effects on fruit responses, in terms of fruit physiology and in terms of fruit diseases	C++: we propose a numerical model of heat conduction within an ellipsoidal fruit. Boundary conditions and diffusivity coefficients can vary in space and over time to mimic variations in atmospheric conditions and changes in tissues thermal conductivity within fruits.	Fruit properties measured or collected from the literature, and the microclimate parameters measured such as air temperature, air humidity, wind velocity, solar and atmospheric radiation. The number of grid points was (nr, nj, nu) = (20, 10, 5) and a simulation time step of 1 min was used.

ID	Author/Year	Paper/Scale	Main conclusion	Type of model	Input
28	Abubakar S. Mahmoud et al 2017	Energy and Economic Evaluation of Green Roofs for Residential Buildings in Hot-Humid Climates  <b>Neighbourhood – climatology and local-building</b>	For the three investigated green roof options, energy saving is found to be in the range of 24% to 35%. The research concludes that though green roofs offer significant energy saving potential, it is currently not an economically promising technology for Saudi Arabia. The tariff increments planned by the Saudi government, however, will improve its economic viability	DesignBuilder software	Extensive green roof model parameters for input in DesignBuilder: Thermal Conductivity (W/(m·K)), Height of Plants (m), Leaf Area Index (LAI), Leaf Reflectivity, Minimum Stomata Resistance (s/m), Maximum Volumetric Moisture Content at Saturation, Minimum Residual Volumetric Moisture Content. Key structural features of the building: Location, orientation, floor to floor height, occupancy density, floor area, window to wall ratio, weather file and relative humidity, exterior walls, roof, infiltration, lighting power density, heating, ventilation, and air conditioning system type, window
29	Elena Palomo Del Barrio 1998	Analysis of the green roofs cooling potential in buildings  <b>Neighbourhood – climatology</b>	Green roofs do not act as cooling devices but as insulation ones, reducing the heat flux through the roof. A relatively small set of parameters have been identified as relevant for green roof design: the leaf area index (LAI) and the foliage geometrical characteristics, the soil apparent density, its thickness, and its moisture content	MATLAB. The green roof model is obtained by coupling the models of green roof components, such models represent the real boundary conditions at the canopy-soil and canopy-support interfaces, satisfying the physical constraint of continuity for the states variables and the flux densities. Finally, several parametric sensitivity analyses are performed in order to identify key parameters for an efficient green roof design.	General: LAI, canopy height, leaves dimensions; Optical: air density, coefficient of extinction; External resistance: canopy crop and leaves dimensions; Internal resistance: minimal stomatic resistance, surface temperature; Aix exchanges
30	F. Convertino, G. Vox & E. Schettin	Heat transfer mechanisms in vertical green systems and energy balance equations  <b>Neighbourhood – climatology</b>	The study investigated the dynamics of heat transfer in the green facade and the energy balance of the elements that compose it. A heat balance equation was written for each layer. The theoretical model was applied to measured data, recorded on an experimental green facade. The analysis of the single terms of the balance pointed out how their contributions influence the overall thermal balance of the green facade. The solar radiation is the most influencing parameter. The presence of green facades affects the building microclimate all day, by reducing heat waves during the warm periods and heat losses from the building in the cold period	The green facade was described by a schematic representation, four layers were defined: the green layer, the external surface of the building wall, the internal surface of the building wall, the air inside the building. The energy balance was defined for each layer and all the terms involved in the energy exchange between the layers were defined as a function of the plant, the weather conditions and the constructive characteristics of the wall.	External air temperature and relative humidity, solar radiation, wind velocity and direction, plants and building characteristics

## APPENDIX 2

Table of fixed parameter used in the literature.

Characteristic	Concrete	Asphalt	Sand	Loam	Clay	Plants (grass and creepers)
Specific thermal capacity (MJ/m <sup>3</sup> K)	1,60	2,00	1,46	1,21	1,09	2,60
Thermal conductivity (W/mK)	1,70	1,30				
Vapour diffusivity (10 <sup>-6</sup> m <sup>2</sup> /s)	0,55	1,58				
Ratio of vapour diffusion coefficient to total moisture diffusion coefficient	0,20	0,10				
Emissivity	0,94	0,81				0,94
Albedo	0.23	0,10				0,30
Convective heat resistance (s/m)						200
Resistance expressing the plant type (s/m)						100
Canopy extinction coefficient						1,4
Level of soil moisture below which permanent wilting of the plant occurs (m <sup>3</sup> /m <sup>3</sup> )						0,25
Coefficient <i>b</i>			4,05	5,39	11,4	
Hydraulic conductivity (m <sup>4</sup> m/s)			1,76	0,072	0,013	
Moisture potential, when soil is saturated (cm)			-12,1	-47,8	-40,5	
Maximum volumetric water content (m <sup>3</sup> /m <sup>3</sup> )			0,395	0,451	0,482	
Factor accounting for reduction in transpiration due to drying up of the soil toward the wilting point (m <sup>3</sup> /m <sup>3</sup> )			0,068	0,155	0,286	
Soil liquid water content at field capacity (m <sup>3</sup> /m <sup>3</sup> )			0,135	0,240	0,367	

Source: Adapted from Alexandri et al (2016) and Jacobson (2004)

APPENDIX 3

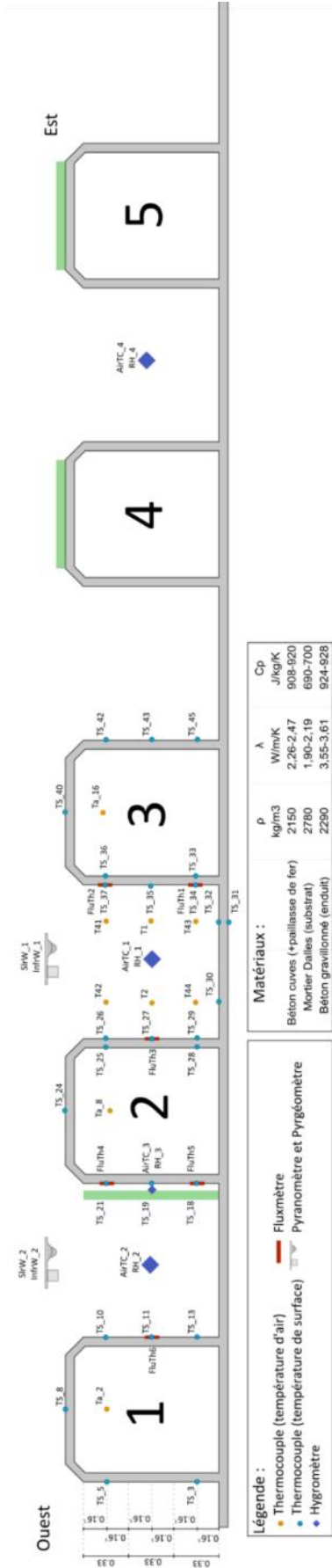


Fig. A : Coupe sur la plateforme expérimentale

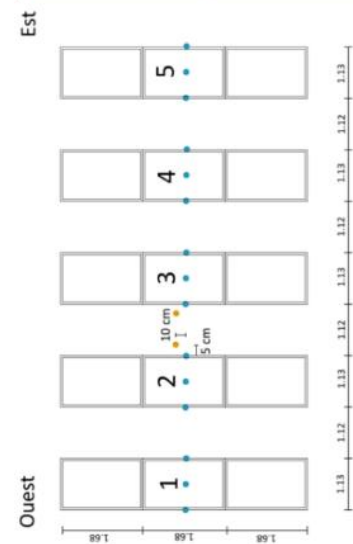


Fig. B : Vue du dessus de la plateforme expérimentale

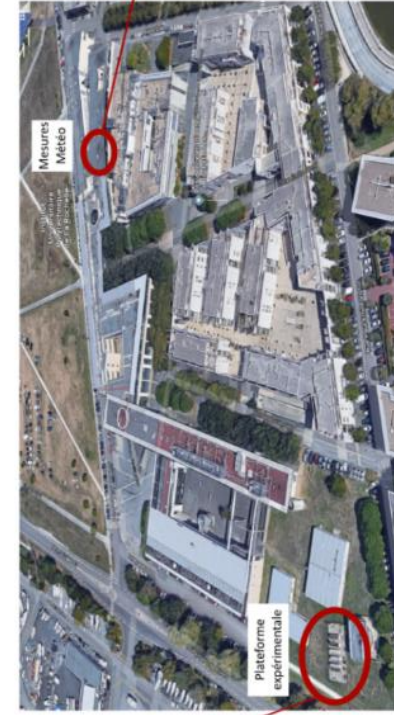


Fig. C : Vue Google Map du site

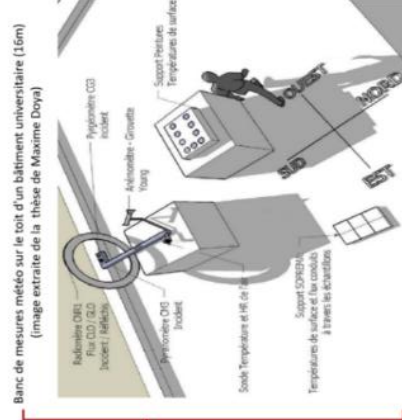
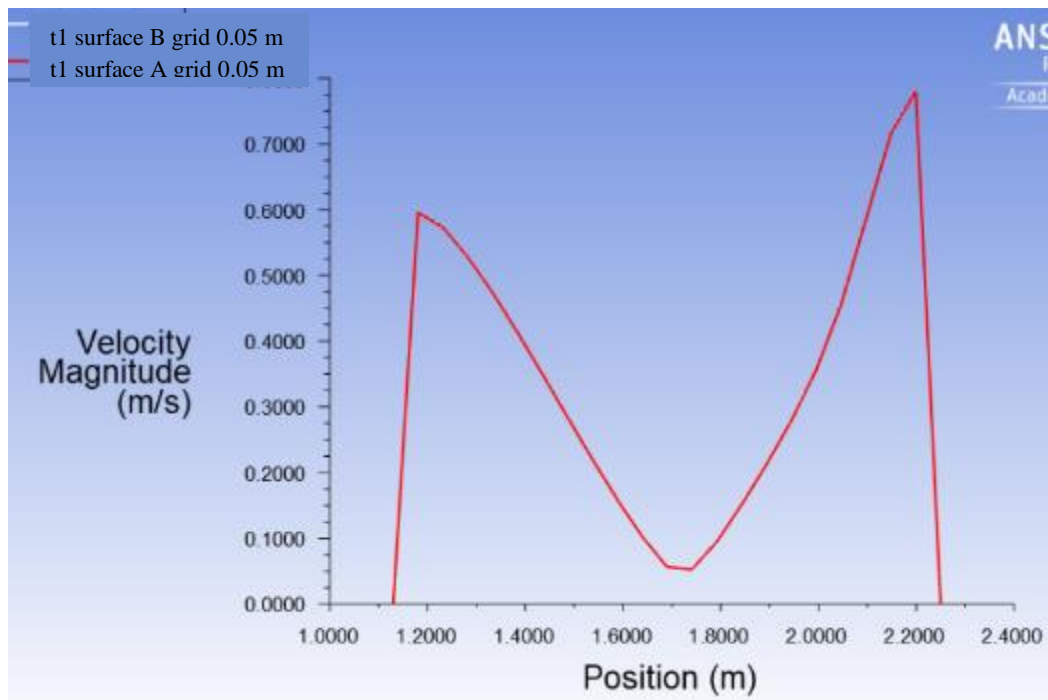


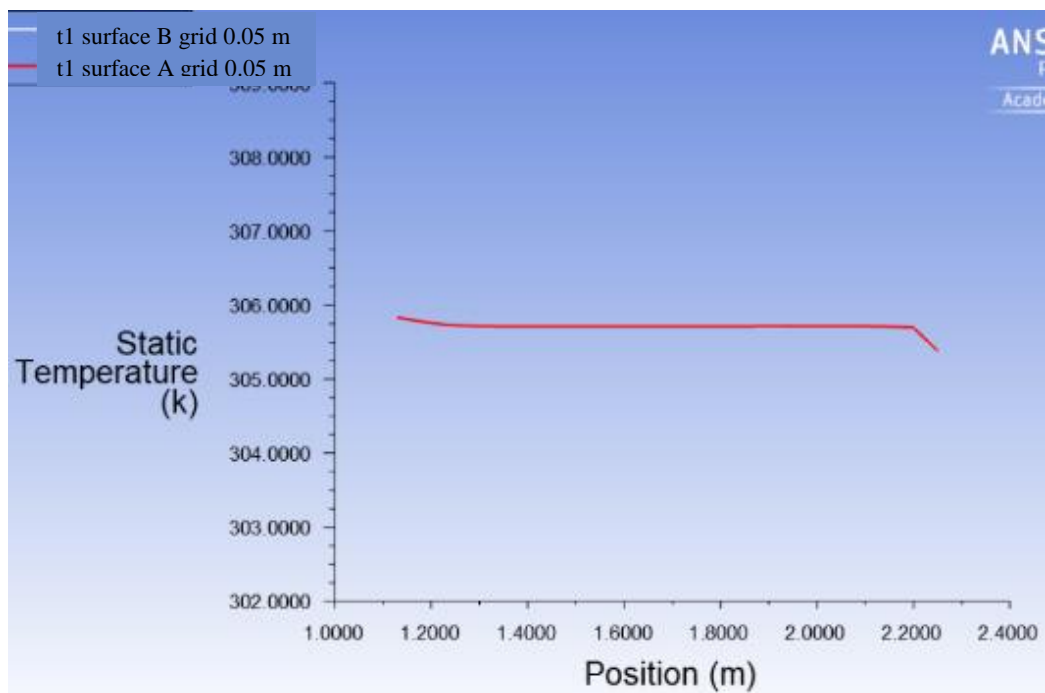
Fig. D : Disposition des mesures météo

Illustration of the location of the pilot ClimaBat, sensors and meteorological measurement bank of the VegDud project developed at La Rochelle University. (Musy et al ,2012 ; Djedjig, 2013)

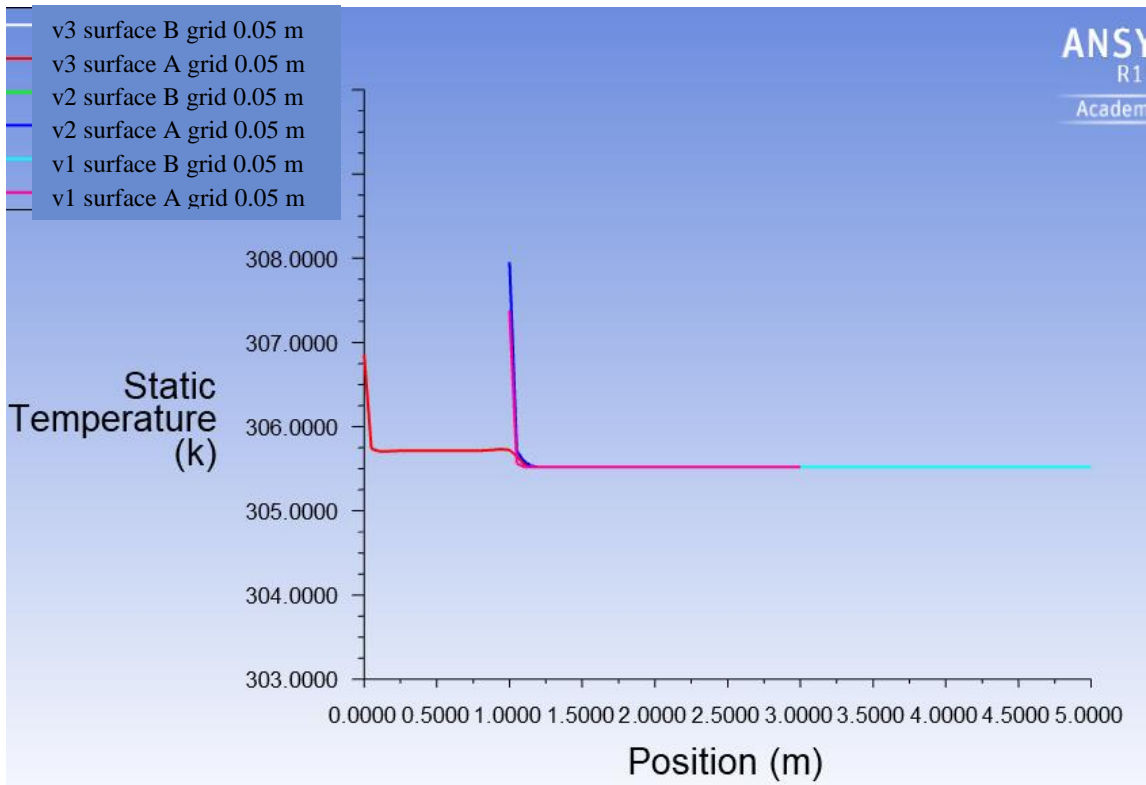
## APPENDIX 4



Graphic of the transverse (t1) profiles for the velocity within the canyon A and B



Graphic of the transverse (t1) profiles for the temperature within the canyon A and B



Graphic of the vertical (v1, v2 and v3) temperature profiles within the canyon A and B